TAMPEREEN TEKNILLINEN YLIOPISTO
TAMPERE UNIVERSITY OF TECHNOLOGY

Ville Mylläri

Melt Spinning, Functionalization and Durability of Polyetheretherketone-Based Fibres

Julkaisu 1466 • Publication 1466

Tampere 2017

Tampereen teknillinen yliopisto. Julkaisu 1466
Tampere University of Technology. Publication 1466

Ville Mylläri

Melt Spinning, Functionalization and Durability of Polyetheretherketone-Based Fibres

Thesis for the degree of Doctor of Science in Technology to be presented with due permission for public examination and criticism in Festia Building, Auditorium Pieni Sali 1, at Tampere University of Technology, on the 7th of April 2017, at 12 noon.

Tampereen teknillinen yliopisto - Tampere University of Technology
Tampere 2017

Doctoral candidate	Ville Mylläri Department of Materials Science Tampere University of Technology, Finland
Supervisor	Professor Jyrki Vuorinen Department of Materials Science Tampere University of Technology, Finland
Pre-examiners	Professor Ulf Gedde School of Chemical Science and Engineering KTH Royal Institute of Technology, Sweden Professor Carl-Erik Wilen Laboratory of Polymer Technology Åbo Akademi University, Finland
Opponents	Professor Jukka Seppälä Department of Biotechnology and Chemical Technology Aalto University, Finland Professor Ferrie van Hattum Lightweight Structures research group Saxion University of Applied Sciences, Netherlands

ISBN 978-952-15-3926-8 (printed)
ISBN 978-952-15-3928-2 (PDF)
ISSN 1459-2045

Abstract

Polyetheretherketone (PEEK)-based polymer fibres have attracted much interest due to their many outstanding properties. Along with one of the highest use temperatures among thermoplastics, PEEK also has excellent mechanical properties and chemical resistance. Because of these properties, PEEK and PEEK fibres are often used in demanding conditions. In this dissertation, PEEK-based polymer fibres were pushed to the limit in four different situations: melt spinning of fine filaments, photoageing, maximum recommended use temperature, and contaminants. To fight contaminants, PEEK was modified via a sulfonation reaction into sulfonated polyetheretherketone (SPEEK) and then melt compounded with polypropylene (PP) to produce antimicrobial and self-cleaning properties. The goal of this dissertation was not only to measure changes in the properties but also to improve the properties.

The general spinnability of PEEK was good with viscosity control deemed crucial to improving that spinnability. In addition to a long and large die and a short spinning path, a low viscosity PEEK grade and a high processing temperature are recommended. Tests provided new information on the quantitative effects of processing parameters on the smallest spinnable fibre diameter. The smallest obtained fibres had an average diameter of 18 µm and a mechanical strength of approximately 280 MPa.

Photodegradation was one of the main weaknesses of PEEK fibres. Ageing PEEK for up to 1056 h in a UV chamber degraded the fibres rapidly from elastic to brittle. Thermal ageing, for up to 128 d at 250 °C, produced effects similar to those of photoageing, including embrittlement, but also some different effects. In both cases, ageing caused crosslinking, which was verified by rheological measurements. Changes in the carbonyl group absorption band, measured by Fourier transform infrared spectroscopy (FTIR), were significantly bigger in photodegradation than in thermal degradation. Differential scanning calorimetry (DSC) turned out to be a poor method to detect ageing in photodegradation, but in thermal degradation it revealed a decrease in the melting temperature and an increase in the glass transition temperature. In both cases, decreased thermal stability was verified by thermogravimetric analysis (TGA).

A SPEEK/PP blend was successfully produced in various compositions. Compounding produced an immiscible polymer blend, in which approximately 1-µm SPEEK particles were homogenously dispersed in the PP matrix. According to electron paramagnetic resonance (EPR) measurements, this blend formed stable radicals with their number correlating with the SPEEK concentration. The thermal properties of SPEEK were inferior to those of PEEK, a reason that made the melt spinning of SPEEK/PP blend challenging. At 200 °C, stable melt spinning process was achieved and good quality yarns were produced. The mechanical tenacity of SPEEK/PP 5:95 yarns was approximately 20% lower than that of otherwise similar PP yarns.

Preface

This thesis was made at Tampere University of Technology, Department of Materials Science. The beginning of this thesis originates to June 2010 when I started my Master's thesis titled "Production of filament yarns made of PEEK". After graduation I had the opportunity to continue with this topic towards doctoral degree. It would not have been possible to finalize this thesis without the financial support of FP7 project "SAFEPROTEX" (FP7-NMP-2008-SME-2, contract number 228439), Academy of Finland project UVIADEM (Grant no 253655), the Federation of Finnish Textile and Clothing Industry (Finatex) and Finnish Foundation for Technology Promotion (TES).

I would like to thank the supervisor of my work Prof. Jyrki Vuorinen for helping in the final stages of this dissertation. I would also like to thank my previous mentors Prof. Pentti Järvelä, Dr. Seppo Syrjälä and Prof. Mikael Skrifvars for instructing me in the beginning of this thesis. I was lucky to have four experts with different backgrounds to guide me. I would also like to express my sincere gratitude to the pre-examiners of this thesis, Prof. Ulf Gedde and Prof. Carl-Erik Wilen, for the valuable comments.

Most of my publications were made in cooperation with different organisations and laboratories. I would like to thank Dr. Enrico Fatarella, M.Sc Tero-Petri Ruoko, Prof. Helge Lemmetyinen, M.Sc. Marco Ruzzante, Prof. Rebecca Pogni, and PhD Maria Camilla Baratto for their contribution in these five articles. I express my gratitude to Jyri Öhrling, Tommi Lehtinen, Sinikka Pohjonen, Maija Järventausta, M.Sc Arja Puolakka, Esa Leppänen, and Dr. Marja Rissanen for the experimental help. I would like to thank Dr. Anu Heikkilä for her help in the characterization of the UV chamber. I would also like to thank my fellow researches and research assistants in the research group for the favours you have done for me during these six years.

Finally, I would like to express my warmest thanks to my family for all the support.

Tampere, March 2017

Ville Mylläri

List of publications

This thesis is based on the original experimental work presented in the following five publications. They are referred to *publications I-V* in the text and shown in appendices.

I. Mylläri Ville, Skrifvars Mikael, Syrjälä Seppo, Järvelä Pentti. The effect of melt spinning process parameters on the spinnability of polyetheretherketone. Journal of Applied Polymer Science 126 (2012) 1564–1571.

II. Mylläri Ville, Ruoko Tero-Petri, Järvelä Pentti. The effects of UV irradiation to polyetheretherketone fibres – characterization by different techniques. Polymer Degradation and Stability 109 (2014) 278–284.

III. Mylläri Ville, Ruoko Tero-Petri, Vuorinen Jyrki, Lemmetyinen Helge. Characterization of thermally aged polyetheretherketone fibres – mechanical, thermal, rheological and chemical property changes. Polymer Degradation and Stability 120 (2015) 419–426.

IV. Fatarella Enrico, Mylläri Ville, Ruzzante Marco, Pogni Rebecca, Baratto Maria Camilla, Skrifvars Mikael, Syrjälä Seppo, Järvelä Pentti. Sulfonated polyetheretherketone/polypropylene polymer blends for the production of photoactive materials. Journal of Applied Polymer Science 132 (2015) 41509.

V. Mylläri Ville, Fatarella Enrico, Ruzzante Marco, Pogni Rebecca, Baratto Maria Camilla, Skrifvars Mikael, Syrjälä Seppo, Järvelä Pentti. Production of sulfonated polyetheretherketone/polypropylene fibers for photoactive textiles. Journal of Applied Polymer Science 132 (2015) 42595.

Author's contribution

The author is responsible for the main part of the experimental work and writing in *publication I* with the help of the comments of the co-authors. In *publications II and III*, the author is responsible for planning the experimental work and performing the main part of it. Author has written these articles, excluding parts involving chemistry, with the help of the comments of the co-authors. In the experimental part of *publication IV*, the author is responsible for melt compounding of SPEEK/PP blend, performing rheological measurements, and organising TGA and SEM tests. Author has also written these sections as well as has had a major role in the introduction, FTIR and conclusion sections. In *publication V* the author is responsible for the written and experimental parts excluding SPEEK sulfonation, EPR measurements and mechanical tests. This publication was improved with the help of the comments of the co-authors.

List of symbols and abbreviations

^{1}H-NMR	Nuclear magnetic resonance
ATR	Attenuated total reflectance
BP	Benzophenone
BPK	Benzophenone ketyl
CH_3	Methyl group
CO_2	Carbon dioxide
DS	Degree of sulfonation
DSC	Differential scanning calorimetry
FDA	US Food and drug administration
FTIR	Fourier transform infrared spectroscopy
EPR	Electron paramagnetic resonance
ESIPT	Excited state intramolecular proton transfer
H_20	Water
HVAC	Heating, ventilation, and air-conditioning systems
I_{max}	Maximum measured radical intensity
L/D	Length/diameter
M_n	Number average molecular weight
M_w	Weight average molecular weight
N_2	Nitrogen
O_2	Oxygen
PE	Polyethylene
PEEK	Polyetheretherketone
POY	Partially oriented yarn
PP	Polypropylene
PVA	Polyvinyl alcohol
PVB	Polyvinyl butyral
Q	Mass flow
SEM	Scanning electron microscope
SPEEK	Sulfonated polyetheretherketone
RPM	Revolutions per minute
SO_3H	Sulphonic acid
T_g	Glass transition temperature
TEM	Transmission electron microscope
TGA	Thermogravimetric analysis
TiO_2	Titanium dioxide
T_m	Melting temperature
UV	Ultraviolet
v_0	Fibre velocity at die
v_l	Fibre take-up velocity
VOC	Volatile organic compound
WAXS	Wide angle X-ray scattering

Contents

1. Introduction

A fundamental goal in material development is to be able to use materials in more and more demanding conditions. Such conditions may pose a risk not only to the material but also to its users. However, risks can be minimized by thoroughly characterizing the material as well as by developing them further. Such development may comprise fine-tuning of the processing parameters or compounding with other materials. In this thesis, polyetheretherketone (PEEK)-based polymer fibres were pushed to the limit in multiple ways and then characterized thoroughly.

PEEK is a semicrystalline thermoplastic, often used in applications too extreme for conventional thermoplastics. PEEK has excellent mechanical and thermal properties and chemical resistance [1, 2]. Of easily spinnable polymer and typically manufactured by melt spinning, PEEK fibres are currently used in many high-technology applications from tennis racket strings to protective clothing [2, 3]. The fibres differ from bulk material not only in dimensions but also in morphology. In fibres, polymer chains are aligned in the same direction as a result of fibre drawing, which also increases crystallinity and improves mechanical properties. Decreased fibre size increases the surface area to volume ratio, high value being desirable in many applications, including fibre reinforcement and photocatalysis. However, reduced fibre size has its drawback in that despite the best precautions, yarn breaks tend to proliferate [4].

PEEK is often exposed to degrading conditions. Various types of degradation such as thermal, mechanical, ultrasonic, hydrolytic, chemical, biological, and radiation can damage materials. Among these, thermal degradation and radiation, often caused by exposure to sunlight, are the most important for polymers. Degradation causes changes in the physical and chemical properties of polymers, typically, decreased molecular weight and mechanical properties, loss of gloss, surface erosion, and changes in chemical structure. [5] The most striking characteristics of ageing PEEK are crosslinking and embrittlement by photo-irradiation [6] and an initial improvement in mechanical properties in the early stages of thermal exposure [7, 8, 9]. However, despite the wealth of literature available on polymer degradation, many problems remain unsolved because results are contradictory and difficult to compare owing to differences in samples, and because many theoretical mechanisms have not been proved experimentally [10].

The repeating unit of PEEK contains benzophenone (BP) as a part of its structure. BP is commonly used as a photosensitizer in photochemistry to provide functionality, for example, antimicrobial and self-cleaning properties, to materials [11, 12, 13]. Harnessing the power of BP in PEEK would be greatly beneficial, and this approach could challenge titanium dioxide (TiO_2), the current standard in the market, because, unlike TiO_2, this fully polymeric approach would contain no potentially harmful nanoparticles. Unfortunately, the photocatalytic reaction is quenched in virgin PEEK. Sulfonation, or other modification, of PEEK is required to acquire these properties. In addition, a proper hydrogen transfer agent is needed. [14] A modification of PEEK as well as the necessary melt compounding are likely to change material properties and complicate melt spinning. Nevertheless, this approach harbours considerable novelty and potential.

The objective of this thesis was to characterize and develop PEEK-based polymer fibres for use in demanding conditions. This objective was approached from three angles: first, to manufacture and characterize fine PEEK filaments; second, to degrade PEEK fibres by heat and light; and, third, to manufacture PEEK-based polymer fibres with antimicrobial and self-cleaning properties. The thesis comprises seven chapters, the introduction being the first. Chapters 2 and 3 constitute the theoretical background with chapter 2 focusing on the material and chapter 3 on demanding conditions. Chapter 4 covers the aim and different approaches of the thesis whereas chapter 5 introduces the experimental procedure, consisting of the materials, compounding, melt spinning, ageing, and characterization. Chapter 6 reports the results and discusses the main findings, and chapter 7 concludes the thesis. Appended to the end are five publications presenting the original experimental work of this thesis.

2. Polyetheretherketone (PEEK)

2.1. General properties

Polyetheretherketone or PEEK or poly(oxy- 1,4-phenyleneoxy- 1,4-phenylenecarbonyl- 1,4-phenylene) is a linear, aromatic, semicrystalline thermoplastic. PEEK was first synthetized by the Imperial Chemical Industries chemists in 1964 and commercialized by the same company in 1982 under the trade name Victrex PEEK [2]. PEEK can be polymerized using two different routes: nucleophilic or electrophilic processes, the first being more common [15]. The repeating unit of PEEK, presented in Fig. 1, is composed of three phenyl rings that are linked to each other either with an ether or a carbonyl group. The molecular weight of the repeating unit is 288.3 g/mol, typical number average molecular weight (M_n) 6200–15000 g/mol, and typical mass average molecular weight (M_w) 14300–100000 g/mol. The crystallinity of PEEK can vary between 0 and 40 % but is typically around 35 %. [15]

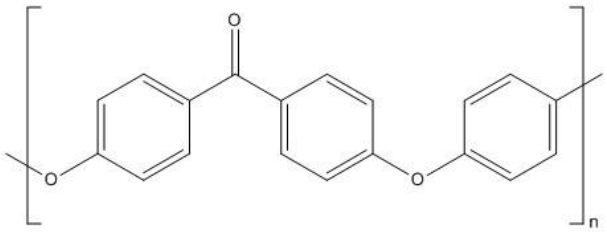

Fig. 1. The chemical structure of PEEK. *Publication II*.

PEEK has unique properties among thermoplastics and therefore it is commonly used in harsh conditions including metal replacement applications, medical implants and space applications. Apart from the high processing temperatures, the processing of PEEK is easy and can be done using all typical thermoplastic processing techniques. PEEK is FDA (US Food and Drug Administration) approved so it can be used in a wide range of applications. [1, 2]

Thermal properties of PEEK are known to be one of the best among synthetic polymers. PEEK has a glass transition temperature (T_g) of 143 °C, continuous use temperature of 260 °C, a melting point (T_m) of 343 °C, and decomposition onset temperature of 575 °C [16]. The chemical properties are excellent as well and PEEK is resistant to most chemicals with some exceptions [15]. PEEK can perform well in weak acids but very strong acids can dissolve them. Halogens (bromine, chloride and fluorine) can attack on the aromatic rings of PEEK and halogenate them. Some amines, like aniline, can damage PEEK on elevated temperatures. Also certain aromatic esters and ketones can attack on PEEK at high temperature. [3]

PEEK has good mechanical properties, low water absorption and flammability, good radiation and abrasion resistance and good electrical insulation properties. The use of PEEK is limited because of its high price and by the need of special processing equipment capable of extreme temperatures. [1, 3, 17] The general properties of PEEK are summarized in Table 1.

Table 1. The properties of Victrex PEEK 151G [18].

Property	Unit	Typical value	Test method
Tensile strength, yield	MPa	110	ISO 527
Tensile modulus	GPa	3.9	ISO 527
Elongation at break	%	25	ISO 527
Charpy impact strength	kJ/m^2	4.0	ISO 179/1ea
Glass transition temperature	°C	143	ISO 11357
Melting point	°C	343	ISO 11357
Coefficient of thermal expansion, average, below T_g	ppm/°C	55	ISO 11359
Heat deflection temperature, 1.8 MPa	°C	156	ISO 75A-f
Thermal Conductivity	W/m °C	0.29	ISO/CD 22007-4
Melt viscosity, 400 °C	Pa.s	130	ISO 11443
Density, crystalline	g/cm^3	1.30	ISO 1183
Density, amorphous	g/cm^3	1.26	ISO 1183
Water absorption, 3.2mm tensile bar, 24 h, 23 °C	%	0.07	ISO 62-1
Dielectric strength, 2.5 mm thickness	kV/mm	16	IEC 60243-1
Dielectric constant, 23 °C, 1 kHz	n/a	3.3	IEC 60250
Volume resistivity, 23 °C	Ωcm	10^{15}	IEC 60093
Flammability rating	n/a	UL94	V-0 @1.5 mm
Limiting oxygen index, 3.2 mm thickness	% O_2	35	ISO 4589

2.2. PEEK fibres

2.2.1. Melt spinning

Melt spinning of PEEK fibres is not a new invention. In fact, it has been successfully done since the 1980s [3]. Melt spinning is a method suitable only for polymers that can be melted. There are many kinds of setups available. Typically, granulates are fed into an extruder through a hopper. A single screw extruder conveys, melts and homogenizes the material, and a filter system removes the remaining impurities. Before entering a spinneret, the polymer mass goes through spinning pumps, which ensures steady material flow. The working principle of a spinneret is similar to a bathroom shower head. It distributes the melt polymer through one (monofilament) or multiple (multifilament) orifices. After the spinneret, the material starts solidifying in an air quench chamber and forms a fibre structure. The fibres are drawn with a winding unit, which decreases the fibre diameter significantly compared to the diameter after the spinneret. The winding velocity can be over 5000 m/min for certain textile yarns. Hot or cold godets or different texturizing setups can be used before a take-up machine to modify the properties of the yarns. At the end of the line, on the take-up machine, there is a spin finish system. In addition, the melt spinning equipment often contains different control units, sensors and accessories for controlling and monitoring stable spinning process. [4]

In laboratory conditions, the mass throughput of an extruder system is often too large. To avoid this problem, piston-based systems have been developed [19]. This kind of system makes it possible to use mass throughputs as low as a few grams per hour providing filaments in the ultra-fine range, below 0.1 dtex at best. The basic principle of a piston system is similar to an extruder system previously described. Melted material is pushed through a small hole, air cooled and drawn with a winder. The difference is that material conveying is done with a piston which makes the process discontinuous. Both extruder and piston-based systems are presented in Fig. 2.

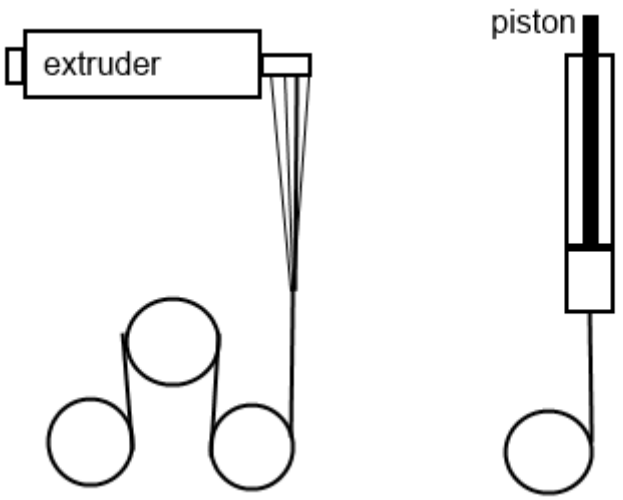

Fig. 2. Extruder and piston-based melt spinning systems.

2.2.2. Properties

PEEK fibres possess many of the same properties as PEEK in bulk form: excellent thermal properties, low smoke and gas emissions, excellent chemical and abrasion resistance, cleanliness for food contact applications, and proven track record of biocompatibility [20, 21]. Initially, the mechanical properties were in the range of 0.3–0.4 N/tex, the monofilament diameter being from 0.4 to 1.0 mm, and elongation at break 30–40 %. By the mid-1980s, the production of 5–15 dtex (20–40 μm) multifilaments was possible as a result of improved polymer quality. This improved the tenacity up to 0.65 N/tex, modulus to 4–5 N/tex, and decreased extensions below 25 %. In the 1990s, different types of PEEK filaments have been further developed, and the filament finesse in the case of multifilaments have been reduced to 3 dtex (20 μm) simultaneously improving the tenacity of the material. [3]

2.2.3. Uses

Due to the high price of PEEK, the commercial applications are currently limited, yet rapidly expanding, and located mainly in the niche market sector. PEEK filaments can be woven to fine screens and used in frame filters which are used for example for the production of board products. PEEK monofilament braids are used in aerospace, automotive and industrial applications. Conveyor belts made of PEEK are used in many industrial sectors. PEEK-based medical products have been developed as non-metallic alternatives, one example being braiding for catheter shafts. PEEK is used in the wiring of robotics in nuclear installations where typical thermoplastics would degrade too rapidly due to the gamma radiation. PEEK multifilaments are used to reinforce synthetic rubber gaskets and bellows. They are also used in industrial bristles, protective clothing, tennis racket strings, music strings, and thermoplastic composites. [2, 3, 20, 21]

3. Demanding conditions

"Demanding conditions" is an inaccurate expression. In this study the demanding conditions for PEEK fibres are chosen to be very small fibre size, maximum recommended use temperature, photo-irradiation, and situations where antimicrobial properties would be desirable.

3.1. Fine filaments

3.1.1. Fibre size reduction

There has been variation on the definitions and terminology of thin fibres [22]. Fourne defined microfilaments to have single filament titers between 0.3 and ca. 1.1 dtex [4]. Below 1 dtex fibres (9 µm for PEEK) are called as ultra-fine filaments [19] and below 0.1 dtex they are sometimes referred to as super ultra-fine fibres [22]. Golzar defined fine PEEK filaments, similar to those manufactured in this study, to have fibre diameter of 10–30 µm [23].

Spinning and texturizing processes for microfilaments were developed around year 1990. The spinning machines are fairly similar to those used for conventional filaments but certain aspects have to be taken into account in the case of microfilaments. According to Fourne, these aspects are very clean and homogenous polymer, absence of dead spots and short residence time, very good polymer filtration with minimal time variation, filter finesse, higher melt temperature than for standard filaments, larger capillary hole distances, shorter quench and lower airflow rate, spin-finish applicator soon after the quench, reduced POY (partially oriented yarn) spinning speed, short yarn path, correctly optimized traverse for winding, yarn wind up tension, good and uniform intermingling, and filament titer before drawing of. [4]

Since changing the processing parameters is much easier than the configuration of the melt spinning equipment or the material quality, the parameters are in key role to further improve the spinnability of polymer fibres. It is useful to understand the difference between limit of spinnability and spinning stability. Stability is investigated in connection with time whereas spinnability is independent of time. Spinnability can be defined as the limits to which satisfactory spinning condition can be achieved. [23] Optimization of the process is needed when smaller and smaller fibre diameters are aimed at. Ziabicki was the first to state the six processing parameters affecting spinnability in the melt spinning process: processing temperature, dimensions and the number of spinneret holes, mass throughput, length of the spinning path, take-up velocity and cooling conditions [24].

3.1.2. The effect of processing parameters

Literature data suggests that to improve spinnability, a high processing temperature should be used [4, 23]. However, processing temperature cannot be raised endlessly due to the thermal degradation of the material. The melting point of PEEK is 343 °C and recommended processing temperature 360–400 °C [18]. According to a previous PEEK melt spinning study, using a processing temperature of 400 °C reduces spinning line breakages compared to lower temperatures and the stability of time variation variables also improves [23]. Higher processing temperature enlarges the solidification length, decreases internal stress, and possibly even improves the structure formation.

The number of spinneret holes can vary from one (monofilament) to tens of thousands in the case of staple fibres. The spinneret holes can have various shapes, round being the most common. In round hole spinnerets, the hole diameter can vary from 0.04 mm to over 1 mm, L/D being typically 1–20 [4]. To improve the spinnability, the control of die swell has an important role. Die swell is a long-known

phenomenon where polymer mass swells after the capillary causing irregularities to fibres. High L/D ratio has shown to decrease die swell, thus being preferable close to the spinnability limit [25]. An early melt spinning study indicated that increasing the diameter of the capillary would decrease the number of failures [26]. In Golzar's study the stable melt spinning conditions were tested alternating the mass throughput and diameter of the holes [23]. The effect for lowest spinnable fibre diameter cannot be obtained from the data but increasing the hole diameter increases the draw down ratio (v_l/v_0). As a concluding remark of the literature, the capillary should be long and large to improve spinnability.

The filaments are usually cooled in vertical tubes preferably below the T_g of the polymer. Initially, the length of the spinning path was 4–8 m when only relative movement of air was used. In 1956, the cross flow quenching zone below the spinneret started to become more common to reduce costs and improve the fibre quality. The minimum length was reduced to 2–3 m at a spinning speed of 6000 m/min, 1.3 m at a spinning speed of 1800 m/min, and 0.4 m at a spinning speed of 40–50 m/min [4]. The spinning path length should be long enough for the filaments to solidify. The maximum spinning path length is limited by the spinning path stress the filament can withstand without breaking. Air friction increases the filament stress almost linearly as a function of the spinning path length [24, 27]. Tests with PEEK indicate that the spinning path length should be as short as possible [23]. According to this study, a long spinning length increases the fibre speed in two steps. The first corresponds to the conventional melt spinning, and the second to either plastic or elastic deformation. Long spinning path increases the stress at the solidification point and the maximum speed gradient also increases. Additional heating tube after the spinneret has not shown to improve the stability of PEEK melt spinning [23].

Take-up velocity of a commercial melt spinning line is nowadays 6000–8000 m/min and the tendency is towards 10 000 m/min [4]. If the mass throughput remains constant, higher take-up velocity evidently leads to a decreased fibre diameter. Almost a linear correlation has been found between the take-up velocity and the spinning line stress [24]. The drag force increases and as a result the rheological force and induced filament stress increase as well [23]. At a certain point this causes necking and finally filament breakages. The general recommendation is to reduce the spinning line speed in case of fine filaments [4] even though PEEK fibres have been spun under relatively high spinning speed [23].

Very low mass throughputs are required to spin fine filaments. Ultra-fine 0.1 dtex PEEK monofilaments have been produced with a piston-based system using a mass throughput as low as 15 mg/min [19]. In order to produce fibres this small, the mass throughput has to be very constant. According to the equation of continuity, the filaments will break unless: [24]

$$Av_l\rho = Q = \text{constant}$$

Where A is the cross-sectional area of the fibre, v_l take up-velocity, ρ density, and Q mass flow of the polymer. Previous studies have shown that decrease in the mass throughput also decreases the maximum take-up velocity [23].

3.2. Photodegradation

Ultraviolet (UV) light is a part of electromagnetic spectrum (100–400 nm) comprised of photons. UV radiation is divided into three categories based on the wavelength: UV-C 100–280 nm, UV-B 280–320

nm, and UV-A 320–400 nm. The solar spectrum maximum is in the visible region of light, approximately at 500 nm, and therefore the UV-B radiation contributes typically less than 1% and UV-A 6-7% of the solar spectrum at the Earth's surface. [28] The short wavelength UV-C radiation is the most harmful of these but fortunately it is filtered almost entirely by the atmospheric oxygen (<240 nm) and ozone (<280 nm). Some of the UV-B radiation is filtered as well, which explains the lower levels of radiation compared to UV-A measured at the Earth's surface. [29]

UV radiation has a key role in polymer degradation even though it is not the only environmental factor ageing polymers [30, 31]. Photoageing is usually iniated by solar UV radiation, air or pollutants. Factors like water, organic solvents, temperature or mechanical stresses can accelerate the process. The polymer macromolecule is activated by the absorption of a photon, which can lead to a formation of free radicals. The secondary process follows this primary process where free radicals initiate number of side reactions, which are independent of the light. [10] Typical chemical groups in polymer structure like C-C, C-O, C-H, or C-Cl do not absorb light wavelengths longer than 190 nm [31]. The explanation for polymers to absorb radiation is the chromophores they contain. These chromophores can be divided into two groups. The group A chromophores are impurities in the polymer chain or low molecular external impurities originating from the polymer processing. The group B chromophores are a part of molecular structure of the polymer. [5, 31] PEEK belongs to the group B as the chromophoric groups in the polymer structure extend the light absorption up to almost 400 nm [32].

In polymer fibres the degree of crystallinity is often high. Crystalline regions have very little free volume below T_m so the free volume is located only in the amorphous regions. Most photochemical reactions can occur only in the amorphous region because of rigidity of the crystalline lattice, possible delocalization of the excitation through the crystal, the lack of free volume imposed by the rigidity of the crystal lattice, and the lack of oxygen in the crystalline lattice. [10, 31].

Photodegradation affects the molecular weights (M_n and M_w) and molecular weight distributions (M_w/M_n) of polymers through two competitive processes, chain scission and crosslinking. If the chain scission tendency is dominant, both M_n and M_w/M_n decrease, and if the crosslinking is dominant the polymer eventually forms a network at the same time as M_w and M_w/M_n increase. [10, 31] Among these options, PEEK has the tendency to crosslinking during photodegradation [6].

It has been estimated that half of the plastics produced annually are employed outdoors [10]. Degradation limits a typical lifetime of an outdoor plastic product to a few months or years. The UV degradation can be observed as discolouring (yellowing), embrittlement, loss of mechanical properties and as a result a significantly shortened lifetime of products which can cause great economic losses [33–36]. In many cases, the first step leading to weathering related failure is the formation of brittle surface layer. In photo-oxidative ageing the surface is affected the most because the intensity of the UV radiation is the highest on the surface and there is sufficient amount of oxygen available. [31] Like previously mentioned, fibres have high area/volume-ratio which is likely to be an accelerating factor in degradation.

Typically, polymers are protected against UV and heat with various stabilizers [5]. However, most UV and heat stabilizers cannot be used with PEEK due the high processing temperatures needed. The largest PEEK provider, Victrex, is not currently selling any PEEK grades with UV- or heat stabilizers [18]. Therefore, the function and properties of different stabilizers are not further treated in this thesis.

3.3. Thermal degradation

The amount of thermal degradation depends on the polymer structure, temperature and presence of oxygen. Oxygen is crucial for the degradation processes, and in the absence of it, most polymer systems are relatively stable. [5] The thermal stability is related to chemical bonds in the repeating unit of the polymer: the stronger the bonds the better is the stability. PEEK has three aromatic rings in the repeating unit and these rings are known to have excellent stability.

Thermal degradation may be classified into three groups at high temperatures: depolymerisation reactions where low molecular weight components similar in the structure of the polymer are scissioned from the polymer, elimination reactions where low molecular weight components unrelated to the original polymer (like H_2O) are formed, or substituent reactions where chemical nature of the repeat unit is changed even though the chemical structure remains intact. In the presence of oxygen most polymer systems undergo chain scission reactions below their T_m point due to reactions of macroradicals with oxygen. These reactions will produce unstable hydroperoxides that break down and form more free radicals accelerating the degradation process. The most prevalent oxidation products in polymers are carbonyl and hydroxyl groups. The formation of these groups can easily be followed with FTIR and corresponding wavenumbers 1710 and 3400 cm^{-1}. [5]

Thermal degradation is similar to photodegradation in many respects. Both degradation mechanisms include initiation, chain propagation, chain branching, and termination steps. The main differences occur in the initiation step: in thermal degradation initiation results from the thermal dissociation of chemical bonds in macromolecules and in photodegradation from the photodissociation (singlet or triplet states). Both degradation types can also be initiated by the presence of external free radicals from impurities, additives or photoinitiators. [31] Because of the similarities in degradation mechanisms, the effects on material properties are also fairly similar.

Presence of oxygen is crucial for degradation of PEEK that is tested to be relatively stable in nitrogen atmosphere. High temperature oxidative environment has shown to cause chain scission and crosslinking reactions in PEEK. Chain cleavage is suggested to occur adjacent to carbonyl functional groups and the following hydrogen abstraction to crosslinking between aryl rings. [37] Therefore, crosslinking behaviour is dominant in PEEK in both degradation types, thermal- and photodegradation.

3.4. Sulfonation of PEEK to provide functional properties

PEEK can be modified by sulfonation reaction to provide functional properties. In this context, functional equals antimicrobial, self-cleaning and antipollution properties achieved by photocatalytic reactions. The repeating unit of PEEK contains benzophenone (BP). These BP chromophoric groups are commonly used as photosensitizers in photochemistry to provide functional properties [11–13]. When BP is exposed to UV radiation, a light-excitation from n to π* triplet states occurs [12]. This photo-irradiated BP is highly reactive to abstract a hydrogen atom from a suitable hydrogen donor such as amine or alcohol to form a stable benzophenone ketyl radical (BPK). This radical is then capable of decomposing organic substances, which leads to functional properties. [11]

The problem with PEEK is that it cannot generate BPK radicals in its native state but modification with e.g. sulfonate groups is required [14]. In the sulfonation of PEEK one hydrogen atom is replaced by SO_3 group. Nowadays, sulfonation of PEEK is a standard procedure and the effects of different processing parameters are well known [38–40]. The degree of sulfonation is shown to increase by

increasing processing temperature or -time. After modification, SPEEK is able to abstract the hydrogen atom after light excitation. Without modification the process would be suppressed by the competitive ESIPT (excited state intramolecular proton transfer) reaction leading to loss of photoreactivity [41–43]. In ESIPT, the proton is not obtained from outside (intermolecular) but instead it moves intramolecularly. The excitation reaction and radical formation of SPEEK are presented in Fig. 3.

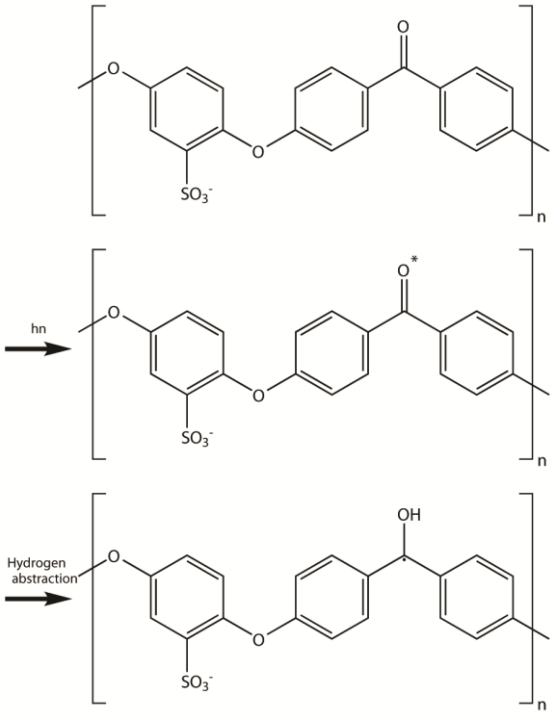

Fig. 3. Excitation reaction and radical formation of SPEEK. *Publication V*.

In order to this reaction to work, a proper hydrogen transfer agent is needed. Polyolefins such as polypropylene (PP) and polyethylene (PE) have a labile hydrogen atom in their polymer chain, which can be used in the transfer reaction. In addition, polyolefins are largely available, inexpensive, and easy to process with conventional methods. SPEEK has been previously blended in solution with polymers such as polyvinyl alcohol (PVA) and polyvinyl butyral (PVB) to be used as a direct methanol fuel cells [44, 45], metal reduction material [46, 47] and for the production of functional thermoplastic materials such as advanced composites [48]. However, the idea to mechanically compound SPEEK with polyolefins is relatively new.

So, in theory, compounded SPEEK/PP blend would have functional properties. However, there are several requirements for the industrial success in textile use. First of all, the blend should be spinnable. For this, the particle size of SPEEK in the blend should be small enough because studies have shown that when the particle size approaches the fibre diameter the spinnability reduces drastically [49]. The second requirement is that the photocatalytic efficiency of the fibre is good enough for the products it is used in. The third requirement is some kind of competitive advantage against current products. This could be price but it could be safety as well. TiO_2 blends, which would the main competitor of this product, often contain nanoparticles. The particle size is reduced to a nanoscale to increase efficiency [50]. However, the safety of the nanoparticles is under investigation and according to current knowledge, TiO_2 nanoparticles are possible carcinogenic to humans [51].

4. Aims of this study

This study concentrated on PEEK-based polymer fibres in demanding conditions. The main research questions were: what occurs when PEEK-based polymer fibres are pushed to the limit and how can these limits be moved further? This study has been divided into three parts, each of which having own more specific research question:

- **Publication I**: What are the effects of different processing parameters on the spinnability of PEEK monofilaments?
- **Publication II, III**: How does photo- or thermal ageing affect PEEK fibres?
- **Publication IV, V**: Is it possible to modify PEEK so that it would provide antimicrobial properties based on photocatalysis?

As described in Fig. 4, the study has been divided into three parts, each of which having the same object: increase knowledge and improve the properties of PEEK-based fibres and thus create new application possibilities and safer products.

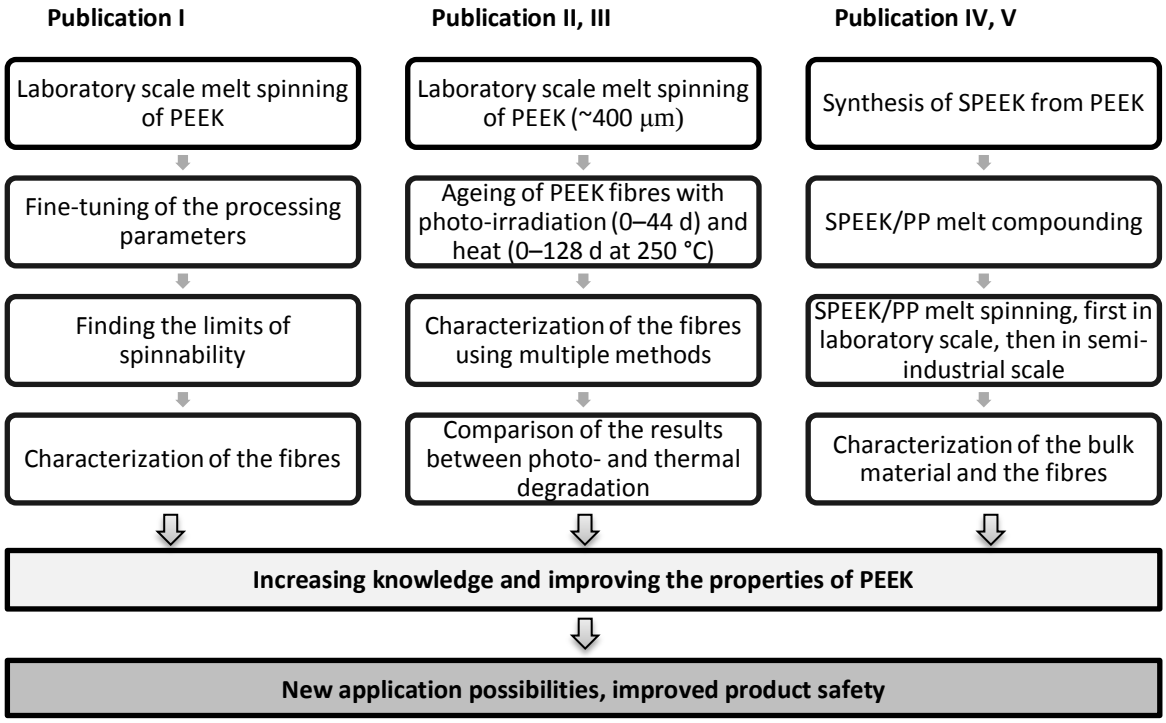

Fig. 4. The process chart in this study to improve the properties of PEEK fibres.

The scientific contribution of this thesis is:

- Generate deeper understanding regarding the relationship between processing parameters and the best spinnable (PEEK) fibre diameter.
- Age PEEK fibres using photo-irradiation and heat, characterize the samples with wide range of methods, and compare the results.
- Manufacture and characterize totally new photocatalytic fibres based on the blend of SPEEK/PP.

5. Experimental procedures

5.1. Materials

Victrex PEEK grade 151G was used in *publications I, II and III*, and powder form Victrex PEEK 704 in *publications IV and V*. Victrex PEEK grades 381G, 450G and powder grade 704 were also briefly tested in *publication I* before choosing the grade 151G. PEEK sulfonation in *publications IV and V* was performed according to the generally accepted processing parameters by a partner company Next Technology Tecnotessile. 98% sulphuric acid was mechanically stirred with powder form Victrex PEEK 704 in 250 ml reactor for 3 h at 45 °C. The obtained SPEEK was then precipitated by dropwise addition of the solution to 500 ml of ice-cooled distilled water. The precipitate was washed until the excess acid was removed and then dried in an oven at 70 °C for 12 h.

5.2. PEEK compounding

Laboratory scale compounding. SPEEK/PP laboratory scale compounding in *publications IV and V* was performed using a DSM Xplore micro compounder with a counter rotating double screw. The maximum batch size for this compounder is 5 ml. The materials were weighted, loaded into the compounder and mixed for 5 min at 200 °C at a screw speed of 150 revolutions per minute (RPM).

Semi-industrial scale compounding. SPEEK/PP semi-industrial scale compounding in *publication V* was performed using a Brabender W50 single screw extruder. The material was repeatedly processed four times to get a homogenous compounding quality. Processing temperature of 200 °C and screw rotation speed of 30 RPM were used.

5.3. PEEK melt spinning

Laboratory scale melt spinning. PEEK laboratory scale monofilament melt spinning was based on a modified Göttfert Rheograph 6000 capillary rheometer. It is a piston-based system with a maximum processing temperature of 400 °C and volume of 26 cm^3. In *publication I*, different processing temperatures, capillary diameters, cooling lengths, and piston speeds were tested to find the limits of spinnability. Optimal tested processing parameters were Victrex PEEK grade 151G, 400 °C processing temperature, 5 cm cooling length and 30/1 mm capillary when using draw velocity of 100 m/min. Lowest achieved spinnable mass throughput using these parameters was 0.031 g/min. *In publications II and III* this same setup was used without a spinning motor so that the fibres were drawn by gravity. This provided very stable fibre diameter of 410 ± 10 µm. The used processing temperature was 380 °C, capillary size 30/1 mm, and mass throughput 5.5 g/min. In *publication V*, the optimal processing parameters of *publication I* were used, except the processing temperature was tested between 180 and 220 °C and the mass throughput was higher.

Semi-industrial scale melt spinning. The semi-industrial SPEEK/PP melt spinning in *publication V* was performed in a Fourne melt spinning system comprised of a single-screw extruder system with a filament count of 10. The used die size was 8/0.5 mm, screw rotation speed 57 RPM, drawing speed 250 m/min, winder traverse 198 1/min, and spinning path length 4.8 m

5.4. Ageing of PEEK fibres

Photoageing. The PEEK fibre photodegradation was studied in *publication II*. The UV irradiation chamber, size of 1260 x 710 x 450 mm, is equipped with four Q-Lab UVA-340 fluorescence lamps with peak intensity at 340 nm. Irradiance of the UVA-340 lamps corresponds well with sunlight in the critical

short wavelength region [52]. The oldest lamp was changed every 400 h so the total working life of the lamps was 1600 h. The UV irradiation chamber was characterized by the Finnish meteorological institute using Bentham DM150 double-monochromator spectroradiometer equipped with measurement head UV-J1002 from CMS Schreder. The chamber was symmetrically divided into nine measuring points and the average of these was used. The focal plane of the measurement head was approximately at the height of 16 cm from the bottom. The dose rate at the UV-B range (290–315 nm) was 0.7 W/m^2, at the UV-A range (315–400 nm) 12.1 W/m^2, and at the visible range (400–600 nm) 3.1 W/m^2. For the UV irradiation tests, PEEK fibres were cut and taped to a 600 x 400 mm frame. PEEK samples were kept in the chamber for 0, 144, 384, 720 and 1056 h so that both sides of the samples were irradiated for the same amount of time. The corresponding total doses were 0, 8.25, 22.0, 41.3 and 60.5 MJ/m^2. Temperature of the UV chamber was 33 °C.

Thermal ageing. Thermal degradation of the PEEK fibres was studied in *publication III*. The samples were aged using a modified Ahma GO600 oven. The original temperature controller was replaced with an Omron E5CN control unit and a PT100 platinum resistance thermocouple. The annealing conditions were kept stable at temperature of 250 ± 0.1 °C during the artificial ageing process. The samples were attached to a horizontal grill attached on the same level as the thermocouple. The aged fibres were cut from the grill so that the fibres in close contact with metal were discarded because the high thermal conductivity of the grill results to accelerated ageing.

5.5. Characterization

Mechanical testing. The mechanical testing in *publication I* was performed according to the standard ISO 5079:1995 with Lenzing Vibroskop and Vibrodyn. Instead of the recommended 50 measurements, only 20 were done because of the difficulties in the measuring procedure of the synthetic PEEK fibre. First, the Vibroskop was used to determine the fibre fineness number and then the same fibre was stretched until breaking with Vibrodyn. In *publication II*, the tensile testing of the fibres was made with an Instron 5967 according to the standard ISO 5079:1995. The initial length was 20 mm and the drawing rate 20 mm/min. Instead of the recommended 50 measurements, only 10 samples per irradiation time were measured due to the long duration of the testing procedure. The modulus was calculated by the software using linear regression techniques according to the standards EN10002 and ASTM E8. Tests were made with a 2 kN force cell. In *publication III*, similar testing procedures were used as in *publication II* except the initial length was increased to 50 mm and 15 samples were measured. In *publication V* the testing was performed by Next Technology Tecnotessile. These tests were performed according to the ISO 2062 standard using an ADF Brustio Tessile tensile testing machine. A 200 mm clamping length and 1800 mm/min drawing speed were used. A total of 10 measurements per sample were made. Young's modulus was calculated in 0–10% strain. Prior to the mechanical analyses, these samples were conditioned at 20 °C and humidity of 65% for 24 h.

Differential scanning calorimetry (DSC). DSC tests in *publications I, II,* and *III* were carried out with Netzsch DSC 204 F1 heat-flux DSC. PEEK was heated from room temperature to 400 °C, then cooled down to room temperature and then heated again to 400 °C. The heating/cooling rate was 20 °C/min. Number of parallel measurements in *publications I, II,* and *III* were 1, 5, and 2, respectively. DSC tests in *publication IV* were made by NTT with a Mettler Toledo 822 e. Samples were heated in 80 ml/min nitrogen flux at a heating rate of 10 °C/min but only once due to the degradative behaviour of SPEEK at higher temperatures.

Thermogravimetric analysis (TGA). TGA measurements in *publications I–IV* were recorded with PerkinElmer TGA 6. The samples were heated in nitrogen atmosphere (*publications I, II,* and *IV*) and in air atmosphere (*publications II* and *III*). The heating rate was 10 °C/min in *publications I–III* and 20 °C/min in *publication IV*. The degradation onset temperature in *publications II and III* was defined as the intersection point of the extrapolated baseline and the tangent of the inflection point.

Fourier transform infrared spectroscopy (FTIR). FTIR spectra in *publications II and III* were measured with a Bruker optics tensor 27 using ATR (attenuated total reflectance) mode. Samples were tested between 400 and 4000 cm^{-1}, using 16–32 measurements and a resolution of 4 cm^{-1}. Measurements were made using 4 parallel fibres and the average of 3–5 measurements was used to minimize errors. The data was baseline corrected using the average absorbance of 3800–4000 cm^{-1} as a reference. The carbonyl index was calculated as the ratio of the aged and unaged peak intensities at 1716 cm^{-1} (*publication II*) and 1740 cm^{-1} (*publication III*). To calculate the peak areas for the crystallization measurements in *publication II*, the baseline corrected FTIR data was integrated using OPUS software. ATR-FTIR spectrum in *publication IV* was measured by Next Technology Tecnotessile with Perkin Elmer Spectrum One spectrometer in HATR reflection mode. A zinc selenide crystal and a resolution of 4 cm^{-1} were used.

Capillary rheometer. Capillary rheometer tests in *publication I* were made with Göttfert Rheograph 6000 capillary rheometer. A 30/1 mm capillary, 140 MPa pressure sensor, and processing temperature of 365–400 °C were used. Test runs were carried out from low to high shear rates and then back and the results were corrected using the Rabinowitsch correction.

Rotational rheometer. Rotational rheometer tests in *publications I–IV* were carried out with Anton Paar Physica MCR 301 using 25 mm plate-plate geometry and nitrogen atmosphere. In *publication I*, the constant shear rate measurements were performed from low to high shear rates. In *publications II–IV*, oscillatory shear measurements were carried out using angular frequency range of 0.1–562 rad/s and decreasing frequency. In *publication IV* the time dependence of viscosity was tested using constant angular frequency of 10 rad/s, strain amplitude of 10% and measuring time of 30 min.

Scanning electron microscope (SEM). A Philips XL30 scanning electron microscope was used to investigate the morphology of PEEK, SPEEK/PP, and PP in *publications I-V*. The samples were gold sputtered before investigations. 15 kV accelerating voltage was used in the tests.

Optical microscope. A conventional optical microscope was used in *publication I* to measure the fibre thickness at 1000x magnification. A bunch of fibres was spread onto the microglass plate, and by using the microscopes rotating measuring scale the filament diameter was read. The diameters of total of 60 individual fibres were measured to ensure reproducibility.

UV-Vis. UV-Vis diffuse reflectance spectra in *publication III* were measured with a Shimadzu UV-3600 UV-Vis-NIR spectrophotometer and ISR-3100 integrating sphere. All spectra were recorded in the wavelength range of 350–750 nm.

Nuclear magnetic resonance (^{1}H-NMR). The ^{1}H-NMR spectra in *publication IV* were recorded using a Bruker 200 MHz spectrometer. The spectra were recorded at 60 °C, without internal standard and using deuterated dimethyl sulfoxide (DMSO-d6) as a solvent, with a polymer concentration of about 30 mg mL^{-1}. Experimental data were elaborated with the 1D Win-NMR software, applying the Lorentze

Gauss enhance function and using appropriate Line broadening and Gaussian broadening parameters in order to improve the resolution of the peaks. These measurements were performed by the University of Siena.

Electron paramagnetic resonance (EPR). EPR spectroscopy in *publications IV* and *V* was used to confirm the free-radical characteristics of the photoactive species. Continuous wave (CW) X-band (9 GHz) EPR measurements were carried out at room temperature on a Bruker E500 ELEXSYS Series, using the Bruker ER 4122 SHQE cavity. The sample was placed into a 4.0 mm ID Suprasil tube, exposed to UV irradiation generated by a UV lamp (effective irradiative power of 8 W/m^2 in the range of 390–490 nm) at a distance of 11 cm for 15 min. Then the specimen was immediately measured by EPR spectroscopy. In *publication V*, the fibres were also measured repeatedly for a total of 10 times. The 24 h measuring cycle consisted of 15 min irradiation, immediate measurement and a waiting period. The relative radical amount was calculated from the EPR peak areas by a double integration of the signal, centered at $g = 2.0035 \pm 0.0003$ with a narrow scan of 50 G avoiding Mn(II) contribution. These measurements were performed by the University of Siena.

6. Results and discussion

6.1. Melt spinning of fine PEEK fibres

6.1.1. Fibre size reduction

Reducing the size of PEEK filaments is desirable in many kinds of applications. PEEK is increasingly used in medical product, often as carbon fibre reinforced composites, but also in a fibre form. PEEK fibres have been developed as guide wires in aortic stenting [53] and braiding material for catheters [21]. Reduced fibre size could open new possibilities for improved medical operations in this huge market sector. In filtration, where PEEK fibres are often used, the benefits of reduced fibre size are apparent, as it would improve the filtration capability. In composite reinforcement the amount of fibres needed depends heavily on the fibre size. When the fibre size approaches the nano-scale only a fraction of the amount of them is needed to provide the same properties as in the case of conventional micro fibres [54].

Material development has improved the properties of PEEK fibres since the 1980s as well as some of the technical innovations in the equipment. Yet, fine-tuning of the processing parameters has remained as an important tool for improving the properties as well as reaching for even smaller diameters. There are a few studies in the literature of melt spinning of PEEK filaments [23, 55, 56]. However, these studies lack information of the effects of processing parameters on a quantitative level. As previously discussed in paragraph 3.1, the effects of different processing parameters are well known on a qualitative level but more information should be received what are the actual effects to the best spinnable fibre diameter. There are several reasons to further develop the melt spinning process and the spinnability of PEEK. Improvements in the spinning process could lead to better mechanical properties of the fibres, decreased fibre diameters, improved process stability and money savings.

6.1.2. Effect of processing parameters

The effect of processing parameters on the spinnability was tested by first estimating the importance of them and then moving from the more important to less important and using the obtained values. The selected order was PEEK grade, processing temperature, capillary dimensions, and the length of the spinning path. The effect of take-up velocity was not tested due to the somewhat inaccurate, analogically controlled, motor unit. Testing of all possible combinations was not possible due to the slowness of the testing procedure. The results of the six different trials are presented in Table 2.

According to the definitions, the goal of these melt spinning tests have the characteristics of both melt spinning stability and limits of spinnability [23]. During the tests, the process was estimated to be stable if the fibre did not break in 60 s. A total of five trials were allowed for each mass throughput and if one of these trials was successful the mass throughput was decreased until the limit was found.

Table 2. The effect of processing parameter on the best spinnable PEEK fibre diameter. Partly modified from *publication I.*

Trial number	1	2	3	4	5	6
Grade	381G	151G	151G	151G	151G	151G
Temperature [°C]	400	400	385	370	400	400
Capillary diameter [mm]	1.0	1.0	1.0	1.0	0.75	1.0
Length of the spinning path [cm]	40	40	40	40	40	5
Shear rate [1/s]	19.0	4.6	4.8	7.9	18.0	4.0
Lowest stable piston speed [mm/s]	0.0165	0.0040	0.0042	0.0069	0.0066	0.0035
Theoretical mass throughput [g/min]	0.15	0.036	0.038	0.062	0.059	0.031
Theoretical diameter [µm]	39	19	19	25	24	18
Theoretical fineness [dtex]	15.4	3.7	3.7	6.5	6.2	3.3

According to the results, the viscosity of the grade has a major effect on the spinnability. The best spinnable fibre diameter of grade 381G is roughly twice as much compared to grade 151G. Since the number corresponds with the viscosity of the grade (Pa.s at 1000 1/s, 400 °C), lower number in the grade indicates better spinnability. Also the processing temperature affects the viscosity of the material and at least partly for that reason the increase in the temperature improves spinnability. On a qualitative level this result was expected [4, 23] but the magnitude was a surprise. 370 °C is between the recommended processing temperature range of the materials, and yet, 15 °C increase in the processing temperature improved the minimum spinnable fibre diameter from 25 µm to 19 µm. Further increase to 400 °C improved the spinnability only slightly.

Testing of capillary dimensions was challenging. Testing was initiated with a 30/1 mm capillary, which is a typical choice for rheological measurements, the main purpose of the equipment. The 30 mm capillary length was the longest possible for this system and therefore the first choice according to the previous literature [4, 24, 25]. It was impossible to use larger capillary diameters since the gravitational self-flow exceeded the required mass throughput of the fibre. Also testing of shorter capillaries caused problems. Due to the structure of the equipment, the capillary hole is inside the barrel when a shorter than 30 mm capillary is used. The air temperature inside this barrel is very high which reduces the viscosity of the material. A high number of fibre breakages occurred when this viscosity reduction was combined with the extreme take-up elongation. Therefore, only 30/1 and 30/0.75 mm capillaries were compared. Between these two, the spinnability was better with the 30/1 mm capillary. When two spinning path lengths, 5 and 40 cm, were compared, small differences were found giving advantage to the shorter length.

6.1.3. Fibre properties

It has to be noted that due to the structure of the laboratory scale melt spinning equipment, the draw down ratio is significantly higher than in the case of conventional extruder melt spinning systems. Multiple godets and cold drawing are used to improve the properties in industrial scale spinning machines and therefore the results in e.g. mechanical properties are not comparable with these laboratory scale spinning tests.

The mechanical tests (Table 3) and SEM micrograph (Fig. 5) reveal that the diameter of the fibres is not constant. For these tests, 25 µm fibres were manufactured using the optimal processing parameters found in trial 6. According to the results, the fluctuations in the fibre diameter have a

significant effect on the elongation at break and Young's modulus. The tenacity of the material, however, is relatively homogenous.

Table 3. Mechanical properties of 25 µm PEEK fibres. Partly modified from *publication I*.

	Fineness [dtex]	Tenacity [cN/dtex]	Elongation at break [%]	Young's Modulus, 1% [cN/dtex]
Average	6.19	2.15	151	19.7
Std. Dev.	2.27	0.24	48	4.9
Maximum	9.90	2.62	218	34.3
Minimum	3.09	1.72	59	13.9

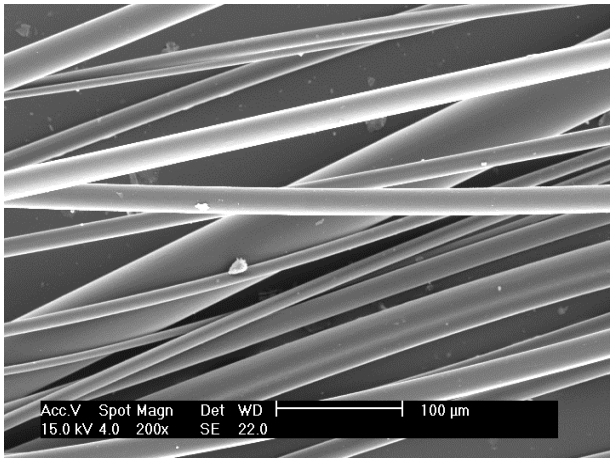

Fig. 5. SEM micrograph of melt spun PEEK fibres. *Publication I*.

6.1.4. Problems, improvements, and benefits

These results indicate that there are certain problems in the equipment that should be solved before manufacturing of finer fibres is possible. There are a few alternative explanations for the non-homogeneity of the fibres: the resonance caused by the old-fashioned spinning motor, unstable mass throughput, or the combination of these two. The size of the capillary is very large compared to the size of the fibre. Drawing reduces the diameter of the fibre very rapidly after a few centimetres from the capillary. When this thinning of the fibre is combined with the absence of proper filtering and gear pump systems of the piston-based equipment and with the small variations in the take-up speed, non-homogeneities in the fibre diameter can be expected.

Reduction in the capillary size is not the solution for this problem since it has a negative effect on the spinnability. Many of the problems observed are related to the structure of the equipment and the removal of them would require a total re-design of the machine. Due to the lack of commercial interest, piston-based melt spinning machines are not that common and many of them are self-built [19]. According to our tests, following aspects should be considered in the piston-based machine to obtain finer filaments: material mixing and filtering before the capillary, accurate and smooth take-up motor, accurate piston movement, wide range of capillaries, controllable air temperature after the capillary, controllable quenching distance, and elimination of quenching turbulence. The smallest fibre parts with this equipment, during a stable process, were approximately 10 µm. At least this level is expected to be achievable if the variations could be eliminated.

When the melt spinning process is upscaled to extruder level, many of these recommendations above are not valid any more. Modern extruder systems have proper filters and gear pumps as well as accurate take-up control and wide range of capillaries to select from. The length of the cooling path is limited by the material solidification and is typically several metres instead of centimetres. However, many of the optimal processing parameters are likely to be transferable from laboratory scale tests to larger scale. On a qualitative level, the results are consistent with previous studies. On a quantitative level, the viscosity control of the fibres is essential. This should be done by first choosing the material grade correctly, and secondly, optimizing the processing temperature. The importance of the die dimensions was larger than expected and should be carefully considered when upscaling the production of fine fibres.

6.2. Under photo-irradiation

6.2.1. PEEK fibres in outdoor applications

It is a well-known fact that most linear polyaromatics, like PEEK, degrade under UV radiation [6, 57, 58]. Considering all the good properties PEEK possesses, photodegradation may be the most significant weakness of it. Because of the chemical structure that involves polyaromatic groups, PEEK absorbs almost all UV radiation of wavelengths under 380 nm [32]. Since the solar spectrum on the Earth's surface starts at 290 nm, a significant amount of photochemical oxidation reactions occurs at PEEK resulting to a formation of new chemical groups that further accelerate the reaction rate of photodegradation.

Even though PEEK fibres are not mainly used in outdoor applications, some of the current products have to withstand UV exposure. A portion of PEEK fibre based industrial bristles, protective clothing, sports strings, conveyer belts, and thermoplastic composites are used outdoor. Since many of the PEEK products have high safety requirements, the degradation would not only be undesirable but also dangerous. No literature has been found of photodegradation of PEEK fibres but the mechanical properties of PEEK photodegraded sheets have been previously tested [6, 58]. According to these tests, PEEK crosslinks readily and this causes embrittlement of the material. In addition to the rapid decrease in elongation, crosslinking reactions also increase the material hardness and yield strength.

UV irradiation studies are often focused on chemical reactions during the photo-oxidation [32, 59–61]. According to the FTIR analysis of photo-irradiated PEEK samples, an increase in the hydroxyl and carbonyl region intensities are observed. New bands at 2954, 2926 and 2854 cm^{-1} in the range of C-H stretching of non-aromatic hydrocarbons and decrease in the intensity of 3067 cm^{-1} peak (assigned to the C-H stretching of aromatic rings) indicate that UV irradiation causes PEEK to loss its aromaticity. One reason for the good thermal properties of PEEK is the structure of it, which contains aromatic groups [5]. Therefore, UV radiation could also affect the thermal stability of PEEK.

More research is needed to study the effects as a function of irradiation time. This would be important when making better estimations of the product lifetime in outdoor conditions. These estimations would be beneficial for wide range of products, not just for fibres. In our research, PEEK fibres have been aged various times and multiple characterization methods have been used. These tests provide new information about the usability of PEEK fibres in outdoor conditions.

6.2.2. Fibre properties

The results in the mechanical tests are presented in Table 4. The mechanical strength and modulus decrease slowly with the irradiation time. The differences are minimal between the pristine and 1056 h aged samples: 6 % in yield strength and 15 % in modulus. According to a previous study, the mechanical strength can even increase at the first due to the solidification of the material [6]. This solidification process evidently occurred at these samples as well since the elongation decreased rapidly. Where unaged PEEK samples are ductile, aged samples have turned brittle. The difference is 96 % between the 0 h and 1056 h samples.

Table 4. Tensile properties of UV irradiated PEEK fibres. Partly modified from *Publication II.*

Time [h]	Yield strength [MPa]	Tensile strength at rupture [MPa]	Elongation at rupture [%]	Modulus [MPa]
0	83.2 ± 2.0	87.6 ± 1.9	311 ± 9	2340 ± 55
144	80.5 ± 1.0	78.6 ± 0.8	173 ± 25	2290 ± 95
384	78.7 ± 1.5	78.0 ± 1.3	137 ± 23	2400 ± 71
720	79.6 ± 1.0	74.4 ± 1.0	49 ± 8	2200 ± 50
1056	77.8 ± 2.0	72.3 ± 1.6	13 ± 1	1980 ± 80

According to Fig. 6, the elongation-time plot is almost a straight line in logarithmic scale. Based on this result, it could be estimated that the maximum working life of these kinds of fibres in this kind of environment is not more than two months (1440 h). The correlation between artificial ageing and natural weathering is difficult but in any case the actual working life in outdoor applications seems to be relatively short considering the high technology nature of PEEK fibres. Also the statistical Weibull analysis for the elongation at rupture data (Table 5) clearly indicates that even a short period of ageing decreases the reliability of the fibre.

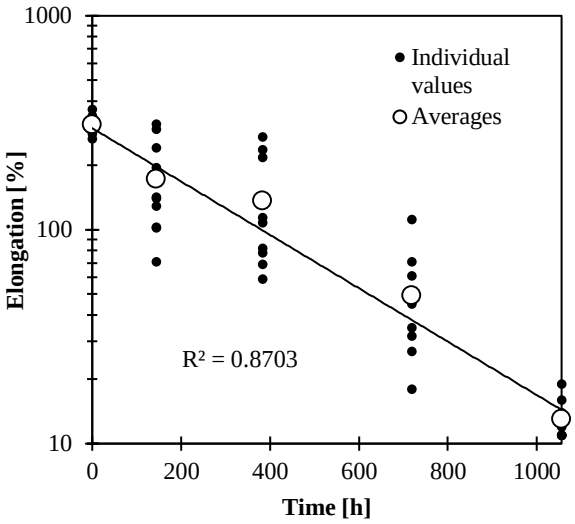

Fig. 6. Elongation of the PEEK fibres as a function of irradiation time. *Publication II*.

Table 5. Weibull analysis for the elongation at rupture data.

Ageing time [h]	0	144	384	720	1056
Samples	10	10	10	10	10
Shape parameter	11.3	1.95	1.93	2.10	3.96
Scale parameter	324	196	157	56.1	14.0
0.05 reliability [%]	357	344	278	95	18
0.10 reliability [%]	349	301	242	83	17
0.50 reliability [%]	314	163	130	47	13
0.90 reliability [%]	266	62	49	19	8
0.95 reliability [%]	249	43	34	14	7

Previous studies have observed hardening of the surface layer at depths under 250 µm [6]. This 250 µm is more than a typical radius of PEEK fibres indicating that eventually the whole fibre is affected by photodegradation. The loss in elasticity is particularly dangerous in applications where fibres are under alternating external stress and the breaking of fibres would cause safety problems.

The chemical properties at the surface of the fibre were measured using ATR-FTIR. Rapid increases in the carbonyl group (maximum at 1716 cm^{-1}) and hydroxyl group (maximum at 3230 cm^{-1}) absorption peaks are observed. In addition, FTIR spectra show evidence that aromatic rings are broken during photodegradation. There occurs a rise of aliphatic methylene group vibrations, in symmetric CH_3-stretching at 2853 cm^{-1} and antisymmetric CH_3-stretching at 2922 cm^{-1}, and lowering of aromatic CH-stretching vibration at 3065 cm^{-1} during photodegradation.

The carbonyl index, probably the most common unit of polymer photodegradation, increases rapidly during the first 384 h (Fig. 7). Carbonyl index seem to be excellent method especially for the early detection of photodegradation. After 384 h the amounts of carbonyl groups on the fibre surface start to saturate. Mechanical tests show that photodegradation does not end at this point but rather moves closer to the fibre centre line.

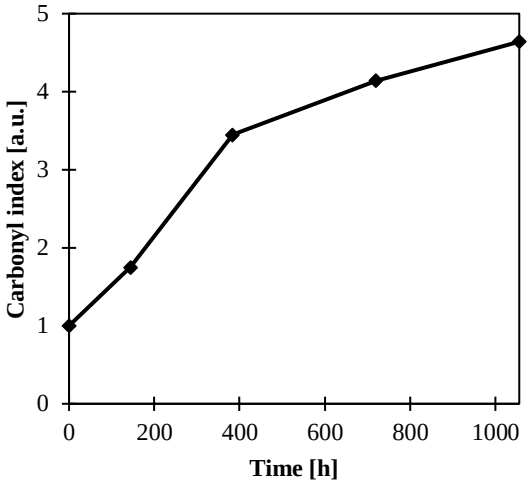

Fig. 7. Carbonyl index of UV irradiated PEEK fibres. *Publication II.*

The formation of new chemical groups on the surface of the fibre does not necessarily mean that the bulk properties are unusable. The properties depend heavily on the sample size and they have to be

reflected to the penetration depth of UV radiation. In case of small diameter fibres, increase in the carbonyl index correlates well with the solidification of the material and decrease in elongation. When the carbonyl index has climbed up to a certain level, the fibre has lost it properties anyway. These results suggest that FTIR could be used as an alternative for mechanical tests to estimate the general usability of the fibres. FTIR is fast and commonly available method and testing of almost any form of samples is possible.

The results of the DSC scans are presented in Table 6. T_m of the samples is 340–343 °C. Increased irradiation time does not change the T_m, and it is therefore considered as poor method to estimate the degradation level. Also the crystallinity of the samples remains unchanged. 36 % crystallinity is relatively high for PEEK but typically fibre form samples have high crystallinity as a result of elongation during manufacturing. T_g increases along with the irradiation time but there is a high variance in the results. If the level of degradation is high, T_g can serve as a directional tool but otherwise thermal tests are inaccurate to estimate the degradation level. UV- or ion irradiation has been shown to increase both the T_{g1} and T_{g2} (the number corresponding to number of heatings) due to crosslinking of the material [62–64].

Table 6. The results of the DSC scans for UV irradiated PEEK fibres. T_{g1}, T_{g2}, T_{m1}, and T_{m2} refer to T_g's and T_m's during the first and the second heating. Partly modified from *Publication II.*

Time [h]	Crystallinity [%]	Tg_1 [°C]	Tg_2 [°C]	Tm_1 [°C]	Tm_2 [°C]
0	36.0 ± 0.5	143.6 ± 0.9	144.7 ± 1.1	342.9 ± 0.4	340.9 ± 0.1
144	36.4 ± 0.3	145.8 ± 0.5	148.4 ± 0.9	342.6 ± 0.2	341.2 ± 0.1
384	35.3 ± 0.4	145.9 ± 2.0	146.0 ± 1.3	342.2 ± 0.1	340.5 ± 0.1
720	35.9 ± 0.3	147.1 ± 1.4	146.0 ± 0.8	342.8 ± 0.1	340.7 ± 0.1
1056	35.4 ± 0.5	149.3 ± 1.3	151.3 ± 2.2	343.0 ± 0.2	340.6 ± 0.2

TGA measurements were performed in air (Fig. 8) and nitrogen atmospheres and they show reduction in thermal stability. Between these two atmospheres, the differences were easier to observe in air. The differences in degradation onset temperatures were only 10–20 °C but depending on the definition of initiation, the difference can be as high as 100 °C between irradiated and pristine samples.

PEEK fibres are more often intended for high temperature rather than outdoor applications. Even though the outdoor temperature is not problem for storage, UV radiation may be. In some applications the fibres may have to withstand, on purpose or by accident, both. In this case the high temperature resistance may be severely damaged by the UV irradiation.

Rheology is typically used to estimate the processability of the material. During the past two decades, rheology has been increasingly used to study the ageing of materials [65–67]. Rheology can detect the changes in molecular weight and molecular weight distribution, which occur through competing chain scission and crosslinking reactions.

The crosslinking of PEEK fibres was evident in the mechanical tests as reduced elongation and in DSC tests as increased T_g. In rheological tests this same crosslinking was visible as steady increase in zero-shear-viscosity and shear thinning behaviour (Fig. 8). Rheology was found to be rather accurate method to study the degree of photodegradation in PEEK fibres. However, it has a few drawbacks that limit the use of it. The samples used in this study have a large fibre diameter, approximately 400 µm. If the fibre size would have been smaller, as much as several kilometres of fibres would have been

required for the measurements. In addition, rheology is not as fast method as FTIR. One measuring cycle took approximately 20–30 min in this case.

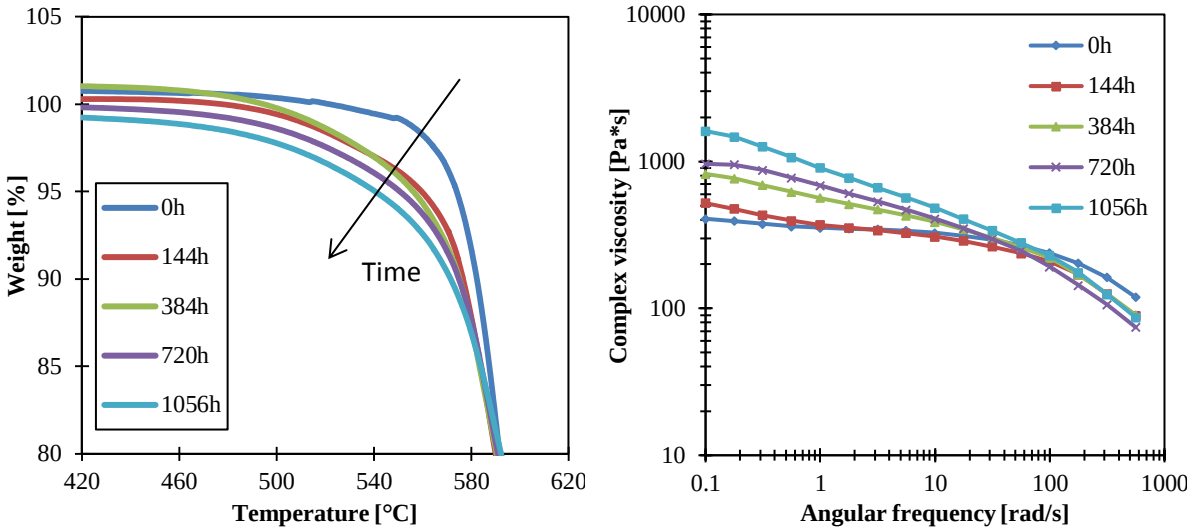

Fig. 8. TGA curve of UV irradiated PEEK fibres measured in air (left), Complex viscosity of UV irradiated PEEK fibres (right). Partly modified from P*ublication II*.

Previously, SEM and optical microscope have been successfully used to estimate degree of photodegradation in PP fibres [68–70]. In theory, cracking of the surface is an expected result since the solidification of the material shrinks the outer layer. This solidification is generally believed to be caused by increased crystallization and reconstruction of the amorphous content in the surface [69, 70].

In PEEK fibres, SEM cannot be recommended as a good method to study the degree of degradation. There are no visible changes in longitudinal samples and only 1056 h aged sample show signs of degradation in transverse breaking surface (Fig. 9). The cracks in the 1056 h aged sample penetrated up to 20 µm depth which is significant compared to a typical size of synthetic fibres.

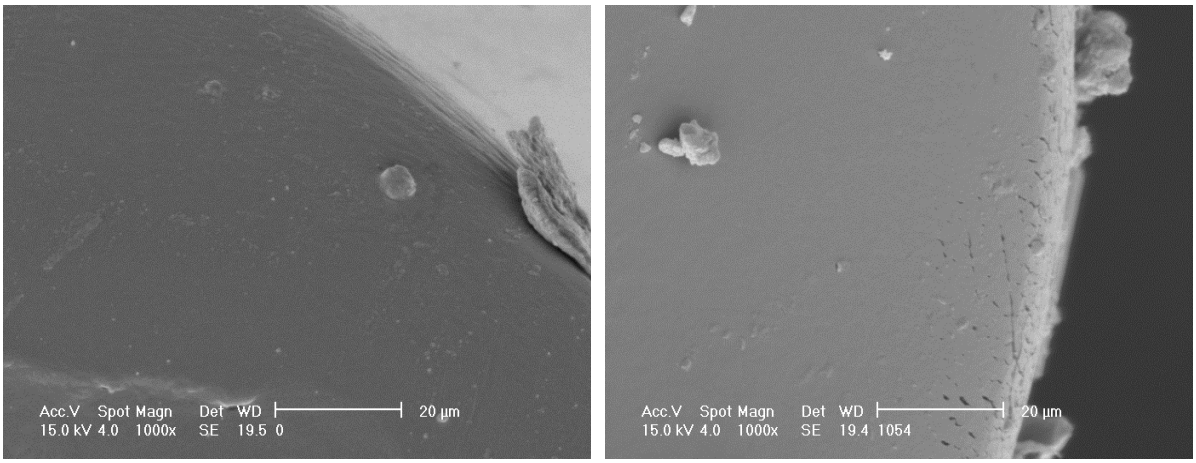

Fig. 9. Transverse SEM micrograph of 0 h (left) and 1056 h (right) photo-irradiated PEEK fibres. Partly modified from *Publication II.*

6.2.3. Benefits of the study

PEEK fibres were artificially aged under UV-light for 0–1056 h. The fibres were then characterized with FTIR, DSC, TGA, rheology, SEM, and mechanical tests and the results were compared. From the results it is possible to state that PEEK is sensitive to UV radiation. Even a few weeks in direct solar light can change the properties of the fibres irreversibly and cause safety problems. A significant amount of crosslinking occurs during the ageing process and this leads to a rapid decrease in elongation and increase in the zero shear viscosity (molar mass). UV irradiation reduces the thermal properties of the fibres and causes solidification of the surface layer. This study provides new information of photodegradation of fibre from samples, photodegradation of PEEK and comparison between different methods.

6.3. Under heat

6.3.1. High temperature applications

PEEK fibres are often used at high temperatures. Protective clothing, automotive applications, space products or industrial bristles may have to face high temperature requirements in use. In bulk products the number of high temperature applications is even greater. Many of these uses include potential risks to users and therefore knowing the high temperature behaviour is essential.

There has been a notable amount of high temperature studies of PEEK with different characterization methods such as FTIR [71, 72], TGA [73–75], mass spectroscopy [76, 77], UV–Vis [78], ^{1}H-NMR spectroscopies [78], DSC [7, 79, 80], Wide Angle X-ray Scattering (WAXS) [79], and mechanical tests [7, 80–82]. These studies include both short- and long-term material testing as well as characterization of the decomposition products. However, the comparison of results between characterization methods has been limited and, according to the best knowledge, no systematic studies regarding PEEK fibre thermal degradation have been published. Testing of fibre form samples is interesting due to the previously described facts: high degree of orientation, high crystallinity, and small sample size. In this study PEEK fibres, similar to photodegradation study, are aged various times in 250 °C. The fibres are then characterized and the results are compared. Usually many age-related phenomena operate simultaneously and/or interactively. However, the continuous use temperature of PEEK is so high that outdoor degradation due to heat is estimated to be negligible compared to UV. On the other hand, elevated temperature close to 250 °C rarely involves UV. Therefore, the cooperative action of heat and UV is not studied in this thesis.

6.3.2. Fibre properties

Even though thermal exposure is typically considered as harmful to plastics, this is not always the case. Annealing of PEEK is performed by heating it between the T_g, 143 °C, and T_m, 343 °C, for various times. This type of heat treatment for PEEK has been studied since the 1980's. Typical annealing conditions are 40 h at 250 °C according to manufacturer's recommendations [7]. Annealing has been reported to have many positive effects on the fibre morphology and properties. Annealing improves the mechanical properties [7, 80], increases the crystallinity [7], and changes the crystal morphology [8, 9, 80]. Previous TEM micrographs have revealed that PEEK has two populations of crystals [83] and according to previous DSC scans, annealing increases the size of these crystals [80].

In previous studies, these secondary crystals have been visible in DSC scans at a temperature slightly over the annealing temperature [80]. In this study, the secondary peak becomes visible in the least aged 1 d sample (Fig. 10). The location of this secondary peak moves slowly towards the primary peak.

Between 32–64 d the primary melting peak starts to shift to lower temperature and at 128 d the two peaks merge. The first heating in the DSC scan resets the thermal history of the material thus removing the secondary peak.

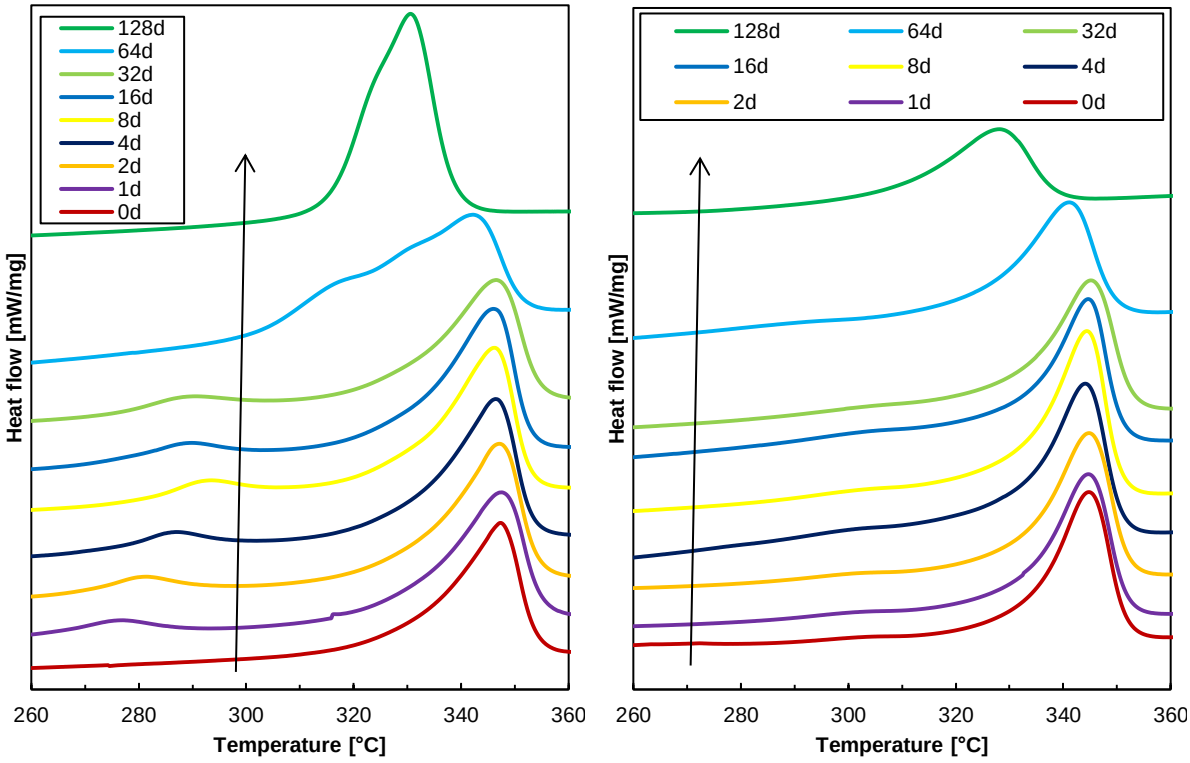

Fig. 10. DSC traces of thermally aged PEEK fibres. First heating (left) and second heating (right). Partly modified from p*ublication III*.

T_m of the material is relatively stable until 32 d after which it starts to drop rapidly (Fig. 11). By 128 d of ageing, T_m has dropped by 15 °C suggesting that a significant amount of degradation has occurred in the bulk of the fibres. Typically, most photochemical reactions occur at the amorphous regions of the material [10, 31]. However, the decrease in T_m is estimated to be caused by the reduction in the crystal content due to thermal degradation [78, 79]. The continuous growth and perfection of the secondary crystals in the amorphous regions of the material is evident in the DSC thermograms as well as in the earlier literature [79, 84]. In principle, this growth can continue until the amorphous regions are totally consumed [85]. Decrease in T_m is slightly visible in the 64 d sample and clearly visible in the 128 d sample. This decrease in T_m in the 128 d sample combined with the overlapping of the primary and secondary peak melting endotherms indicate that the amorphous regions are well filled with the secondary crystals but the (primary) crystals has started to show signs of degradation.

The formation of secondary crystals is clearly visible in the T_g. Already the first day of ageing increases T_{g1} from 148 °C to 164°C (Fig. 11). These secondary crystals presumably lead to changes in the amorphous portions of the fibres and cause crosslinking induced tensions. On the other hand, increase in T_{g2} becomes visible roughly at the same time as changes in T_m, between 16 d and 32 d samples. According to previous studies, this change is caused by crosslinking induced decrease in the molecular mobility [6, 62]. The latter study claims that if both the T_g and Young's modulus are increased simultaneously, this can only be justified by the material crosslinking. The crosslinking of the material is later verified by the rheological measurements and increase in the Young's modulus by the mechanical tests.

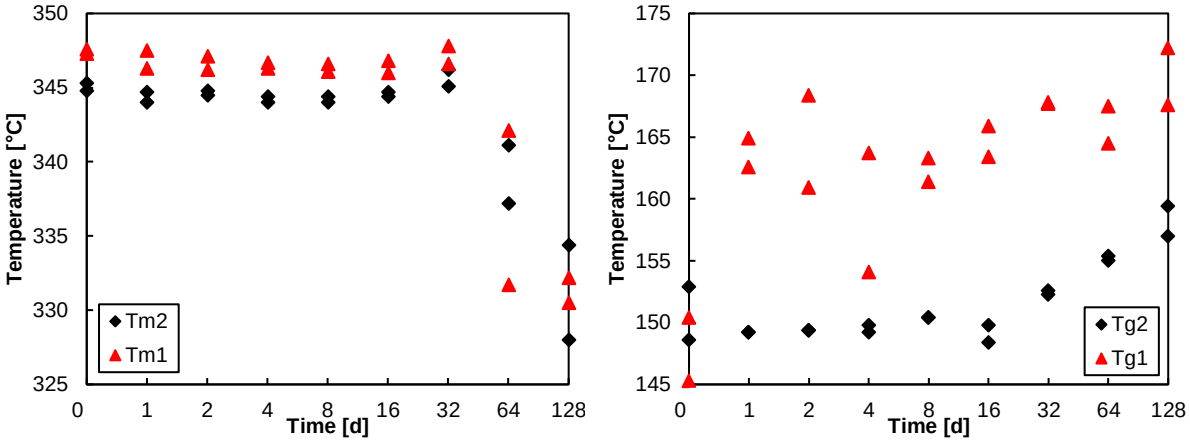

Fig. 11. Melting temperature (left) and glass transition temperature (right) of thermally aged PEEK fibres. T_{m1} and T_{g1} during the first heating and T_{m2} and T_{g2} during the second. *Publication III*.

The changes in the FTIR spectrum, like the formation of the carbonyl and hydroxyl group absorption bands, are similar to photodegradation study but smaller in magnitude. The rise in the carbonyl index is presented in Fig. 12. In thermal degradation study the peak intensity maximum is located at 1740 cm^{-1}, which is different from the photodegradation study peak intensity maximum of 1716 cm^{-1}. This result indicates that the degradation route is different between thermal- and photodegradation. Hydroperoxide mechanism [86, 87] is typical for aliphatic polymers and general thermal degradation but the differences in peak intensity maximums illustrate that photodegradation of PEEK is likely to occur with a different mechanism.

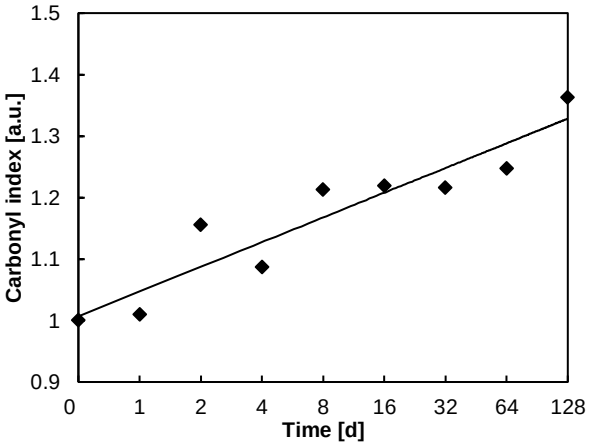

Fig. 12. Carbonyl index [1740 cm^{-1}/1740 cm^{-1} (t = 0)] of PEEK fibres aged at 250 °C. *Publication III*.

The good thermal stability of polymers is linked to aromatic groups in the molecular structure [5]. The repeating unit of PEEK includes three phenyl rings. FTIR tests show that the relative number of aromatic groups decreases and the number of aliphatic groups increases during ageing. This result is similar to the photodegradation study and indicates that ring opening reactions occur during ageing. These ring opening reactions may be one reason why T_m has decreased so much in the 64 d and 128 d samples. Even though photodegradation caused severe damage to fibres, it did not affect the T_m of the material. This again illustrates the different degradation mechanisms of thermal- and photodegradation. From the application point of view FTIR is not the most obvious choice since it does not give any results related to material properties but only changes on the fibre surface. However,

changes in the carbonyl index can be used to estimate the general degradation of the fibres and the dominant degradation mechanism can even be differentiated from the peak intensity maximum.

Thermal ageing causes somewhat similar rheological effects as photodegradation (Fig. 13). The zero shear viscosity increases slowly at first but rapidly after 16 d. Even the first day of thermal ageing causes a significant reduction in the viscosity at high angular frequencies. This behaviour differs from the photodegradation study, where more changes occurred at low angular frequencies. It was impossible to measure 64 d and 128 d samples, since they did not melt during the tests (Fig. 13). This is very interesting results and is evidently caused by the material crosslinking which leads the material to behave more like a thermoset than a thermoplastic.

From the zero-shear-viscosity and M_w power-law connection [88] it is possible to state that a significant amount of crosslinking occurs because of the ageing. Crosslinking is observed with rheology roughly at the same time (32 d) as T_m and T_{g2}, measured with DSC, start to change. This is an expected result, since increased crosslinking, combined with changes in the relative amounts of crystalline and amorphous material, is directly observable as changes in the T_m and the T_g with DSC. This crosslinking is often undesirable in products since it makes the fibres brittle.

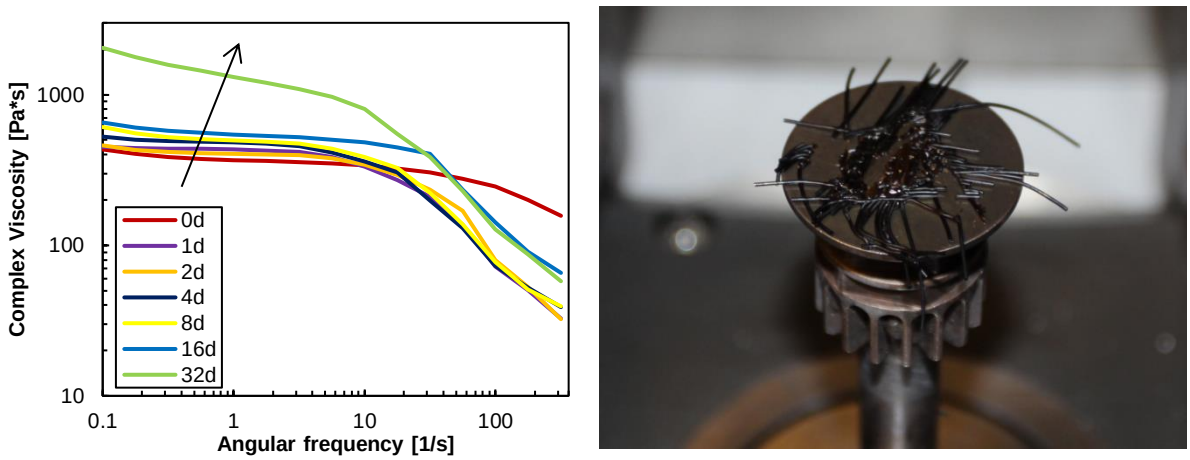

Fig. 13. Complex viscosity curves of PEEK fibres aged at 250 °C (left). 128 d aged PEEK fibres after rotational rheometer measurement. The fibres were heated 15 min at 450 °C using 50 N compression without changes in the fibre form. The photo was taken while heating was still on (right). Partly modified from *Publication III*.

A decrease in the T_m of the material and thus reduction in the thermal stability was observed in the DSC tests. This result was confirmed by the TGA measurements (Fig. 14) where significant changes occurred in the samples aged at least 8 d. Differences in the degradation onset temperature are small, only 13 °C between the virgin sample and the 128 d aged samples, but is due to the shapes of the curves. The mass loss begins at lower temperature when sample is aged more. If 2% mass losses are compared, the difference is almost 40 °C. Compared to photodegradation, the results are similar.

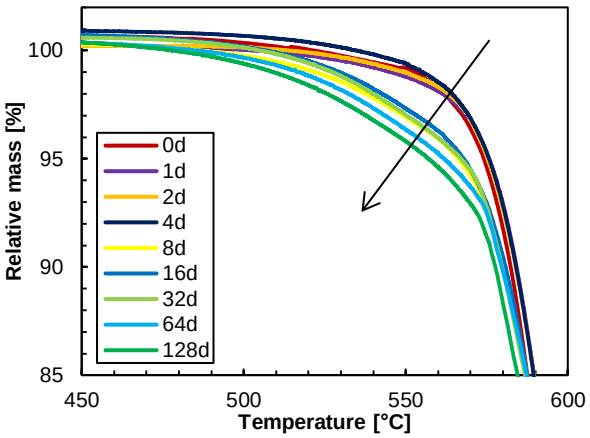

Fig. 14. TGA of PEEK fibres aged at 250 °C. Partly modified from *Publication III*.

Rheological investigations might have led to conclusion that highly crosslinked PEEK fibres have excellent thermal stability, but this is not the case according to TGA measurements. In fact, the thermal stability is the worst in 64 d and 128 d aged samples. These samples behave like thermosets that, upon heating, do not melt before degrading. In comparison, this gap between the T_m and the degradation onset is over 200 °C in virgin PEEK. The loss of aromaticity, observed with FTIR, also supports this decrease in thermal stability, since phenyl rings have better stability than aliphatic chains in the polymers. Both rheology and TGA are methods that give information on the whole sample volume and their ability to detect degradation was tested to be fairly similar. On the other hand, FTIR is a surface sensitive method. Since the first signs of degradation occur at the fibre surface, FTIR can detect changes, like the loss of aromaticity, much earlier than rheology or TGA.

Previous literature data clearly states that annealing have positive effects on the mechanical properties of PEEK [80, 82]. Tensile strength and tensile modulus improve significantly during the first day of ageing: tensile strength increases from 92 to 105 MPa (Fig. 15) and modulus from 2.6 to 2.9 GPa (Fig. 15). These values remained relative unchanged until 64 d of ageing. The highest values were measured in 128 d samples, 123 MPa tensile strength and 3.0 GPa modulus. The elongation behaviour was very similar to photodegradation study (Fig. 15). Virgin PEEK fibres were really elastic whereas aged samples had turn brittle. Confirmed and progressing crosslinking of the material during ageing is another explanation for the improved mechanical strength and reduced elongation [6, 81]. Crosslinking is often undesirable in the case of fibres because it eventually turns them brittle which reduces usability.

The measuring procedure for the elongation was modified from the photodegradation study in which average values were used. In this study, the highest value of 15 measurements was used. Because of equipment limitations and difficult samples, a stress concentration was generated near the jaws of the tensile testing machine, which often caused the fibre to break at the yield point. As long as the number of measurements is high enough, this method should effectively neutralize the phenomenon where fibre breaks down due to the stress concentration in jaws. According to 9 different ageing times, this method turned out to be suitable to follow the degradation process.

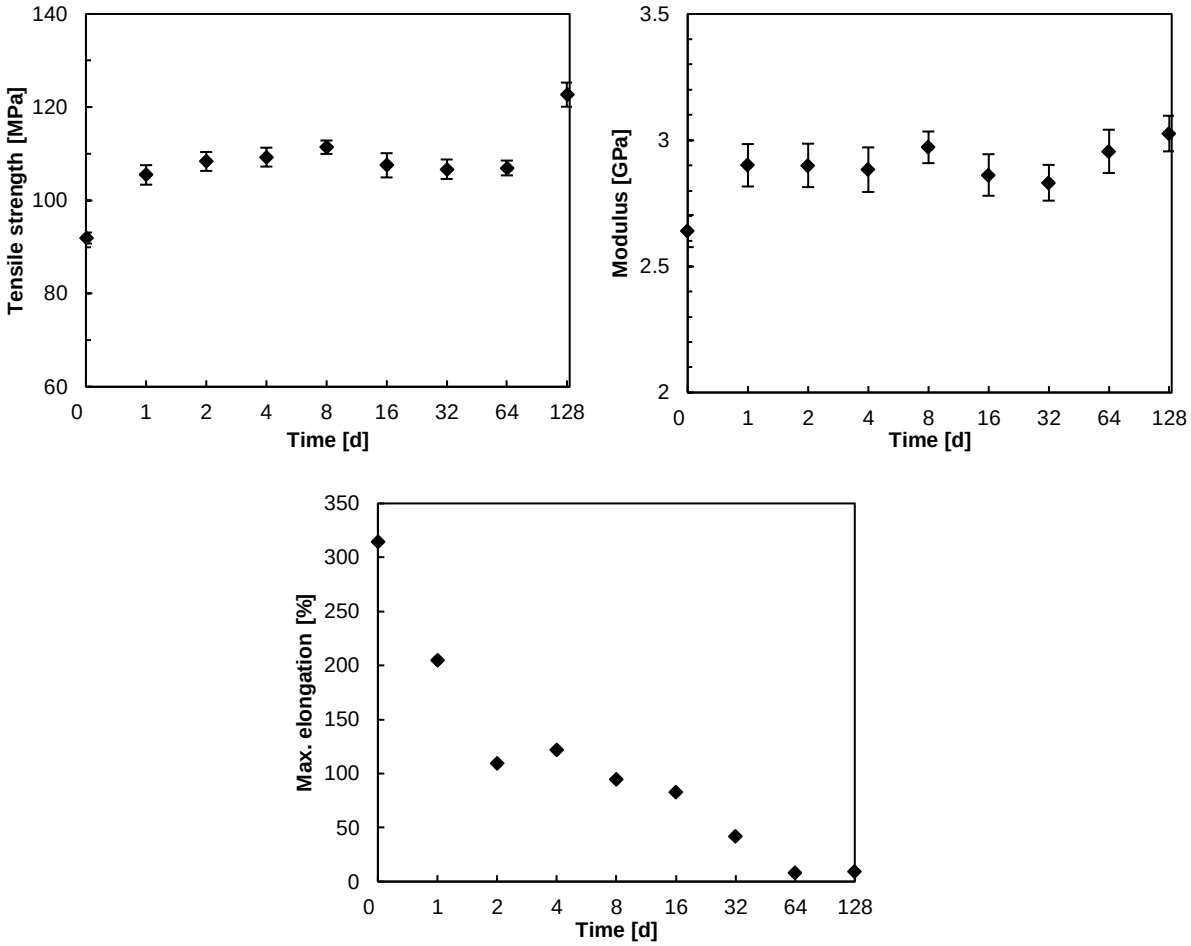

Fig. 15. Tensile strength (up left), modulus (up right), and maximum elongation (below) of PEEK fibres aged at 250 °C. Partly modified from *Publication III*.

The originally yellowish PEEK fibres turned brownish red during ageing. The chromophoric groups in PEEK's structure absorb almost all UV radiation below 380 nm [32]. This result is also confirmed by the UV-Vis diffuse reflectance spectra of the samples (Fig. 16).

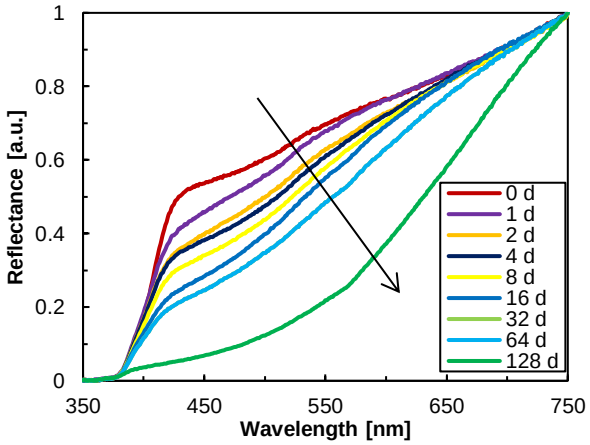

Fig. 16. UV-Vis diffuse reflectance spectra of PEEK fibres aged at 250 °C. Partly modified from *Publication III*.

The onset of the absorption gradually moves to higher wavelengths with increased ageing, the absorption band forming in the visible region between 400 and 750 nm. The 128 d aged fibres have an absorption onset of 550 nm, this corresponding to a brownish red colour. Surface oxidation of the fibres is a likely explanation for the colour changes. The phenomenon is similar to what is observed during the burning of polymers.

6.3.3. Benefits of the study

The aim of this part of the thesis was to test PEEK fibres in elevated temperature (250 °C) and characterize them using a wide range of methods. Tested fibres were the same as in the UV irradiation study, which makes comparison possible. The ultimate goal was to expand the uses of PEEK fibres in extreme temperatures and generate new information to increase the safety of these products.

According to the results, as well as the earlier literature, the initial effects are mostly positive due to the formation of secondary crystals. Surface sensitive methods like FTIR are able to detect changes roughly at 8–16 d. At this point the usability of the fibres is still good even though the elongation of the fibres reduces at a fast rate. The reduction in usability occurs at 32–64 d. The fibres become more and more brittle due to crosslinking reactions, thermal stability and T_m decrease and the colour of the fibres turn darker. At 128 d the fibres are not totally destroyed but the use of them in actual products can be hardly recommended.

6.4. Under contamination

6.4.1. Applications of photocatalytic fibres

Photocatalytic fibres are currently utilized in antimicrobial, self-cleaning, and antipollution applications. Antimicrobial textiles include products such as tents, tarpaulins, awnings, blinds, parasols, sails, waterproof clothing, consumer textiles, and medical settings [89]. Clothing industry would benefit from the self-cleaning property and therefore much research has been done in this sector [90–92]. However, these products are not largely available yet and products containing TiO_2 nanoparticles possibly pose a risk to humans [51]. Some commercial air purifiers, also in HVAC (heating, ventilating and air-conditioning) systems, use photocatalytic oxidation to turn harmful substances, including volatile organic compounds (VOCs), into less harmful compounds like H_2O or CO_2. [93, 94]

6.4.2. Manufacturing and characterization of material

SPEEK was compounded with PP at three different mass concentrations 2:98; 5:95; and 10:90. TGA measurements (Fig. 17) indicate that SPEEK has poor thermal stability compared to PEEK and this has to be taken into consideration during material compounding. SPEEK decomposes almost linearly when heated above 50 °C. In a previous study, the mass loss from 50 to 250 °C was shown to occur due to chemically and physically bound water, from 250 to 450 °C due to the decomposition of acid group which induces the elimination of SO_3 and the decomposition of the $–SO_3H$ group, and above 450 °C due to the breakdown of the polymer backbone [38]. Drying of SPEEK for 30 min before the TGA measurement effectively removed the bound water and decreased the mass loss in the TGA curve.

Too high processing time and temperature would have led to thermal degradation and too low to improper mixing. 5 min of compounding at 200 °C at a laboratory scale provided a SPEEK/PP blend with a homogenous character and brown colour. An increase in the processing time clearly changed the colour to darker, this being a typical sign of thermal degradation. Interestingly, SPEEK/PP blends

seem to have better thermal stability than virgin PP. However, the onset of SPEEK/PP blend initiates the earlier the higher SPEEK concentration is.

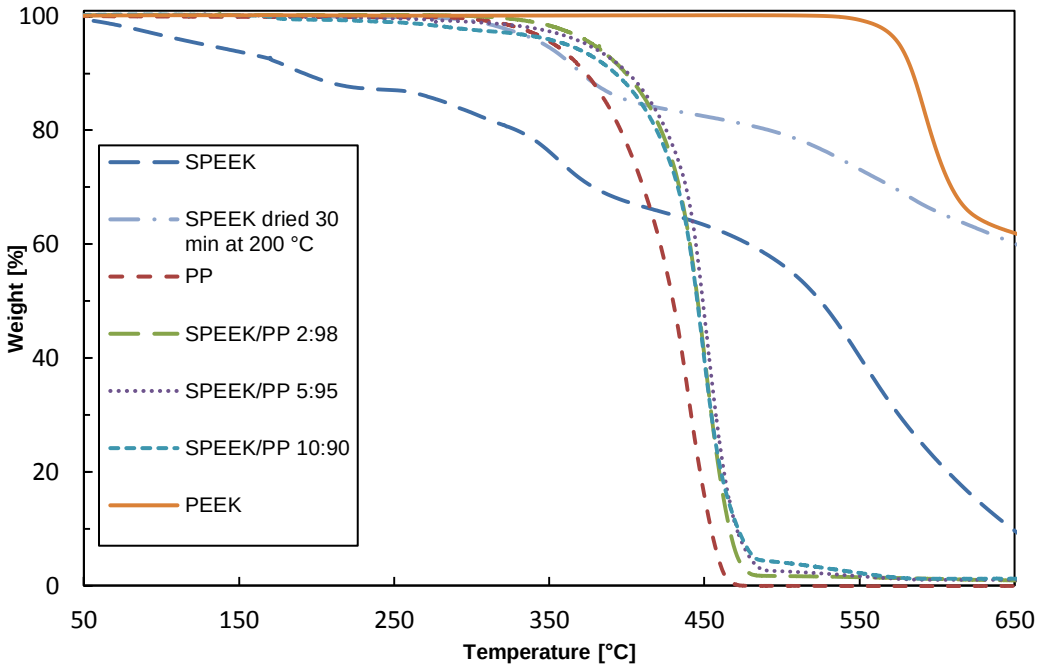

Fig. 17. TGA curve of PEEK, SPEEK, SPEEK dried, SPEEK/PP 2:98; 5:95; 10:90 and PP (20 °C/min, N_2). *Publication IV*.

TGA measurements can be used to estimate the degree of sulfonation (DS) for SPEEK. As previously mentioned, the weight loss between 250 and 450 °C is associated to elimination of SO_3 unit in the polymer chain. Theoretical maximum for the weight loss is 21.7% that is the mass portion of SO_3 of the whole unit. TGA measurements show a weight loss of 23.7% in this range, which corresponds to a theoretical DS of 109 %. The explanation for the value to be over 100 % is that the acid groups may cause random chain scissions, which lead to a loss of phenol groups as well [95]. The limits for SO_3 volatilisation are also somewhat inaccurate.

To confirm the high DS of synthetized SPEEK, a ^{1}H-NMR measurement was performed. PEEK sulfonation generates a single signal for H proton in ortho position to SO_3H, the intensity of the signal being equivalent to the SO_3H group content [96]. The ratio of the area of this proton peak and the area of the other protons equals to a degree of sulfonation. The measured value of 93% confirms that a higher DS was achieved compared to a previous study where values between 70 and 80% were achieved [38].

The results of DSC measurements in Table 7 show that SPEEK does not have a crystallization peak which indicates that SPEEK is completely amorphous polymer. In comparison, PEEK has a maximum crystallinity around 40% [15]. Also the T_g of SPEEK is rather high (225 °C) compared to the one measured in PEEK (159 °C). SPEEK/PP blends have a T_m (~168 °C) and two T_g's, one T_g (~2 °C) similar to PP and a second T_g similar to the one in SPEEK (~225 °C). Two distinct T_g's is perhaps the most typical sign of an immiscible (heterogeneous) polymer blend [97].

Table 7. Thermal properties of PP, PEEK, SPEEK and SPEEK/PP 2:98, 5:95, and 10:90 blends measured by DSC (10 °C/min, N_2). Partly modified from *Publication IV*.

Sample	T_{g1}	T_{g2}	T_m
PEEK	159.4 °C	-	346.6 °C
SPEEK	-	225.2 °C	-
PP	2.3 °C	-	168.2 °C
SPEEK/PP (2:98)	3.1 °C	221.9 °C	169.4 °C
SPEEK/PP (5:95)	2.0 °C	225.8 °C	167.5 °C
SPEEK/PP (10:90)	2.8 °C	219.7 °C	168.6 °C

A high-viscosity PP grade (melt flow index 3 g/10 min) was selected because it was estimated that compounding causes chain scission reactions in PP decreasing the viscosity [98]. According to the rheological measurements in Fig. 18, SPEEK/PP 2:98 blend has similar viscosity as PP but in the case of SPEEK/PP 5:95 and SPEEK/PP 10:90 blends the viscosity is significantly dropped. SPEEK degrades at elevated temperatures, which could explain the decrease in viscosity. Decomposition products, such as the acid groups mentioned in TGA section, are one likely explanation for the chain scission reactions.

There are no differences in shear thinning behaviour in SPEEK/PP 5:95 samples measured at 180, 200, 220, and 240 °C (Fig. 18). The shape of the 240 °C curve is a somewhat different in small shear rates, probably due to thermal degradation. These measuring points take the longest time of the approximately 10 min measuring cycle. A drop in SPEEK/PP 5:95 viscosities (Fig. 18) can be observed as a function of time but the amount of the decrease is unclear because of the measuring procedure: it takes several minutes to heat the sample, trim it, and start the measurement. Therefore, 200 °C sample seem to have higher drop compared to 220 and 240 °C samples. After roughly 5 min the viscosities are stabilized in all three samples.

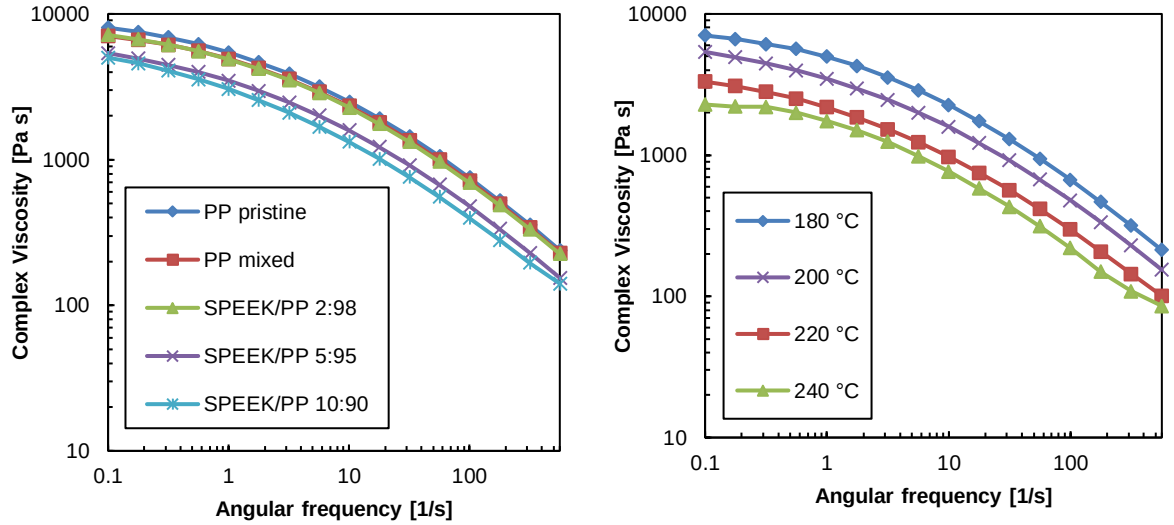

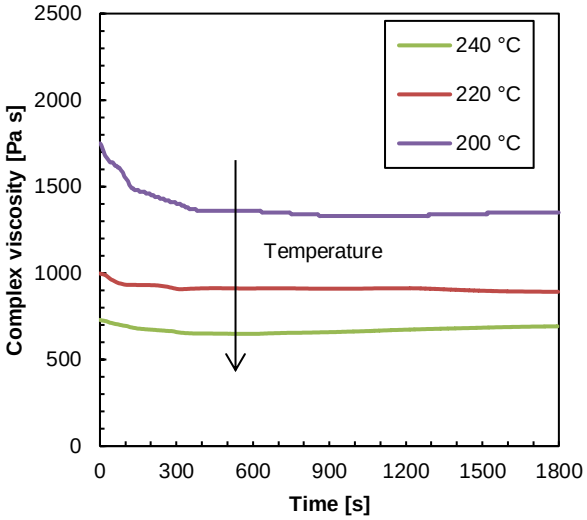

Fig. 18. Complex viscosity of PP, PP mixed and SPEEK/PP 2:98; 5:95; 10:90 (200 °C, N_2) (up left). Complex viscosity of SPEEK/PP 5:95 (180, 200, 220 and 240 °C, N_2) (up right). Complex viscosity of SPEEK/PP 5:95 as a function of time (200, 220 and 240 °C, N_2) (below). Partly modified from *Publication IV*.

DSC measurements revealed the heterogeneous nature of the SPEEK/PP blend. This is confirmed by the SEM micrographs (Fig. 19) that show two different domains in the SPEEK/PP blends implying that the blend is not miscible. The SPEEK particles have a size of a few micrometres, which should not be a problem during fibre spinning where the fibre size is typically in tens of micrometres. The shear forces of the compounder seem to be able to homogenously disperse the SPEEK particles into the PP matrix.

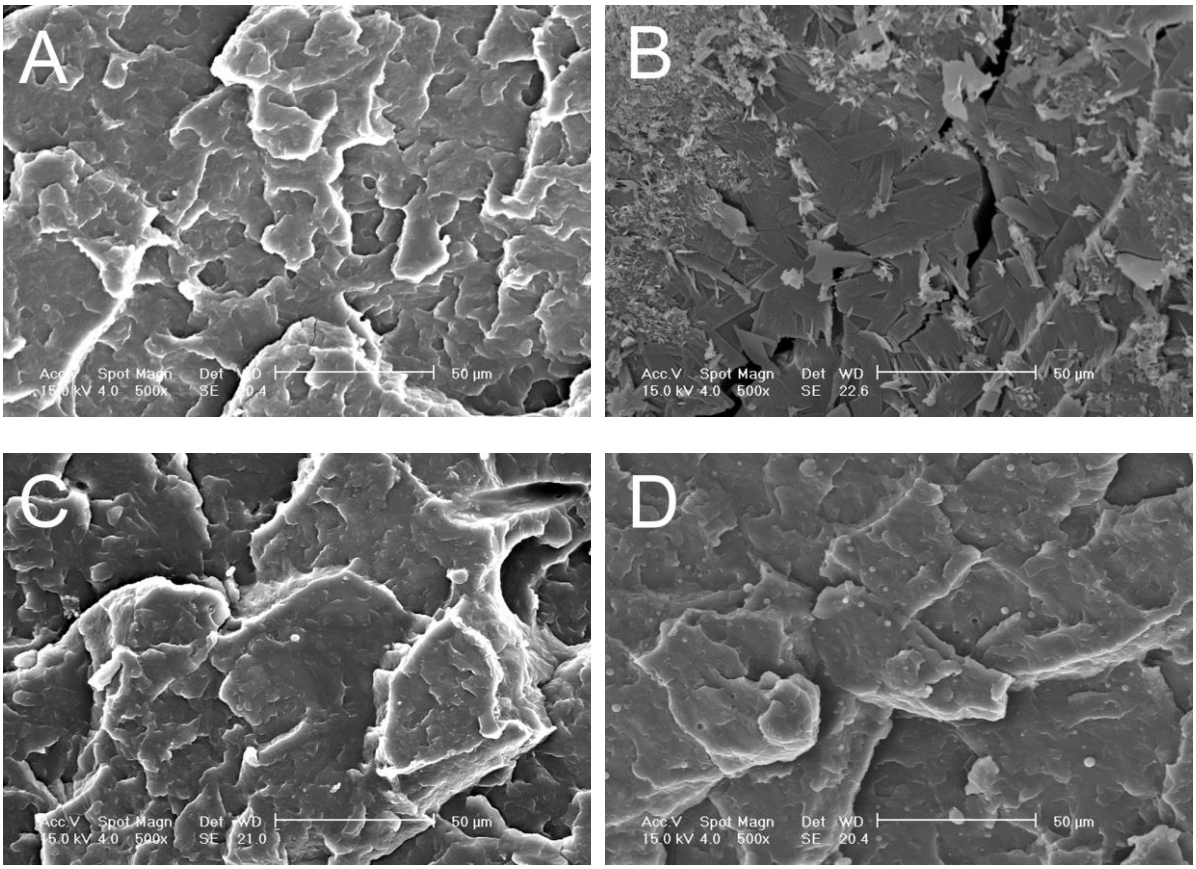

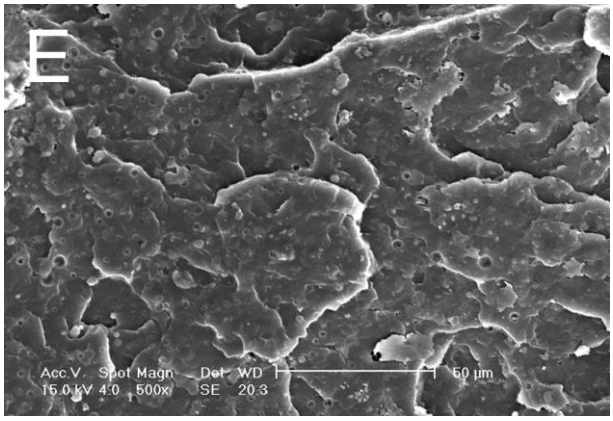

Fig. 19. SEM micrograph of PP (A), SPEEK (B), SPEEK/PP 2:98 (C), SPEEK/PP 5:95 (D), and SPEEK/PP 10:90 (E). *Publication IV*.

6.4.3. Fibre melt spinning

The fibre spinning was performed using two different melt spinning systems. The laboratory scale system was used to test the melt spinning processing parameters and the semi-industrial system to manufacture sufficient amount of fibres for characterization. In laboratory scale tests, most of the processing parameters are the same as found optimal for PEEK in *publication I*: capillary dimensions 30/1 mm, spinning path length 5 cm, and take-up speed 100 m/min. The mass throughput, material composition, and processing temperature were altered to found the optimal spinning conditions. For evaluation of the fibre spinning properties, a very simple three-step grading scale was created. The descriptions for different spinning qualities are presented in Table 8.

Table 8. Spinning quality table. Partly modified from *Publication V*.

Quality	Description
Excellent	No problems in fibre quality or spinning stability.
Good	Fibre spinning was possible but there were problems in the spinning stability or fibre quality and spinning of very thin fibres was not possible.
Not spinnable	Fibre spinning was not possible or the process was stable for a few seconds at best.

The laboratory scale spinnability and fibre quality turned out to be excellent at best even though the very simplified structure of the Göttfert capillary rheometer does not allow using filters or gear pumps before the die. Generally, increasing the processing temperature improves spinnability [4, 23]. Among the three tested processing temperatures, 200 °C was a good compromise between spinnability and thermal degradation (Table 9). 180 °C is so close to the T_m of PP that the spinnability was not quite as good. Spinnability of PP was excellent at 200 and 220 °C. On the other hand, the spinnability of SPEEK/PP at 220 °C was strongly time-dependent. Initially excellent spinnability reduced to good in 5 min and after 10–15 min the material was not spinnable at all.

SPEEK/PP 5:95 and 10:90 had almost similar spinnability at the same temperature. This spinnability of PP was rather similar to SPEEK/PP blends as long as the residence time was short. Rheological investigations support this finding since the SPEEK concentration had only a small effect on the viscosity. There was no point of testing the limits of spinnability in the laboratory scale setup. The smallest spun SPEEK/PP 5:95 fibres had an average diameter of 45 µm.

Table 9. The results of the spinning tests. Partly modified from *Publication V*.

Test number	Processing temperature [°C]	SPEEK concentration [%]	Quality
1	180	0	Good
2	200	0	Excellent
3	220	0	Excellent
4	180	5	Good
5	200	5	Excellent
6	220	5	Excellent → Good → Not spinnable (depending on the residence time)
7	180	10	Good
8	200	10	Excellent
9	220	10	Excellent → Good → Not spinnable (depending on the residence time)

Up-scaling of the process to semi-industrial scale was tested. The goal of these tests was to estimate the spinnability in scale closer to real applications and to manufacture sufficient amount of fibres for characterization. SPEEK/PP concentration of 5:95 was chosen for the tests. Optimal processing temperature from the laboratory scale spinning tests, 200 °C, was used. Theoretically, the fibre properties should be more stable in the semi-industrial tests since the equipment includes a 50 µm filter, more accurate drawing system, and more stable material flow. The spinnability was excellent from the beginning and no fine-tuning was required. A total of 4 bobbins (Fig. 20) were spun and no broken filaments were observed during the semi-industrial scale spinning tests. The colour of spun SPEEK/PP 5:95 fibres was brown whereas PP fibres were light-coloured.

Fig. 20. Melt spun SPEEK/PP 5:95 filaments. *Publication V*.

6.4.4. Fibre properties

Filaments obtained from the semi-industrial tests, SPEEK/PP 5:95 and PP, were characterized by photocatalytic tests, mechanical tests, and SEM. Testing of photocatalytic properties is crucial considering the applications of these fibres. The amount of generated radicals should be sufficient, they should have a long life-time, and the effectiveness should not decay too much during multiple irradiations. X-band (9 GHz) EPR spectra of the samples was measured at different times after the irradiation and after several irradiation cycles. A BPK radical signal as well as six Mn(II) impurities were detected.

The EPR signal area as a function of time, obtained by double integration of the experimental spectra, is presented in Fig. 21. The maximum value of the BPK signal is measured immediately after the irradiation after which it starts to decay. Considering the potential applications, the lifetime of the radical is relatively long. After 15 min, the radical intensity is dropped to 59% and after 60 min to 18% of the maximum measured radical intensity (I_{max}). The residual radical intensity is approximately 5% of the I_{max}. 16 h monitoring of the radical signal reveals no further decay in the intensity. BPK radicals have slow dimerization/disproportionation coupling reaction, which explains their long lifetime [46]. In the solid state, the mobility of the radicals is slow which increases the life-time. Also SPEEK/PP 5:95 samples that were not irradiated showed a small BPK peak as a result of the irradiation during material handling. In PP samples, with or without irradiation, BPK peak was not visible.

Relative radical amount was monitored 10 irradiation cycles to simulate the effectiveness of the fibre in continuous use (Fig. 21). The first irradiation cycle drops the effectiveness to about one third of I_{max}. Stable radical intensity level around 20 % of I_{max} is quickly reached. Evidently, the radical formation ability reduces in use, this being very typical challenge for such fibres. It is difficult to estimate whether 100% or 10% I_{max} intensity is enough to provide functional properties and therefore e.g. antimicrobial tests should be performed to verify the usability.

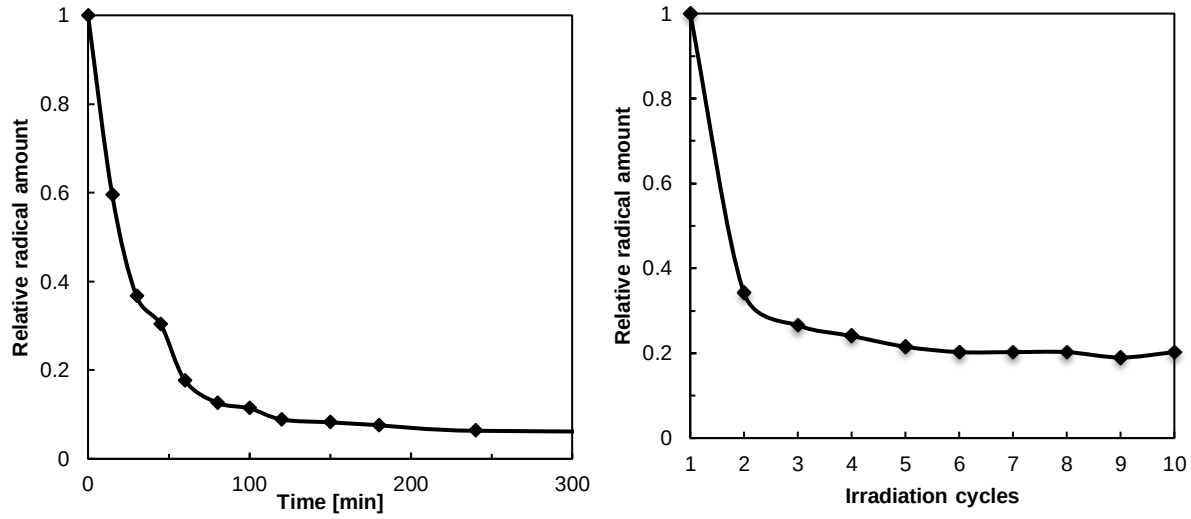

Fig. 21. Relative radical amount after the first irradiation compared to I_{max} as a function of time (left) and relative radical amount after irradiation compared to I_{max} as a function of irradiation cycles (right). *Publication V*.

The mechanical properties of the yarns are presented in Table 10. Compared to the otherwise similar PP yarn, the mechanical tenacity of SPEEK/PP 5:95 yarn is 20% lower. A lack of material during testing

forced to draw the fibres directly into the bobbing which is the simplest option. The orientation of the polymer chains by using heatable godets and cold drawing could not been performed and this affected the mechanical properties of the yarns that are below the commercial levels [99]. Another choice that can cause speculation is the PP grade. A high-viscosity PP grade was chosen to improve the compounding quality but in fibre melt spinning higher melt-index grades (lower viscosity) are typically used. In contrast to the low mechanical strength, the yarns are very elastic with over 250% strain at break.

Table 10. Mechanical properties for SPEEK/PP 5:95 and PP filaments. Partly modified from *Publication V*.

Sample	Fineness [tex]	Tenacity at break [cN/tex]	Strain at break [%]	Young's modulus [cN/tex]
SPEEK/PP 5:95	23	9.1±1.2	267±59	19.5±2.9
PP (pristine)	23	11.6±1.8	268±47	24.7±2.2

SEM analysis reveals no problems in the fibre quality of SPEEK/PP 5:95 fibres (Fig. 22). The surface of these fibres is, however, a little rougher compared to the PP fibres. The reason for this is the SPEEK particles but the differences are small. In the characterization of SPEEK/PP bulk blend the particle size of SPEEK was found to be a few micrometres with a homogenous dispersion and these micrographs confirm this finding.

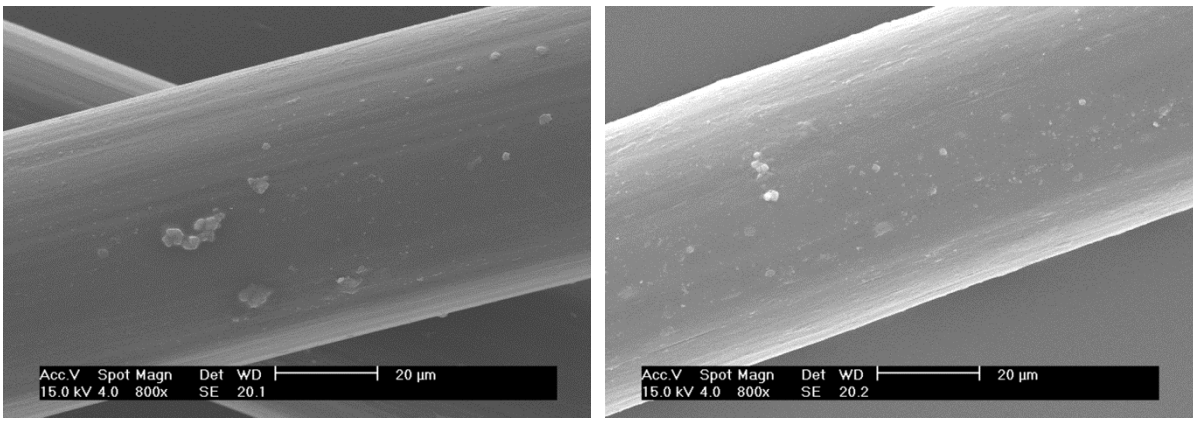

Fig. 22. SEM micrograph of the PP fibre (left) and SPEEK/PP 5:95 fibre (right). *Publication V*.

6.4.5. Benefits

In this study, nanoparticle-free photocatalytic fibres were developed. The study included many challenging aspects such as totally new polymer blend, thermal degradation of SPEEK and the blend, and SPEEK particles that could interfere the melt spinning. Despite these challenges, a fibre with good overall performance was developed. Characterization of the fibre revealed long-lasting BPK radicals but also decay in use. This decay is a typical challenge for the current products as well and slows down the growth rate of these products. The mechanical properties of them were only slightly affected by the addition of SPEEK compared to the PP fibres. It should be possible to manufacture this fibre into textiles and then use this textile in products such as carpets or filters. Even though the formation of BPK radicals was verified, more research of the actual performance in textiles is recommended.

7. Conclusions

PEEK is a specialty thermoplastic often used in conditions that conventional thermoplastics cannot withstand. PEEK has been melt-spun for over 30 years, during which time its number of applications has increased dramatically. There is a clear, market-driven need to improve the properties of PEEK fibres. In this work, PEEK-based polymer fibres were pushed to the limit and beyond under demanding conditions. The results show that the spinnability of the fibres can be improved by fine-tuning the processing parameters, though eventually filament breaks increase in number despite the best efforts. Both photo-irradiation and thermal ageing significantly and progressively degrade the fibres and turn them from elastic to brittle and eventually to unusable. PEEK sulfonation into SPEEK, melt compounding this SPEEK with PP, and melt spinning this blend produced fibres with functional properties.

The main findings for the specific sub-questions of this thesis are as follows:

- PEEK is an easily spinnable polymer. The optimal processing parameters for fine PEEK fibres on a laboratory scale were low viscosity PEEK grade, high processing temperature, long and large capillary, and short spinning path length. Quantitatively, the selection of the PEEK grade and capillary dimensions had the highest impact on the obtained fibre diameter. The smallest directly-to-the-bobbin-spun PEEK fibres were 18 µm in average diameter.
- Photodegradation is harmful to PEEK. Exposure to UV radiation causes crosslinking, especially on the surface of the fibre. The extent of this crosslinking can be estimated with rheological measurements, and mechanical tests show the transformation of originally elastic fibres to brittle. The carbonyl index, measured by FTIR, was the easiest tested method to estimate the degree of photodegradation. Changes were also visible in TGA and SEM measurements, but DSC turned out to be a poor method for characterization.
- Thermal exposure at the maximum recommended use temperature (250 °C) significantly degraded the fibres during the 128-d test period. At first, changes were mostly positive due to the formation of secondary crystals improving mechanical properties. After 8–16 d, changes became visible with surface sensitive methods, but the fibres remained usable. Between 32–64 d, usability slowly deteriorated. Finally, samples aged for 128 d, though not fully destroyed, were yet highly crosslinked, brittle, and significantly compromised in thermal stability.
- SPEEK and its melt compounded blend with PP provided photocatalytic properties, which were confirmed by EPR measurement. During melt spinning, the processing temperature had to be carefully optimized because of the poor thermal stability of SPEEK. At 200 °C, the 5:95 SPEEK/PP blend showed excellent spinnability and mechanical properties of only slightly below the PP reference.

The melt spinning of fine filaments was also linked to other approaches of this study. Reduction in fibre size increases the surface area to volume ratio. Since oxygen affects the degradation rate, and since there is more oxygen on the surface of than inside the fibre, degradation is faster in fine fibres. An increased surface area is highly beneficial in photocatalytic applications because more radicals can then be generated.

Comparison of photo- and thermally aged PEEK fibres reveals both similarities and differences. In both cases, crosslinking makes fibres brittle, their thermal stability drops according to TGA, T_g increases, and FTIR shows generation of carbonyl groups. A few useful tips can be given to distinguish thermal degradation from photodegradation. The easiest is probably the location of the carbonyl absorption band maximum in FTIR. In photodegradation, the maximum is located at around 1716 cm^{-1}, whereas in thermal degradation it is at around 1740 cm^{-1}. In photodegradation, the intensity of the peak is also significantly higher. If a reference sample is available, thermal degradation is likely to increase yield strength and modulus, whereas in photodegradation change is not so obvious, or the effect can even be negative. A secondary endotherm at around 270–320 °C can be observed in DSC only in thermally aged samples. Furthermore, T_m changes in thermal degradation but not in photodegradation. If a reference sample is available, changes in rheological behaviour can be used to differentiate between the ageing methods. In thermally aged samples, a rapid change in the slope occurs at around 10–50 1/s angular frequency. The curve of photodegraded samples is more linear on a logarithmic scale. Finally, SEM is not an accurate method to estimate the degree of degradation, though some changes may be visible in photodegraded samples.

The antimicrobial properties of the SPEEK/PP blend highlight the material versatility of PEEK. Its chemical structure of aromatic rings accounts for its excellent thermal stability and enables its photocatalytic activity after modification. Furthermore, SPEEK/PP fibres were verified on a laboratory scale to be a potential alternative to competitors containing nanoparticles.

Though this study concentrated on PEEK-based polymer fibres, its results can be exploited for other materials and processes as well. For example, the spinnability results apply, at least to some degree, to other thermoplastics. However, it is more complicated to compare degradation processes. The internal chromophores of PEEK that extend its light absorption up to 400 nm are another reason for its excellent thermal properties. Many thermoplastics contain no such internal chromophores; instead, their degradation is initiated by the impurities they contain. This difference makes it difficult to use these results extensively. Regardless of the type and rate of degradation, the multiple characterization methods in these studies provide new information for efficient characterization of aged fibres. One important result of the SPEEK/PP fibre study is the distribution of small SPEEK particles in the PP matrix to stabilize the spinning process. Different blends must often be compounded to produce functional properties. If the compounding quality is not sufficient, spinning process will not be stable. In fact, particles distributed evenly in the matrix help secure the best possible properties.

All the three approaches could be further studied. Besides laboratories, the limits of spinnability could also be tested on a semi-industrial scale. Because of its excellent chemical resistance, PEEK is used in applications where it ends up in contact with chemicals. Consequently, its ageing could well be tested using chemicals and characterized as in thermal and photodegradation studies. Photocatalytic SPEEK/PP fibres could also be processed into textiles and thereby be tested in real-life conditions for functional properties such as antimicrobiality. On the whole, there are still many possibilities to further develop PEEK-based polymer fibres.

References

[1] Sabu, T., Visakh, P.M. *Handbook of Engineering and Speciality Thermoplastics*: Polyethers and Polyesters. Wiley, New York, USA, 2011.

[2] Wypych, A. *Handbook of polymers*. ChemTec Publishing, Toronto, Canada, 2012.

[3] Hearle, J.W.S. *High performance fibres*. Woodhead publishing limited, Cambridge, UK, 2001.

[4] Fourne, F. *Synthetic fibers: Machines and equipment, manufacture, properties.* Hanser Gardner, Munich, Germany, 1999.

[5] Allen, N.S., Edge, M. *Fundamentals of polymer degradation and stabilisation*. Elsevier, London, UK, 1992.

[6] Nakamura, H., Nakamura, T. Noguchi, T. Imagawa, K. Photodegradation of PEEK sheets under tensile stress. *Polymer Degradation and Stability* 91(2006)740–746.

[7] Berer, M., Major, Z., Pinter, G., Constantinescu, D.M., Marsavina, L. Investigation of the dynamic mechanical behaviour of polyetheretherketone (PEEK) in the high stress tensile regime. *Mechanics of Time-Dependent Materials* 18(2014)663–684.

[8] Lee, L.H., Vanselow, J.J., Schneider, N.S. Effects of mechanical drawing on the structure and properties of peek. *Polymer Engineering & Science* 28(1988)181–187.

[9] Ostberg, G.M.K., Seferis, J.C. Annealing effects on the crystallinity of polyetheretherketone (PEEK) and its carbon fiber composite. *Journal of Applied Polymer Science* 33(1987)29–39.

[10] Rabek, J.F. *Polymer Photodegradation: mechanisms and experimental methods*. Chapman & Hall, London, UK, 1995.

[11] Hong, K.H., Sun G. Photoinduced antimicrobial polymer blends with benzophenone as a functional additive. *Journal of Applied Polymer Science* 112(2009)2019–2026.

[12] Hong, K.H., Sun, G. Poly(styrene-co-vinylbenzophenone) as photoactive antimicrobial and selfdecontaminating materials. *Journal of Applied Polymer Science* 109(2008)3173–3179.

[13] Hong, K.H., Sun, G. Antimicrobial and chemical detoxifying functions of cotton fabrics containing different benzophenone derivatives. *Carbohydrate Polymers* 71(2008)598–605.

[14] Korchev A.S., Shulyak T.S., Slaten B.L., Gale W.F., Mills G.J. Sulfonated poly(ether ether ketone)/poly(vinyl alcohol) sensitizing system for solution photogeneration of small Ag, Au, and Cu crystallites. *Journal of Physical Chemistry B* 109(2005)7733–7745.

[15] Kemmish, D. *Updates on the technology and applications of polyaryletherketones*. Smithers Rapra Update, Shawbury, UK, 2010.

[16] Patel, P., Hull, R., McCabe, R., Flath, D., Grasmeder, J., Percy, M. Mechanism of thermal decomposition of poly(ether ether ketone) (PEEK) from a review of decomposition studies. *Polymer Degradation and Stability* 95(2010)709–718.

[17] Platt, D.K. *Engineering and High Performance Plastics Market Report*. Smithers Rapra Technology, Shawbury, UK, 2003.

[18] Victrex. Literature. [www] [July 2016] www.victrex.com

[19] Brünig, H., Beyreuther R., Vogel R., Tändler B. Melt spinning of fine and ultra-fine PEEK-filaments. *Journal of Materials Science* 38(2003)2149–2153.

[20] Zyex. Applications. [www] [June 2016] http://www.zyex.com

[21] Zeus. Applications. [www] [June 2016] http://www.zeusinc.com/

[22] Nakajuma, T. *Advanced Fibre spinning technology*. Woodhead Publishing Limited, Cambridge, UK, 1994)

[23] Golzar M. *Melt spinning of the fine PEEK filaments*. Dissertation. Technische Universitat Dresden, Dresden, Germany, 2004.

[24] Ziabicki, A. *Fundamentals of Fiber Formation*. Wiley-Interscience, London, UK, 1976.
[25] White, J.L. *Fiber and Yarn Processing*. Wiley, New York, USA, 1975.
[26] Repkin, Y.S. The diameter of the spinneret holes as a factor in spinning stability. *Fibre Chemistry* 3(1972)377–378.
[27] Shimizu, J., Kikutani, T. Dynamics and evolution of structure in fiber extrusion. *Journal of Applied Polymer Science* 83(2002)539–558.
[28] Webb, A.R. *UVB instrumentation and applications*. Overseas Publishers Association, Amsterdam, Netherlands, 1998.
[29] Zerefos, C.S., Bais, A.F. *Solar Ultraviolet Radiation: Modelling, Measurements and Effects.* Springer, Berlin, Germany, 1997.
[30] Wypych, G. *Weathering of plastics: testing to mirror real life performance*. William Andrew Inc, New York, USA, 1999.
[31] Rabek, J.F. *Photodegradation of polymers*. Springer, Berlin, Germany, 1996.
[32] Giancaterina, S., Rossi, A., Rivaton, A. Gardette J.-L. Photochemical evolution of poly(ether ether ketone). *Polymer Degradation and Stability* 68(2000)133–144.
[33] White, J., Turnbull, A. Weathering of polymers: mechanism of degradation and stabilization, testing strategies and modelling. *Journal of Material Science* 29(1994)584–613.
[34] Bedia, E., Paglicawan M.A., Bernas C.V., Bernardo, S.T., Tosaka, M., Kohjiya, S. Natural weathering of polypropylene in a tropical zone. *Journal of Applied Polymer Science* 87(2003)931–938.
[35] Rajakumar, K., Sarasvathy, V., Thamarai Chelvan, A., Chitra, R., Vijayakumar, C.T. Natural weathering studies of polypropylene. Journal of Polymers and the Environment 17(2009)191–202.
[36] Andrady, A., Hamid, S., Hu, X., Torikai, A. *Effects of increased solar ultraviolet radiation on materials. Journal of Photochemistry and Photobiology B: Biology* 46(1998)96–103.
[37] Day, M., Sally, D. Wiles, D.M. Thermal degradation of poly(aryl-ether-ether-ketone): experimental evaluation of crosslinking reactions. *Journal of Applied Polymer Science* 40(1990) 1615–1620.
[38] Muthu Lakshmi, R.T.S., Choudhary, V., Varma, I.K. *Journal of Material Science* 40(2005)629–636.
[39] Jin, X., Bishop, M.T., Ellis, T.S., Karasz, F.E. A sulphonated poly(aryl ether ketone). *British Polymer Journal* 17(1985)4–10.
[40] Shibuya N., Porter R.S. Kinetics of PEEK sulfonation in concentrated sulfuric acid. *Macromolecules* 25(1992)6495–6499.
[41] Catalan J., Valle J.C. Toward the photostability mechanism of intramolecular hydrogen bond systems. The photophysics of 1‟-Hydroxy-2‟-acetonaphthone. *Journal of American Chemical Society* 115(1993)4321–4325.
[42] Pospisil, J., Nespurek, S. Photostabilization of coatings. Mechanisms and performance. *Progress in Polymer Science 25*(2000)1261–1335.
[43] Mosquera, M., Penedo, J.C., Rodriquez, C.R., Rodriquez-Prieto, F. Photoinduced inter- and intramolecular proton transfer in aqueous and ethanolic solutions of 2-(2’-hydroxyphenyl)benzimidazole: evidence for tautomeric and conformational equilibria in the ground state. *Journal of Physical Chemistry* 100(1996)5398–5407.
[44] Yang, T. Preliminary study of SPEEK/PVA blend membranes for DMFC applications. *International Journal of Hydrogen Energy* 33(2008)6772–6779.
[45] Molla, S., Compan, Vicente. Polymer blends of SPEEK for DMFC application at intermediate temperatures. *International Journal of Hydrogen Energy* 39(2014)5121–5136.

[46] Korchev, A.S., Konovalova, T., Cammarata, V., Kispert, L., Slaten, L., Mills, G. Radical-induced generation of small silver particles in SPEEK/PVA polymer films and solutions: UV-Vis, EPR, and FT-IR studies. *Langmuir* 22(2006)375–384

[47] Korchev, A.S., Bozack, M.J., Slaten, B.L., Mills, G. Polymer-initiated photogeneration of silver nanoparticles in SPEEK/PVA films: direct metal photopatterning. *Journal of American Chemical Society* 126(2004)10–11.

[48] Conceição, T.F., Bertolino, J.R., Barra, G.M.O, Pires, A.T.N. Poly (ether ether ketone) derivatives: synthetic route and characterization of nitrated and sulfonated polymers. Materials Science and Engineering C 29(2009)575–582.

[49] Lee, S.H., Youn, J.R. Properties of polypropylene/layered-silicate nanocomposites and melt-spun fibers. *Journal of Applied Polymer Science* 109(2008)1221–1231.

[50] Beydoun, D., Amal, R., Low, G., Mcevoy, S. Role of nanoparticles in photocatalysis. *Journal of Nanoparticle Research* 1(1999)439–458.

[51] World health organization International Agency for Research on Cancer. *IARC monograps on the evaluation of carcinogenic risks to humans. Vol. 93 carbon black, titanium dioxide and talc.* Lyon, France, 2010.

[52] Q-lab. Technical bulletin. [www][July 2016] http://www.q-lab.com/documents/public/d6f438b3-dd28-4126-b3fd-659958759358.pdf.

[53] Kos, S., Huegli, R., Hofmann, E., Quick, H.H., Kuehl, H., Aker, S., Kaiser, G.M., Borm, P.J.A., Jacob, A.L., Bilecen, D. First magnetic resonance imaging-guided aortic stenting and cava filter placement using a polyetheretherketone-based magnetic resonance imaging-compatible guidewire in Swine: proof of concept. *Cardiovascular Interventional Radiology* 32(2009)514–521.

[54] Ko, F.K., Wan, Y. *Introduction to Nanofiber Materials*. Cambridge University Press, Cambridge, UK, 2014.

[55] Shekar, R.I., Kotresh T.M., Rao P.M.D., Kumar K. Properties of high modulus PEEK yarns for aerospace applications. *Journal of Applied Polymer Science* 112(2009)2497–2510.

[56] Brünig, H., Beyreuther R., Vogel R., Tändler B. Melt spinning of fine and ultra-fine PEEK-filaments. *Journal of Materials Science* 38(2003)2149–2153.

[57] Rivaton, A., Gardette, J.L. Photodegradation of polyethersulfone and polysulfone. *Polymer Degradation and Stability* 66(1999)385–403.

[58] Massey, L. *The effect of UV light and weather on plastics and elastomers*, 2nd ed. William Andrew publishing, New York, USA, 2007.

[59] Shard, A., Badyal J.P.S. Surface oxidation of polyethylene, polystyrene, and PEEK: the synthon approach. *Macromolecules* 25(1992)2053–2054.

[60] Munro, H.S., Clark, D.T., Recca, A. Surface photo-oxidation of phenoxy resin and polyetheretherketone. *Polymer Degradation and Stability* 19(1987)353–363.

[61] Ferain, E., Legras, R. Modification of PEEK model compounds and PEEK film by energetic heavy ion and ultraviolet irradiations. *Nuclear Instruments and Methods in Physics Research Section B: Bean Interactions with Materials and Atoms* 83(1993)163–166.

[62] Claude, B., Gonon, L., Duchet, J., Verney, V., Gardette, J.L. Surface cross-linking of polycarbonate under irradiation at long wavelengths. *Polymer Degradation and Stability* 83(2004)237–240.

[63] Vaughan, A.S., Stevens, G.C. Irradiation and the glass transition in PEEK. *Polymer* 42(2001)8891-8895.

[64] Sasuga, T., Kudoh, H. Ion irradiation effects on thermal and mechanical properties of poly(ether –ether –ketone) (PEEK). *Polymer* 41(2000)185–194.

[65] Benicek, L., Chvatalova, L., Obadal, M., Cermak, R., Verney, V., Commereuc, S. *Polymer Degradation and Stability* 96(2011)1740–1744.
[66] Moura, I., Botelho, G., Machado, A.V. Journal of Polymers and the Environment 22(2014)148
J. Polym. Environ. 2014, 22, 148–157.
[67] Commereuc, S., Askanian, H., Verney, V. Celli, A., Marchese, P. Berti, C. About the end life of novel aliphatic and aliphatic-aromatic (co)polyesters after UV-weathering: structure/degradability relationships. *Polymer Degradation and Stability 98(*2013)1321–1328.
[68] Schmidt, H., Witkowska, B., Kamińska, I., Twarowska-Schmidt, K., Wierus, K., Puchowicz, D. Comparison of the rates of polypropylene fibre degradation caused by artificial light and sunlight. *Fibres & Textiles in Eastern Europe* 19(2011)53–58.
[69] Aslanzadeh, S., Haghighat Kish, M. Photo-oxidation of polypropylene fibers exposed to short wavelength UV radiations. *Fibres and Polymers* 11(2010)710–718.
[70] Rabello, M., White J.R. The role of physical structure and morphology in the photodegradation behaviour of polypropylene. *Polymer Degradation and Stability* 56(1997)55–73.
[71] Cole, K.C., Casella, I.G. Fourier transform infra-red spectroscopic study of thermal degradation in poly(ether ether ketone)-carbon composites. *Polymer* 34(1993)740–745.
[72] Cole, K.C., Casella, I.G. Fourier transform infrared spectroscopic study of thermal degradation in films of poly(ether ether ketone). *Thermochimica Acta* 211(1992)209–228.
[73] Yao, F., Zheng, J., Qi, M., Wang, W., Qi, Z. The thermal decomposition kinetics of poly(ether-ether-ketone) (PEEK) and its carbon fiber composite. *Thermochimica Acta* 183(1991)91–97.
[74] Nandan, B., Kandpal, L.D., Mathur, G.N. Poly(ether ether ketone)/poly(aryl ether sulphone) blends: thermal degradation behaviour. *European Polymer Journal* 39(2003)193–198.
[75] Huo, R.-Z, Luo, Y.-F., Hang, L.-K, Jin, X.-G., Karasz, F.E., Kinetic studies on thermal degradation of poly(aryl ether ether ketone) and sulphonated poly(aryl ether ether ketone) by thermogravimetry. *Journal of Functional Polymers* 4(1990)426–433.
[76] Perng, L.H., Tsai C.J., Ling Y.C. Mechanism and kinetic modelling of PEEK pyrolysis by TG/MS. *Polymer* 40(1999)7321–7329
[77] Tsai, C.J., Perng L.H., Ling Y.C. A study of thermal degradation of poly(aryl-ether-ether-ketone) using stepwise pyrolysis/gas chromatography/mass spectrometry. *Rapid Communications in Mass Spectrometry* 11(1997)1987–1995.
[78] Day, M., Sally, D., Wiles, D.M. Thermal degradation of poly(aryl-ether-ether-ketone): experimental evaluation of crosslinking reactions. *Journal of Applied Polymer Science* 40(1990)1615–1620.
[79] Buggy, M., Carew, A. The effect of thermal ageing on carbon fibre reinforced polyetheretherketone (PEEK). Part II Morphological changes. *Journal of Materials Science* 29(1994)2255–2259.
[80] Jar, P.-Y., Kausch, H.H., Cantwell, W.J., Davies, P., Richard, H. The effect of annealing on the short and long term behavior of PEEK. *Polymer Bulletin* 24(1990)657–664.
[81] Buggy, M., Carew, A. The effect of thermal ageing on carbon fibre reinforced polyetheretherketone (PEEK). Part I Static and dynamic flexural properties. *Journal of Material Science* 29(1994)1925–1929.
[82] Jar, P.-Y., Kausch, H.H. Annealing effect on mechanical behavior of PEEK. *Journal of Polymer Science Part B: Polymer Physics* 30(1992)775–778.
[83] Lattimer, M.P., Hobbs, J.K., Hill, M.J., Barham, P.J. On the origin of the multiple endotherms in PEEK. *Polymer* 33(1992)3971–3973.

[84] Kampert, W. G., Sauer, B.B. Temperature modulated DSC studies on melting and recrystallization in poly(oxy-1,4-phenyloxy-1,4-phenylenecarbonyl-1,4-phenylene)(PEEK). *Polymer Engineering and Science* 41(2001)1714–1730.
[85] Wang, Z.-G., Hsiao, B.S., Sauer, B.B., Kampert, W.G. The nature of secondary crystallization in poly(ethylene terephthalate)
[86] Carlsson, D., Wiles, D. The photodegradation of polypropylene films. II. Photolysis of ketonic oxidation products. *Macromolecules* 2(1969)587–597.
[87] Carlsson, D., Wiles, D. The photodegradation of polypropylene films. III. Photolysis of polypropylene hydroperoxides. *Macromolecules* 2(1969)597–606.
[88] Han, C.D. *Rheology and Processing of Polymeric* Materials, Volume 1 – Polymer Rheology. Oxford University Press, New York, USA, 2007.
[89] Windler, L., Height, M., Nowack, B. Comparative evaluation of antimicrobials for textile applications. *Environment International* 53(2013)62–73.
[90] Meilert, K.T., Laub, D., Kiwi, J. Photocatalytic self-cleaning of modified cotton textiles by TiO_2 clusters attached by chemical spacers. *Journal of Molecular Catalysis A: Chemical* 237(2005)101–108.
[91] Uddin, M.J., Cesano, F., Scarano, D., Bonino, F., Agostini, G., Spoto, G., Bordiga, S., Zecchina, A. Cotton textile fibres coated by Au/TiO2 films: Synthesis, characterization and self cleaning properties. *Journal of Photochemistry and Photobiology A: Chemistry* 199(2008)64–72.
[92] Yuranova, T., Mosteo, R., Bandara, J., Laub, D., Kiwi, J. Self-cleaning cotton textiles surfaces modified by photoactive SiO_2/TiO_2 coating. *Journal of Molecular Catalysis A: Chemical* 244(2006)160–167.
[93] Zhong, L., Lee, C.-S., Haghighat, F. Adsorption performance of titanium dioxide (TiO_2) coated air filtes for volatile organic compounds. *Journal of Hazardous Materials* 243(2012)340–349.
[94] Yang, L., Cai, A., Luo, C., Liu, Z., Shangguan, W., Xi, T. Performance analysis of a novel TiO2-coated foam-nickel PCO air purifier in HVAC systems. *Separation and Purification Technology* 68(2009)232–237.
[95] Luo, Y., Huo, R., Jin, X., Karasz, F.E. Thermal degradation of sulfonated poly(aryl ether ether ketone). *Journal of Analytical and Applied Pyrolysis* 34(1995)229–242.
[96] Zaidi, S.M.J., Mikhailenko, S.D., Robertson, G.P., Guiver, M.D., Kaliaguine, S. Proton conducting composite membranes from polyether ether ketone and heteropolyacids for fuel cell applications. *Journal of Membrane Science* 173(2000)17–34.
[97] Robeson, L.M. *Polymer Blends*. Carl Hanser Verlag, Munich, Germany, 2007.
[98] da Costa, H.M., Ramos, V., Rocha, M.C.G. Rheological properties of polypropylene during multiple extrusion. *Polymer Testing* 24(2005)86–93.
[99] Vitkauskas, A., Miglinaite, R., Vesa, P., Puolakka, A. Mechanical properties of polypropylene multifilament yarns in dependence of their drawing ratio. *Materials Science (Medziagotyra)* 11(2005)407–410.

The Effect of Melt Spinning Process Parameters on the Spinnability of Polyetheretherketone

Ville Mylläri, Mikael Skrifvars, Seppo Syrjälä, Pentti Järvelä

Laboratory of Plastics and Elastomer Technology, Tampere University of Technology, Tampere 33101, Finland

Received 14 September 2011; accepted 1 February 2012
DOI 10.1002/app.36930
Published online 2 May 2012 in Wiley Online Library (wileyonlinelibrary.com).

ABSTRACT: This study has been carried out to investigate the processing parameters affecting polyetheretherketone's (PEEK) spinnability in a melt spinning process. PEEK has excellent mechanical and thermal properties and fibers made from it could be used in extreme environments. Different PEEK grades were characterized thermally and rheologically to see which one is the most suitable for fiber spinning. The spinning tests made with the most suitable grade (Victrex 151G) show that increased processing temperature, increased capillary diameter or shorter spinning path length improves spinnability. The best fibers made in optimal processing conditions (400°C temperature, 30/1 mm capillary, and 5 cm spinning path) were 18 μm in average diameter. Because of the limitations of the system used, variations in fiber thickness were noticeable and worsened the spinning stability. Scanning electron microscope photos confirmed these variations, and they were also visible in an optical microscope. The selected low-viscosity PEEK grade provided good spinnability but gave filaments with only mediocre mechanical properties, the tensile strength being around 280 MPa. © 2012 Wiley Periodicals, Inc. J Appl Polym Sci 126: 1564–1571, 2012

Key words: PEEK; melt spinning; fiber, spinnability, optimization

INTRODUCTION

Polyetheretherketone (PEEK) is a semicrystalline thermoplastic with excellent mechanical and thermal properties and chemical resistance. PEEK has very low water absorption, low flammability, good radiation resistance, and good electrical properties. PEEK's continuous use temperature of 260°C is one of the highest among all plastics. It is approved by food and drug administration. Because of its high price (100 €/kg) PEEK is normally used in high-tech applications such as medical devices, space applications, and as metal replacement.[1,2] The commercial applications of PEEK fibers are currently dry filtration, chemical separation, sport strings, braids, brushes, and cords.[3]

Melt spinning is a process where melt polymeric material is pushed through a small-hole (spinneret), then cooled down by cold air and finally drawn onto a roll by a winding unit.[4] Melt spinning of PEEK is not a new invention. In fact, it has been done since the 1980s.[3] There have been studies concerning melt spinning of ultrafine PEEK filaments[5,6] and even one dissertation about PEEK melt spinning.[7] Ziabicki first stated the six processing parameters affecting spinnability in a melt spinning process: processing temperature, dimensions and the number of spinneret holes, mass throughput, length of the spinning path, take-up velocity and cooling conditions.[4] There are previous data available on how processing parameters affect spinnability generally[4,8–12] and also for PEEK,[6,7] but in these studies, a deeper understanding regarding the relationship between processing parameters and the best spinnable fiber diameter is lacking. Fourne and Golzar have given fairly similar list of suggestions how to spin very thin filaments.[7,9] However, these recommendations do not state what are the actual effects on the spinnability. Golzar has also created a fiber stability map for Victrex PEEK 151G but this map do not show the effects of PEEK grade, processing temperature, capillary dimensions, and the length of the spinning path to the best spinnable fiber diameter.[7] Although the effects of processing parameters are well known in a qualitative level, there is limited amount of literature data available how these processing parameters affect the best spinnable fiber diameter on a quantitative level.

Theoretically, an increase in processing temperature should improve spinnability as Fourne first suggested in 1995.[9] According to Golzar's tests, this is the case with PEEK also.[7] The normal processing temperature of PEEK is 360–400°C, so 400°C should provide the best spinnability. Repkin have shown that increasing the capillary diameter improves process quality and decreases the number of failures.[12]

Correspondence to: Ville Mylläri (ville.myllari@tut.fi).
Contract grant sponsor: European Union's Seventh Framework Programme; contract grant number: FP7/2007-2013 (grant agreement no. 228439).

In addition to the diameter, the length/diameter (L/D) ratio also affects spinnability. Several publications have shown that the die swell-ratio (the ratio of maximum polymer mass diameter after the capillary and the diameter of the capillary) decreases when L/D-ratio increases.[9,11] It is important to minimize the die swell because it weakens the quality of the fibers by making them more irregular.[4] This means that theoretically capillary should be long and large. Previous studies have shown that short spinning paths should preferably be used when making ultrafine filaments.[7,9] Stress in the spinning line increases along with the spinning path length thus increasing the change of failure.[7,13]

The goal of this project is to manufacture fine PEEK filaments by a lab-scale melt extrusion spinning process and to optimize the most important processing parameters. To get filaments of even quality, and with optimal properties, it is necessary to fine-tune the process parameters (such as piston speed, melt temperature, length of cooling path, etc.). The obtained PEEK filaments where then thoroughly characterized so that any material related problems (e.g., thermal degradation of PEEK, filament breaking) can be minimized during the fiber spinning. The obtained results from the PEEK fiber characterization were then compared with results from previous studies reported in the literature and were also used to evaluate the spinning process.

EXPERIMENTAL

Materials

Four PEEK grades from Victrex (Lancashire, UK) were used in the study. Three of the grades are in granular form: 151G, 381G, and 450G, and one grade, 704, is a powder. These grades have different molecular weights and rheological properties according to the supplier data.[14] The thermal properties are very similar between the grades, whereas the mechanical properties have more variation. The properties for the granulate grades can be seen in Table I. Powder grade 704 is designed for coatings but was briefly tested in the fiber spinning trials also.

TABLE I
Properties of the PEEK Grades Used[14]

Property\grade	151G	381G	450G
Melting point (°C) ISO11357	343	343	343
Glass transition (°C) ISO11357	143	143	143
Melt viscosity (Pa s) ISO11443	130	300	350
Tensile strength (MPa) ISO527	110	100	100
Tensile modulus (GPa) ISO527	3.9	3.7	3.7
Tensile elongation (%) ISO527	25	40	45
Izod impact strength (kJ m^{-2}) ISO180/A	5.0	6.5	7.5

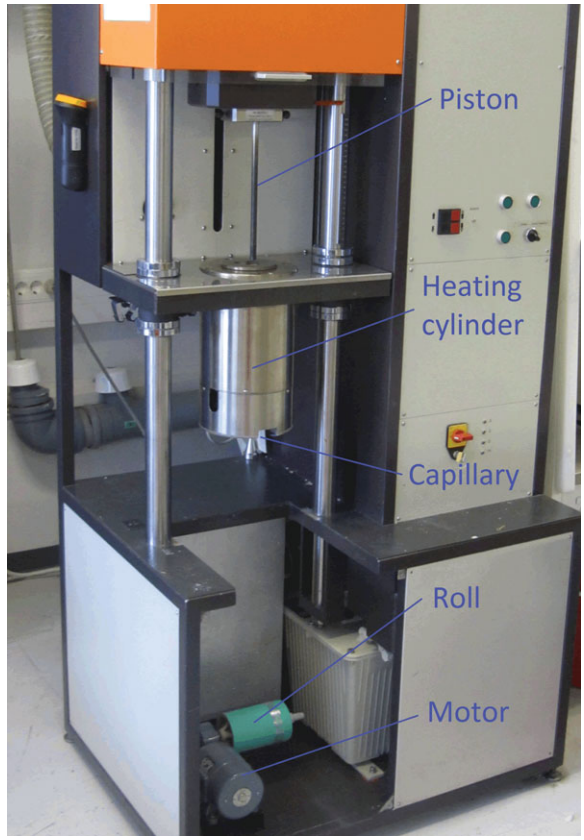

Figure 1 Göttfert capillary rheometer. [Color figure can be viewed in the online issue, which is available at wileyonlinelibrary.com.]

Melt spinning

The PEEK melt-spinning system was based on a modified Göttfert Rheograph 6000 capillary rheometer, which can be seen in Figure 1. It is a piston-based system with a maximum temperature of 400°C and volume of about 26 cm^3. The barrel is 12 mm in diameter and 230 mm in length. The maximum length of the capillary used is 30 mm, and its typical diameter is 1 mm. It is possible to manufacture only monofilaments with the system. The filament winding motor unit is located under the capillary and has a maximum speed of about 350 RPM. The roll used in the winder has a diameter of 87 mm, giving a fiber production rate of roughly 100 m/min at full motor speed.

The limit of spinnability was evaluated experimentally. Step by step, the piston speed (fiber diameter) was decreased until the limit was found. If the fiber did not break in 1 min, the process was estimated to be stable. If this was not the case during the first five trials then the limit was found.

Characterization

Differential scanning calorimetry (DSC) tests were carried out in a Netzsch DSC 204 F1 heat-flux DSC.

All the tests were carried out in nitrogen atmosphere. This corresponds to the melt spinning conditions used, as PEEK is not in contact with oxygen in the closed barrel. During the conventional DSC test, PEEK was heated from room temperature to 400°C, then cooled down to room temperature and then heated once more. The heating/cooling rate was 20°C/min. The PEEK sample was also kept at constant 400°C temperature in a DSC analyser for about 18 h to see whether it degrades thermally. The thermogravimetric analysis (TGA) tests were made with a Perkin-Elmer TGA 6. The PEEK samples were heated in a nitrogen atmosphere at a rate of 10°C/min from room temperature to 1000°C.

Capillary rheometer tests were made with the same Göttfert Rheograph 6000 capillary rheometer which was used in the melt spinning. During the rheometer tests a 30/1-mm capillary was used. Test runs were carried out from low to high shear rates and then back. A 140-MPa pressure sensor was used during the tests. The Rabinowitsch correction was made to the capillary rheometer data. The Bagley correction could not be made because only one capillary was used during the capillary rheometer tests.

Rotational rheometer characterizations were carried out with Anton Paar Physica MCR 301 equipment. Tests were carried out with plate–plate geometry in a nitrogen atmosphere. The used tests were constant shear rate tests from low to high shear rates.

The mechanical testing of the filaments was made according to the standard ISO 5079:1995 "Textiles fibres—Determination of breaking force and elongation of individual fibres" by using Lenzing Vibroskop and Vibrodyn. Instead of the recommended 50 measurements, only 20 were done because PEEK is a synthetic fiber and causes problems with the Vibroskop. First, the Vibroskop was used to determine the Tex number and then the same fiber was stretched until breaking. The advantage of measuring the Tex number first is that more accurate data are obtained because fiber cross-sectional density is known.

A conventional optical microscope was used to measure the fiber thickness at ×1000 magnification. A bunch of fibers was spread onto the microglass plate, and by using the microscopes rotating measuring scale the filament diameter could be read. The diameters of total of 60 individual fibers were measured, to ensure reproducibility. A Philips XL30 scanning electron microscope (SEM) was used to investigate the morphology of the produced PEEK filaments.

Theoretical calculations

The piston speed in the Göttfert capillary rheometer can be controlled by a computer in a fairly accurate manner. The control program calculates the shear rate for different capillaries and piston speeds.

Mass throughput ($m_{\text{throughput}}$) can be calculated from the piston speed (v) if the material density is known, using Eq. (1)—PEEK's melt density (ρ) varies as a function of temperature and pressure, which makes the calculations for exact mass throughput difficult. Therefore, the density's literature value for solid PEEK (1.32 g/cm^3) has been used, which may cause some inaccuracy. Barrel radius (r) is 0.6 cm. The unit for v_{piston} is (cm/s), barrel radius is (cm), and for $m_{\text{throughput}}$ (g/min).

$$m_{\text{throughput}} = v_{\text{piston}} * \pi * r_{\text{barrel}}^2 * \rho * 60\,\text{s/min} \quad (1)$$

The theoretical fiber diameter can be expressed as a function of the piston speed. The very simplified formula for fiber diameter in the system used is:

$$\oslash = 0.30\,(\text{mm/s})^{0.5} * (v_{\text{piston}})^{0.5} \quad (2)$$

where the fiber diameter Ø is in mm, and v_{piston} in mm/s. A more detailed formula can be found in Reference 15.

The Tex number is commonly used to measure sizes in linear and continuous products such as cables and fibers. It is a measure of linear mass density. One tex is the mass in gram for a 1000-m-long filament, and it is commonly regarded as the fiber fineness. Decitex is also used, it is the mass in grams for a 10,000-m-long fiber. The decitex-number can be expressed as a function of the fiber diameter if the density of the material is known. In the calculations, PEEK's density of 1.32 g/cm^3 has been used.

$$\text{dtex} = 250,000 * \oslash^2 * \pi * \rho \quad (3)$$

The unit of dtex is (g/10,000 m), Ø (cm), and ρ (g/cm^3).

RESULTS AND DISCUSSION

Thermal characterization

Before starting the fiber spinning tests, the PEEK grades were characterized thoroughly. Theoretically PEEK should have excellent thermal properties, and the thermal characterization techniques DSC and TGA were used to verify this. These thermal tests were done on the grades 151G and 381G.

A conventional DSC test, where the temperature changes at a constant rate, shows that both grades have good and almost similar thermal properties (Fig. 2). This is in line with the literature data provided by Victrex.[14] The peak melting temperature is around 340°C. The curves for the first and second heating are almost similar, so there is no evident

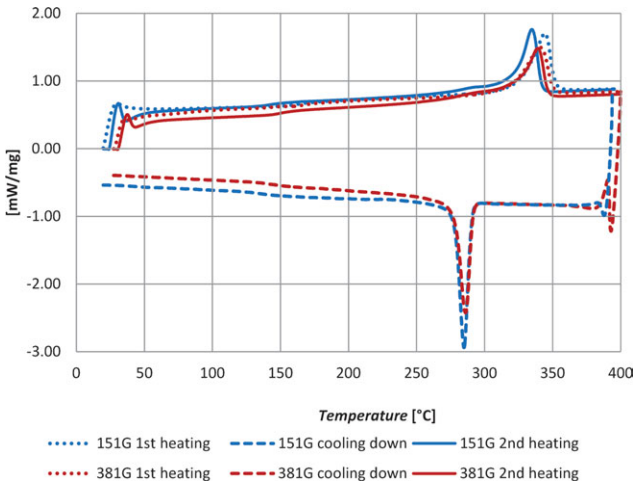

Figure 2 DSC scans for grades 151G and 381G. [Color figure can be viewed in the online issue, which is available at wileyonlinelibrary.com.]

thermal history, and no thermal degradation occurs during the measurements. Victrex recommends the minimum processing temperature to be 360°C, and according to the DSC tests, PEEK is completely melted at this temperature.

A DSC test where the PEEK grades 151G and 381G were kept under nitrogen atmosphere at 400°C for 18 h did not show any signs of thermal degradation, because the curve is a flat line. This is important because during the processing in the equipment PEEK may stay for hours at high temperatures in the barrel. Thermal degradation would worsen the mechanical properties and make fiber spinning more difficult or even impossible. This thermal stability is in line with the expected thermal stability for PEEK.

TGA test data in Figure 3 also shows the excellent thermal properties of PEEK. PEEK's mass remains the same up to a temperature of 550°C for both grades. For some reason, grade 381G loses mass faster than grade 151G at temperatures higher than

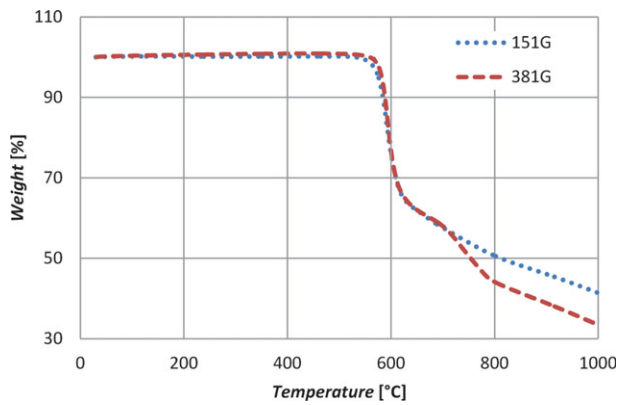

Figure 3 TGA test for grades 151G and 381G. [Color figure can be viewed in the online issue, which is available at wileyonlinelibrary.com.]

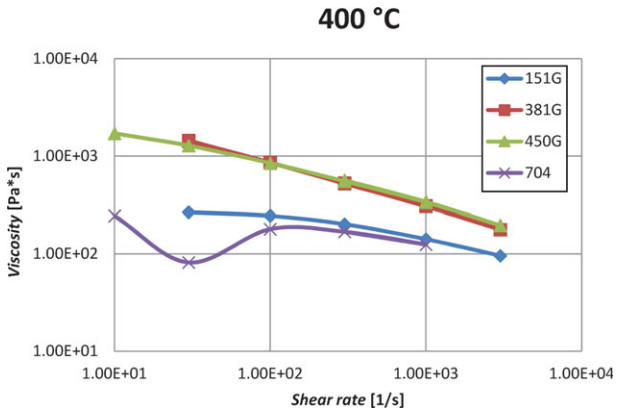

Figure 4 Capillary rheometer test at 400°C for grades 151G, 381G, 450G, and 704. [Color figure can be viewed in the online issue, which is available at wileyonlinelibrary.com.]

700°C, but this difference is not significant in the applications for PEEK fibers. At 1000°C, 40% of the mass of PEEK's grade 151G is still left, which must be considered remarkable for an organic plastic material.

Rheological characterization

Viscosity tests at 400°C were made on all four PEEK grades and at the same time, the rheological behavior in the melt spinning was also evaluated. Figure 4 shows that the viscosities of grades 381G and 450G are almost similar. This is not surprising considering that the grade number indicates viscosity at 400°C temperature and 1000 1/s shear rate according to the Victrex own test TM-VX-12.[14] The viscosity of grade 151G is therefore considerably lower. The grade number does not correlate with the viscosity of the powder grades, in fact the viscosity of grade 704 is the lowest of the used grades. Because of its powder form, it was very difficult to load grade 704 into the rheometer barrel. The powder got stuck into the barrel walls, and during the measurement, the piston had difficulties to move. Therefore, the test results with grade 704 are inconsistent at least with small shear rates, and the test was not repeated.

Capillary rheometer tests were carried out from low to high shear rates and then back. The obtained results give very similar data regardless of the direction of the measurement. The high viscosity grades 381G and 450G have more shear thinning effects than the low viscosity grade 151G. Fiber spinning tests are done at very small shear rates, so the differences in viscosities are in fact greater than the differences in the manufacturer's theoretical values.

Additional viscosity tests were made on grades 151G and 381G (Fig. 5) which seem to be the best candidates for fiber spinning. Grade 704 was not tested because of its powder form and grade 451G

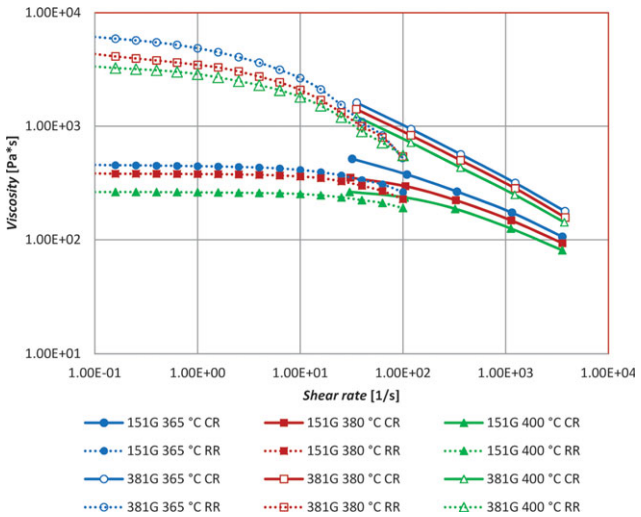

Figure 5 Capillary (CR) and rotational rheometer (RR) tests at different temperatures for grades 151G and 381G. [Color figure can be viewed in the online issue, which is available at wileyonlinelibrary.com.]

was left out of the testing because it is very similar to grade 381G. Grades 151G and 381G were tested at three different temperatures with a capillary and also with a rotational rheometer. Very small shear rates are difficult to test with a capillary rheometer, and therefore, a rotational rheometer was used.

The results show that the used PEEK grade affects viscosity more than temperature. PEEK grade 381G has a higher viscosity at 400°C than 151G has at 365°C. Shear thinning of grade 381G begins at significantly low shear rates compared with grade 151G. Values measured with the capillary rheometer are a little higher than those measured with the rotational rheometer at the same shear rates. One reason for this is that the capillary rheometer tests were made with only one capillary, and therefore, the Bagley correction could not be made. The second possible reason is the melt fracture effect that happens at high shear rates with the rotational rheometer. This is evident at least with grade 381G at shear rates higher than 20 1/s.

Fiber spinning

Four PEEK grades were initially used in the experimental study, and according to the preliminary tests, one of these grades, 151G, was selected for the large-scale melt spinning experiments. The decision was based not only on fiber properties but also on the ease to load and clean the material. The spinning properties of the grades can be found in Table II. To find the optimal melt spinning parameters, a rather extensive experimental program is necessary to do, and therefore the chosen PEEK grade should be not only easy to spin but also easy to load into the barrel and clean afterwards, to minimize the time for the trials.

The differences between fiber properties (minimum fiber diameter) were so remarkable that very precise tests for all grades were not needed. The powder grade 704 was almost impossible to load into the barrel, which is unfortunate because it seemed to give fibers with very good properties. Preliminary tests indicate that good fiber properties are related to low viscosity because lower viscosity grades seemed to have better spinnability. Lower viscosity grades were also easier to clean afterward because they did not stick tightly to the piston and barrel walls.

Testing of all possible process parameter combinations would not have been possible for practical reasons. Therefore, it was decided to first evaluate the more important parameters and then use the obtained results in subsequent experimental work. The importance of a parameter was estimated by the preliminary tests and data obtained from the literature review. The order of the parameters tested was the material grade, processing temperature, capillary dimensions, and the length of the spinning path. The results can be found in Table III.

As the preliminary tests showed, low-viscosity grades have much better spinnability compared to high-viscosity grades. The differences in average filament diameter are significant. The best fibers achieved with grade 381G were 39 μm in diameter and for grade 151G 19 μm in diameter.

The first actual processing parameter tested was the processing temperature. As mentioned in the introduction, an increase in processing temperature should improve spinnability and according to our tests, this is really the case. The best processing temperature was 400°C. However, the improvement is rather small compared to processing at 385°C. At 370°C, it was difficult to get the process stable at all because the fiber diameter varied all the time. At higher temperatures, this problem was not visible to the naked eye.

The second tested parameter was the capillary dimensions. There are a lot of combinations for capillary diameter and length. Unfortunately, there were several problems especially with short capillaries. The only suitable capillary length turned out to be 30 mm, which is the longest possible in the system used. Spinning with shorter capillaries was

TABLE II
Grade Selection Table

Grade	151G	381G	450G	704
Fiber properties	Good	Moderate	Moderate	Very good
Loading	Easy	Easy	Easy	Very difficult
Cleaning	Normal	Difficult	Difficult	Normal

TABLE III
Spinnability in Different Processing Parameters

Grade	381G	151G	151G	151G	151G	151G
Temperature (°C)	400	400	385	370	400	400
Capillary diameter (mm)	1.0	1.0	1.0	1.0	0.75	1.0
Length of the spinning path (cm)	40	40	40	40	40	5
Shear rate (1/s)	19.0	4.6	4.8	7.9	18.0	4.0
Lowest stable piston speed (mm/s)	0.0165	0.0040	0.0042	0.0069	0.0066	0.0035
Theoretical mass throughput (g/min)[1]	0.15	0.036	0.038	0.062	0.059	0.031
Theoretical diameter (μm)[2]	39	19	19	25	24	18
Theoretical tex-number (dtex)[3]	15.4	3.7	3.7	6.5	6.2	3.3

impossible because the process was stable for only a few seconds at best. The reason for this is most likely the high temperature air PEEK encounters when using short capillaries. If a full-length capillary is not used then PEEK comes out inside a hot tube (the capillary is inside the barrel). The second problem was the gravitational self-flow of PEEK when using very large capillaries (>1 mm). With a 1.5 mm capillary, the process was stable without the piston movement. Therefore, only two capillaries were tested: 1.0 and 0.75 mm. Spinnability turned out to be considerably better with a 1.0 mm capillary.

The third tested parameter was the length of the spinning path. Normally, the spinning path is several meters long, but there was not much room under the capillary in the used experimental setup. Therefore, spinning path length could not affect the spinnability in the system used significantly. Most of the tests were made with a 40-cm spinning path, but one test was made with very short spinning path and it improved spinning stability even further. Very thin fibers cool down rapidly, so very short spinning paths can be used.

As a conclusion, the best processing parameters in the system used were the 400°C processing temperature, 30/1 mm capillary, and very short spinning path. The best spun fibers were 18 μm in average diameter. According to these tests, process optimization should be started from the material grade, because it affects more to the viscosity than any other parameter. Mass throughput of grade 381G had to be increased by 317% to get the process as stable as grade 151G is in similar spinning conditions. Processing temperature should be above 385°C because then the increase in stable mass throughput is only 6% from 400 to 385°C but 72% from 400 to 370°C. Changing capillary diameter from 1 to 0.75 mm worsens spinnability nearly as much as decreasing temperature from 400 to 370°C. The length of the spinning path is the least important of these processing parameters because the increase in stable mass throughput is only 16% from 5 to 40 cm. In industrial scale systems, the spinning path is longer thus affecting more to the spinnability. Obtained spun PEEK fibers can be seen in the optical micrographs in Figure 6. The optical microscope confirms the huge variations in fiber thickness, the average being 25 μm and the standard deviation 5.2 μm. The minimum detected value was 14 μm and maximum 36 μm. Variations can also be seen in the more detailed SEM micrograph in Figure 7.

Figure 6 Spun PEEK filaments. [Color figure can be viewed in the online issue, which is available at wileyonlinelibrary.com.]

Mechanical properties and fineness

The obtained filaments were tested to evaluate their fineness and tenacity. For the mechanical tests, a

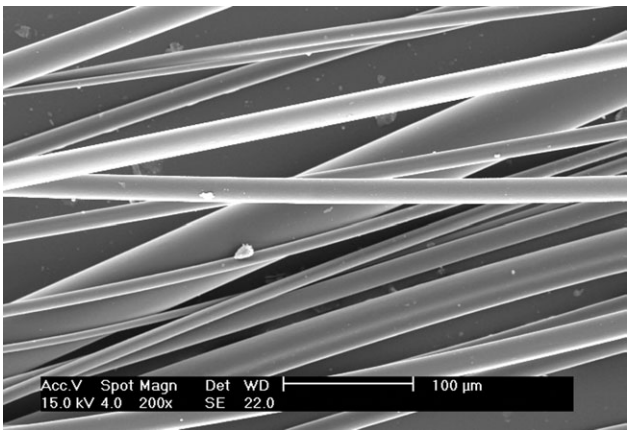

Figure 7 SEM photo of PEEK fibers.

sufficient amount of 25-μm diameter fiber was manufactured according to the otherwise optimal processing parameters (Victrex 151G, 400°C, 30/1 mm, 5 cm, and 100 m/min). The following can be concluded from the test data: The obtained fiber diameter is not homogenous, as Tex numbers vary from 3.1 to 9.9 dtex, with an average of 6.2 dtex. The tensile strength for the filaments is 2.2 cN/dtex, corresponding to about 280 MPa (ratio is 100ρ). This is slightly below the expectations based on previously reported studies made with PEEK.[7] The standard deviation of tensile strength is very small, only 0.24 cN/dtex, which indicates good experimental reproducibility. Elongation at break, however, varies more, the average being 150%, which is much more than anticipated. It is evident that thick fibers have higher elongation at break. This could mean that there is a limit in thickness near 10 μm where PEEK fibers break. Fiber parts that have stretched relatively more during the winding cannot stretch more during the tensile testing and vice versa. Young's modulus at 1% elongation is higher with thinner fibers, the average being about 19.7 cN/dtex (2.6 GPa).

The Victrex grade 151G has a very low viscosity probably as a result of a small molecular weight. This means that many of the mechanical properties are inferior compared to higher viscosity grade PEEK's.[16] Another reason for the low mechanical properties is the low degree of crystallisation of PEEK fibers measured by a DSC test (at 100% crystallization level $\Delta H_F = 130$ J/g).[17] According to this DSC test, 25 μm fiber had only 11% degree of crystallization which is very low compared with the theoretical maximum of about 40%. Golzar's tests show that increasing the take-up velocity or decreasing the mass throughput increases the degree of crystallization.[7] In the spinning system used, the bottleneck is the spinning motor which is not capable of higher take-up speeds than 100 m/min.

CONCLUSIONS

Fiber spinning of PEEK is relatively easy despite the high melt temperatures needed. The results of thermal tests confirm the very unique thermal properties of PEEK polymers. During the fiber spinning tests, the best achieved fibers were 18 μm in average diameter. There are several processing parameters affecting the limits of spinnability. The most important parameters were estimated to be viscosity related; material grade and processing temperature. Spinnability improved when the material viscosity decreased. However, viscosity could not be decreased limitlessly, because at some point, PEEK started to flow out from the capillary faster than piston moved.

The biggest drawbacks of the melt spinning system were related to Göttfert's structure which is designed for viscosity measurements, not for fiber spinning. A typical conventional spinning line cannot be used with PEEK because of the high processing temperatures needed. The biggest downside of the system used is the resulting high variations in obtained fiber thickness. This most definitely affects the limits of spinnability because the thinnest fiber parts were about 10 μm in diameter. The second reason for the big variations may be the motor system used. Although easy to control and use, it is still a bit old-fashioned. The requirements for very thin filaments are high and they do not allow any rough acceleration.

If the setup were to be optimized further then the first step would be a new motor system. The structure of Göttfert cannot be changed, except by replacing the used capillaries with capillaries of another size. However, a basic problem with process is the absence of mixing, which is present in all piston type melt spinning systems.

One important processing parameter which could not be tested in this study was the windup motor speed's effect on the limits of spinnability. The motor system used had no RPM screen and therefore had to be used at full speed. Further and more precise experimental trials would require a more advanced motor system such as a precise AC servo motor.[18] It would also be useful to know the mechanical properties of fibers of a same diameter manufactured at different take-up velocities.

The authors express their gratitude to Enrico Fatarella who provided some of the PEEK grades for testing, the Laboratory of Fiber Material Science at Tampere University of Technology for providing the windup spinning motor, Sinikka Pohjonen for thermal characterization, Jyri Öhrling for help during the spinning tests, and all the other people who contributed in some other way.

References

1. Platt, D. K.Engineering and High Performance Plastics Market Report; Smithers Rapra Technology: Shawbury, 2003.
2. Sabu, T.; Visakh, P. M. Handbook of Engineering and Speciality Thermoplastics: Polyethers and Polyesters; New York: Wiley, 2011; Vol. 3, Chapter 3, p 55.
3. Zyex Ltd. Manufacturer of PEEK fibers. Available at: http://www.zyex.com. Accessed June 13, 2011.
4. Ziabicki, A.Fundamentals of Fiber Formation; Wiley-Interscience: London, 1976.
5. Shekar, R. I.; Kotresh, T. M.; Rao, P. M. D.; Kumar. K. J Appl Polym Sci 2009, 112, 2497.
6. Brünig, H.; Beyreuther, R.; Vogel, R.; Tändler, B. J Mat Sci 2003, 38, 2149.
7. Golzar, M.Melt spinning of the fine PEEK filaments. Dissertation, Technische Universität Dresden, Dresden, 2004.
8. Gupta, V. B.; Kothari, V. K.Manufactured Fibre Technology; Springer: London, 1997.

9. Fourné, F. Synthetic fibers: Machines and Equipment, Manufacture, Properties: Handbook; Hanser Gardner: Munich, 1999.
10. Gupta, V. B.; Mondal, S. A.; Bhuvanesh, Y. C. J Appl Polym Sci 1997, 65, 1773.
11. White, J. L. Fiber and Yarn Processing; Wiley: New York, 1975.
12. Repkin, Y. S. Fiber Chem 1972, 3, 377.
13. Shimizu, J.; Kikutani, T. J Appl Polym Sci 2002, 83, 539.
14. Victrex, PLC. Leading manufacturer of PEEK. Available at: http://www.victrex.com. Accessed June 14, 2011.
15. Mylläri, V. Production of filament yarns made of PEEK. Master of Science Thesis, Tampere University of Technology, Tampere, April 2011.
16. Yuan, M.; Galloway, J. A.; Hoffman, R. J.; Bhatt, S. Polym Eng Sci 2011, 51, 94.
17. Blundell, D. J.; Osborn, B. N. Polymer 1983, 24, 953.
18. Firoozian, R.; Servo Motors and Industrial Control Theory; Springer: New York, 2008.

Polymer Degradation and Stability 109 (2014) 278–284

Contents lists available at ScienceDirect

Polymer Degradation and Stability

journal homepage: www.elsevier.com/locate/polydegstab

The effects of UV irradiation to polyetheretherketone fibres – Characterization by different techniques

Ville Mylläri [a, *], Tero-Petri Ruoko [b], Pentti Järvelä [a]

[a] Department of Material Science, Tampere University of Technology, Tampere 33101, Finland
[b] Department of Chemistry and Bioengineering, Tampere University of Technology, Tampere 33101, Finland

ARTICLE INFO

Article history:
Received 23 April 2014
Received in revised form
10 July 2014
Accepted 4 August 2014
Available online 12 August 2014

Keywords:
PEEK
Fibre
Ultraviolet
Rheology

ABSTRACT

The effects of UV irradiation on polyetheretherketone (PEEK) fibres were investigated in this study. PEEK fibres were manufactured with a melt spinning system and then artificially aged with simulated solar UV light. Fibres were then characterized by mechanical tests, Fourier transform infrared spectroscopy (FTIR), differential scanning calorimetry (DSC), rheology, thermogravimetric analysis (TGA) and scanning electron microscopy (SEM). PEEK, best known for its excellent thermal stability, suffered greatly from the effects of UV irradiation. The low UV stability manifested as embrittlement of the fibres in the mechanical tests, increased crosslinking rate in the rheological tests, formation of carbonyl and hydroxyl groups and changes in the nature of the carbon–hydrogen bonds in the FTIR, diminished thermal properties in TGA, and transverse cracks in the SEM photos. DSC was found to be an inaccurate technique for estimating the degradation level of PEEK fibres, whereas the carbonyl index measured by FTIR was found to be the most convenient technique.

1. Introduction

UV irradiation of polymeric materials is an important area of research since many polymers must withstand extended outdoor exposure. Long exposure to UV light causes polymers to degrade, which can be observed as discolouring, embrittlement, loss of mechanical properties and therefore a greatly shortened product lifetime [1–5]. The study of speciality and high performance polymers has gained more interest because their degradation behaviour, which often occurs only in extreme conditions, is not as well studied as that of commodity plastics [6–9].

Polyetheretherketone (PEEK) is a linear, aromatic, semi-crystalline and rather expensive thermoplastic (Fig. 1). It has excellent thermal properties and chemical resistance, low flammability, low water absorption and good radiation resistance. Because of these properties, PEEK is commonly used in high-tech applications such as space products, medical devices, and as a metal replacement [10,11]. Commercial PEEK fibres can be found in process belting, filtration mesh, wiring harnesses, strings, threads, and composites [12]. PEEK has a high processing temperature of 360–400 °C, which limits the processing possibilities because typical extrusion or injection moulding equipment is not capable of withstanding temperatures that high.

Most degradation studies of PEEK have concentrated on the high-temperature thermal behaviour [13–16] since PEEK has one of the highest continuous use temperatures (260 °C) among plastics. UV degradation of PEEK has been studied primarily from the chemical point of view [8,17–19] and studies of its mechanical properties are not as common [7]. Studies of the UV resistance of PEEK fibres were not found in the literature. Polymer fibres often have special characteristics in properties like mechanical strength, sample thickness, and polymer chain orientation, which makes testing of fibre form samples desirable [20–23].

PEEK, like most linear polyaromatics, degrades under UV irradiation [7,9,24]. As an aromatic chain polymer PEEK absorbs practically all UV radiation of wavelengths under 380 nm [8]. As the incident solar spectrum begins at 290 nm, natural UV radiation is strongly absorbed by PEEK generating photochemical oxidation reactions. Photooxidation forms products in the polymer sample that extend its light absorption well into the visible region, leading to an observable yellowing caused by the absorption of blue light and further accelerating the rate of photodegradation. UV light induced ageing is a major factor affecting the lifetime of PEEK products, and it can also cause great economic losses.

This article will concentrate on artificial UV testing of fibre form PEEK samples. UV testing of fibres has many advantages when

* Corresponding author. Tel.: +358 401981683.
E-mail address: ville.myllari@tut.fi (V. Mylläri).

http://dx.doi.org/10.1016/j.polymdegradstab.2014.08.003
0141-3910/

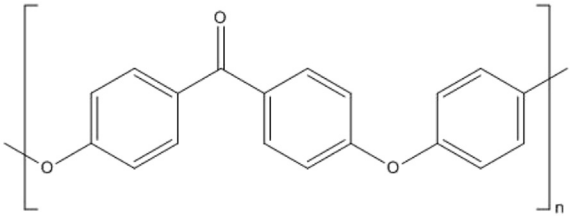

Fig. 1. The chemical structure of PEEK.

compared to the more commonly used sheets or tensile testing specimens. Fibres have a high surface area to volume ratio, which makes ageing faster because the chemical reactions occur primarily in the surface layer. Samples were irradiated for 0–1056 h, after which the mechanical properties, DSC, TGA, FTIR, SEM and rheology were measured. Rheology is rarely used for studying the ageing of materials, but provides useful information on degradation behaviour like relative amounts of competitive chain scission and crosslinking reactions [25–27]. The goal of this article is to use a wide range of characterization techniques to measure changes in the fibres and estimate the suitability of the techniques for the study of photodegraded PEEK fibres.

2. Experimental

2.1. Samples and irradiation

Samples were made of Victrex (Lancashire, UK) PEEK grade 151G. This is a semicrystalline, easy flow grade with no inherent UV stabilizers. PEEK fibres were manufactured by a melt spinning process using a Göttfert Rheograph 6000 to melt and pump the material. The processing temperature was 380 °C, capillary dimensions 30/1 mm and piston speed 0.5 mm/s. Fibres were drawn by gravity because the use of a spinning motor would have led to unnecessarily small fibre diameters. The final diameter of the fibres was very homogenous at 410 ± 10 μm.

The UV irradiation chamber (1260 × 710 × 450 mm) has four Q-Lab UVA-340 fluorescence lambs with peak intensity at 340 nm. Irradiance of the UVA-340 lambs corresponds well with sunlight in the critical short wavelength region [28]. The oldest lamp was changed every 400 h so the total working life of the lamps was 1600 h. The UV irradiation chamber was characterized using Bentham DM150 double-monochromator spectroradiometer equipped with measurement head UV-J1002 from CMS Schreder. The chamber was symmetrically divided into nine measuring points and the average of these was used. The focal plane of the measurement head was approximately at the height of 16 cm from the bottom. The dose rate at the UVB range (290–315 nm) was 0.7 W/m^2, at the UVA range (315–400 nm) 12.1 W/m^2, and at the visible range (400–600 nm) 3.1 W/m^2.

For the UV irradiation tests, PEEK fibres were cut and taped to a 600 × 400 mm frame. PEEK samples were kept in the chamber for 0, 144, 384, 720 and 1056 h so that both sides of the samples were irradiated for the same amount of time. The corresponding total doses were 0, 8250, 22,000, 41,300 and 60,500 kJ/m^2. Temperature of the UV chamber was 33 °C.

2.2. Measurements

The tensile testing of the fibres was made with an Instron 5967 according to the standard ISO 5079:1995. The initial length was 20 mm and the drawing rate 20 mm/min. Instead of the recommended 50 measurements, only 10 samples per irradiation time were measured due to the long duration of the testing procedure. The modulus was calculated by the software using linear regression techniques according to the standards EN10002 and ASTM E8. Tests were made with a 2 kN power shell.

FTIR measurements were made with a Bruker optics tensor 27 using ATR (attenuated total reflectance) mode. Samples were tested between 400 and 4000 cm^{-1}, using 16 measurements and resolution of 4 cm^{-1}. Measurements were made using four parallel fibres and the average of five measurements was used to minimize errors. The data was baseline corrected using the average absorbance of 3800–4000 cm^{-1} as a reference. The carbonyl index was calculated as the ratio of the aged and unaged peak intensities at 1716 cm^{-1}. To calculate the peak areas for the crystallization measurements, the baseline corrected FTIR data was integrated using OPUS software.

DSC tests were carried out in a Netzsch DSC 204 F1 heat-flux DSC. All the tests were performed under nitrogen atmosphere. During the DSC tests, materials were heated from room temperature to 400 °C, then cooled to room temperature and heated once more. The heating/cooling rate was 20 °C/min. To minimize errors each fibre was measured 5 times.

Oscillatory shear measurements within the linear viscoelastic range were carried out on the samples using an Anton Paar Physica MCR 301 rheometer. All the experiments were performed under a nitrogen atmosphere using a 25 mm plate–plate geometry. The measuring points with decreasing frequency in the angular frequency range of 0.1–562 rad/s were recorded at 380 °C.

TGA tests were made with a PerkinElmer TGA 6. Samples were heated from room temperature to 995 °C in synthetic air (20% O_2/80% N_2) and nitrogen (100% N_2) with a heating rate of 10 °C/min.

A Philips XL30 scanning electron microscope (SEM) was used to investigate the morphology of the PEEK fibres. The fibres were broken with liquid nitrogen for the transverse investigations.

3. Results and discussion

3.1. Tensile properties

Breaking strength, yield strength, and Young's modulus decrease only a little as the irradiation time increases (Table 1). Fibres irradiated for 1056 h lost approximately 5–15% of their original strength and elastic modulus. These changes are small when compared to the changes in their elongations, because 1056 h irradiated fibres became brittle and lost 96% of their original elongation at rupture. Pristine PEEK fibres were very ductile with over 300% elongation at rupture. The changes in the elongations at rupture are fairly linear on a logarithmic scale as can be seen in Fig. 2. An exponential trendline gives R^2-value of 0.87.

The relative variance in the elongations is the highest in the medium aged (144 h, 384 h and 720 h) samples. UV irradiation causes chain scission reactions in the polymer chains which has a special significance in the fibres since they have a high degree of orientation. In pristine PEEK the polymer chains are untouched, thus the elongation at rupture is high and the variance relatively

Table 1
Tensile properties of UV irradiated PEEK fibres.

Time [h]	Yield strength [MPa]	Tensile strength at rupture [MPa]	Elongation at rupture [%]	Modulus [MPa]
0	83.2 ± 2.0	87.6 ± 1.9	311 ± 9	2340 ± 55
144	80.5 ± 1.0	78.6 ± 0.8	173 ± 25	2290 ± 95
384	78.7 ± 1.5	78.0 ± 1.3	137 ± 23	2400 ± 71
720	79.6 ± 1.0	74.4 ± 1.0	49 ± 8	2200 ± 50
1056	77.8 ± 2.0	72.3 ± 1.6	13 ± 1	1980 ± 80

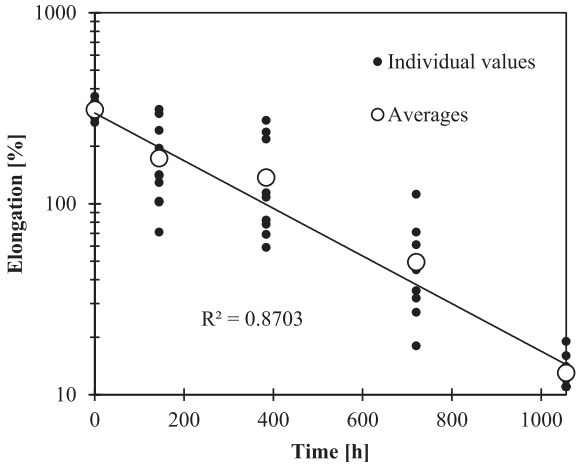

Fig. 2. Elongation at break on a logarithmic scale for UV irradiated PEEK fibres.

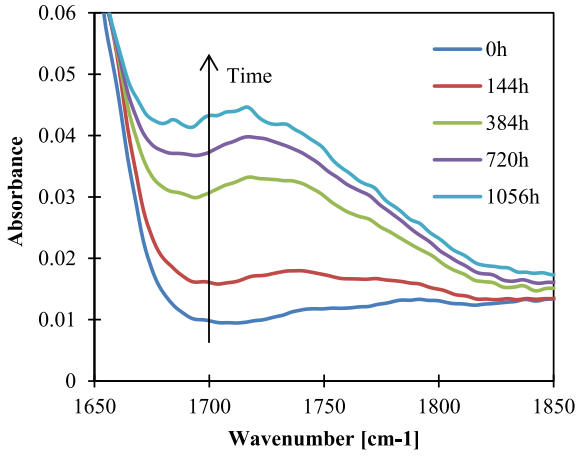

Fig. 4. FTIR spectrum of UV irradiated PEEK fibres in the carbonyl region.

low. UV irradiation starts randomly breaking off the polymer chains leading to a rapid decrease in the rupture elongation. Existing flaws then induce new flaws at an increasing rate. The high variance in the three medium aged samples can be explained statistically. If a sufficient amount of material flaws are concentrated into a single area in any part of the fibre, then it leads to a rupture. In the 1056 h irradiated samples the amount of deterioration is so large that the fibres inevitably rupture very early, which decreases the variance. Some of the variance can be explained by the spinning equipment [29]. There is no mixing in the capillary rheometer which can cause problems in the material homogeneity. Typical tensile testing curves for different samples can be seen in Fig. 3.

Previous mechanical tests for PEEK sheets have shown that photodegradation does not have a significant effect on the yield strength of PEEK and it can even initially increase because of crosslinking and hardening of the material [7,24]. Also, the embrittlement of the material was previously noted with similar magnitudes to what was measured in our tests [7].

3.2. FTIR

The most profound change in the IR spectra of UV irradiated PEEK is the formation of the carbonyl group absorption peak (Fig. 4), with a maximum at 1716 cm^{-1} and numerous shoulders indicating that several different carbonyl species (aldehydes, carboxylic acids and esters) are formed. Another typical change is the formation of the broad hydroxyl group absorption peak (Fig. 5), at 2800–3700 cm^{-1} with a maximum at ~3230 cm^{-1}. In addition the two bands at ~3050 cm^{-1} that correspond to the stretching C–H vibrations of phenyl groups decrease, indicating the opening of aromatic groups due to photodegradation.

The carbonyl index is one of the most used metrics in the study of polymer degradation. This is primarily due to the fact the chemical degradation products often contain carbonyl groups with high extinction coefficient, that makes their peaks very distinct in the FTIR-spectra. Since degradation reactions initially occur in only a thin layer of the sample, the increase in the concentration of carbonyl groups can often be observed well before the mechanical properties change. The carbonyl index of PEEK fibres, shown in Fig. 6, rises with increasing irradiation time. The carbonyl index rises almost exponentially between 144 and 384 h, after which the rise continues at a much slower pace. This indicates a large number of carbonyl groups forming during the photodegradation of PEEK.

The rise of the aliphatic methylene group vibrations (symmetric CH_3-stretching at 2853 cm^{-1} and anti-symmetric CH_3-stretching at 2922 cm^{-1}) and the lowering of the CH-stretching vibration of the aromatic rings (at 3065 cm^{-1}) are clearly visible in Fig. 5. This result indicates that the photodegradation of PEEK fibres leads to a loss in aromaticity due to a ring breaking reaction. The relative changes of the absorptions are presented in Fig. 7.

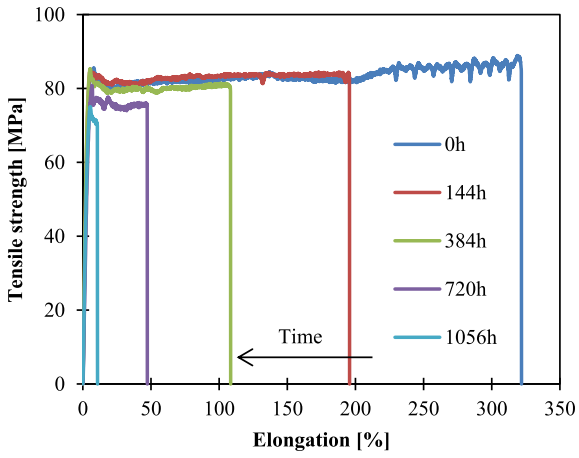

Fig. 3. Typical tensile testing curves for UV irradiated PEEK fibres.

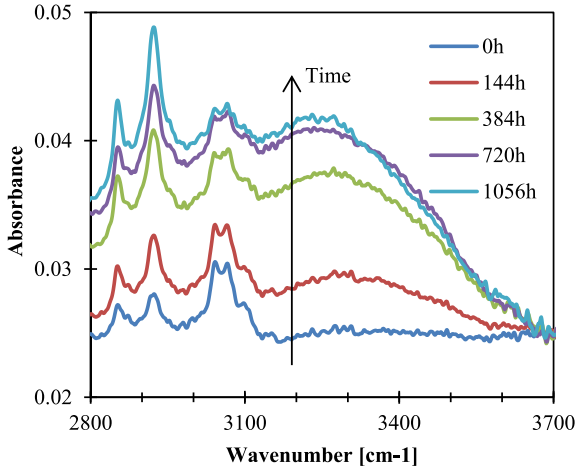

Fig. 5. FTIR spectrum of UV irradiated PEEK fibres in the hydroxyl region.

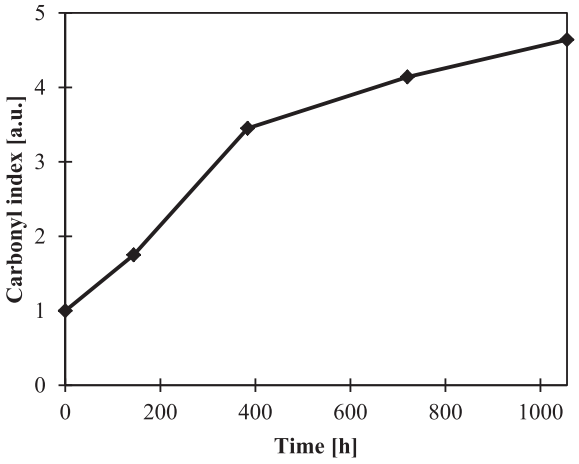

Fig. 6. Carbonyl index of UV irradiated PEEK fibres.

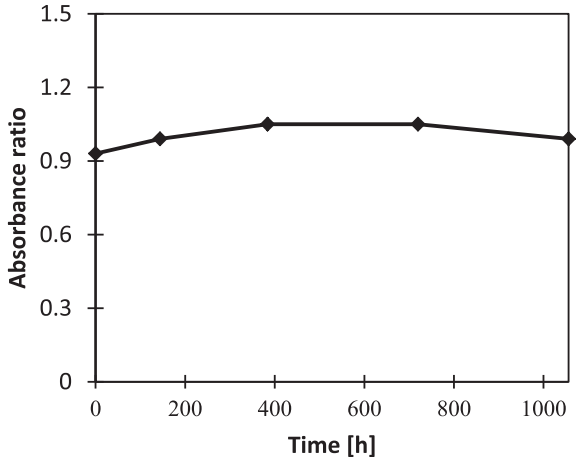

Fig. 8. Absorbance ratio 1305 cm^{-1}/1280 cm^{-1} measured by FTIR to estimate the degree of crystallinity of PEEK.

Previous studies have shown that the degree of crystallinity and the ratio of certain IR absorption peaks have a linear relationship [30,31]. Chalmers et al. [30] reported that the ratios of the peak intensities at wavenumbers 1305 cm^{-1}/1280 cm^{-1} and 970 cm^{-1}/952 cm^{-1} increase as the degree of crystallinity increases. Jonas et al. [32] later discovered that the peak 965 cm^{-1} is not suitable for determination of crystallization degrees above 15%. The ASTM F2778 standard uses the peak intensities at 1305 cm^{-1} and 1280 cm^{-1} to determine the degree of sample crystallinity [33].

Several authors have studied the determination of the degree of crystallinity of PEEK by different techniques. Specular reflectance FTIR (R-FTIR) is commonly considered the best technique for the task [31,34,35]. Also wide-angle x-ray scattering (WAXS) can be used for unfilled grades but is slower and may need complex curve fitting techniques to obtain the degree of crystallinity [34]. It has the advantage of measuring the crystallinity from the whole sample thickness rather than only the surface as in R-FTIR. DSC has been shown to be inaccurate in measuring the degree of crystallinity of PEEK although it is a commonly used technique [34].

ATR-FTIR is a very simple and common technique used to measure the degree of crystallinity of PEEK [31]. It has received criticism due to its poorer absorption intensity and repeatability when compared to R-FTIR [35]. In this study, the PEEK crystallinity was measured using ATR-FTIR (Fig. 8) and the results were compared with the DSC crystallinity measurements (Table 2). Both techniques indicate that photodegradation causes no major changes in the degree of crystallinity. DSC measurements give 35–36% degree of crystallinity for all samples, but this value should be considered with caution because of the previously mentioned limitations.

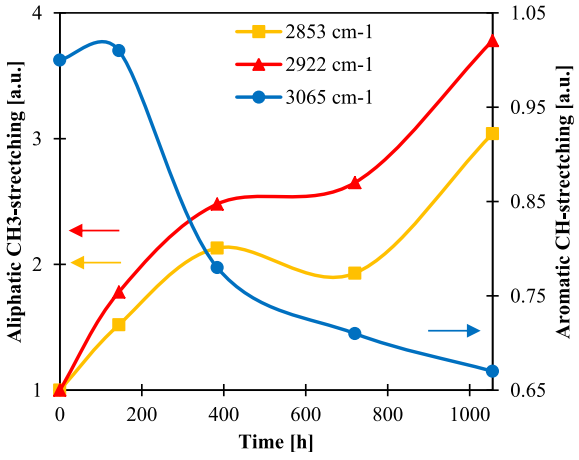

Fig. 7. Methylene CH_3- and aromatic CH-stretching vibration changes as a function of irradiation time.

3.3. DSC

The glass transition temperature of PEEK rises quite linearly with increased irradiation time in both heating runs (Table 2 and Fig. 9). During the photodegradation T_{g2} is usually larger than T_{g1}. This is expected since the glass transition temperature of a polymer is caused by a change in the mobility of the amorphous regions. The photodegradation process induces crosslinking in the amorphous regions, limiting the mobility and free volume of the polymer chains. In the first heating run these tensions lower the energy required to cause the glass transition process because the polymer chains relax to lower tensions exothermically. During the cooling cycle the polymer crystallizes to a relaxed morphology, causing an increase in the temperature required to cause the glass transition.

According to the DSC tests, UV irradiation does not affect the polymer crystallinity and melting point of the PEEK fibres tested.

3.4. Rheology

The results of the rheological tests in Fig. 10 show a steady increase in the zero shear viscosity with increased irradiation time. The amount of shear thinning increases during the irradiation so that the pristine PEEK samples have the lowest viscosity at low angular frequencies and the highest viscosity at high angular frequencies.

Table 2
The results of DSC scans for UV irradiated PEEK fibres.

Time [h]	Crystallinity [%]	T_{g1} [°C]	T_{g2} [°C]	T_{m1} [°C]	T_{m2} [°C]
0	36.0 ± 0.5	143.6 ± 0.9	144.7 ± 1.1	342.9 ± 0.4	340.9 ± 0.1
144	36.4 ± 0.3	145.8 ± 0.5	148.4 ± 0.9	342.6 ± 0.2	341.2 ± 0.1
384	35.3 ± 0.4	145.9 ± 2.0	146.0 ± 1.3	342.2 ± 0.1	340.5 ± 0.1
720	35.9 ± 0.3	147.1 ± 1.4	146.0 ± 0.8	342.8 ± 0.1	340.7 ± 0.1
1056	35.4 ± 0.5	149.3 ± 1.3	151.3 ± 2.2	343.0 ± 0.2	340.6 ± 0.2

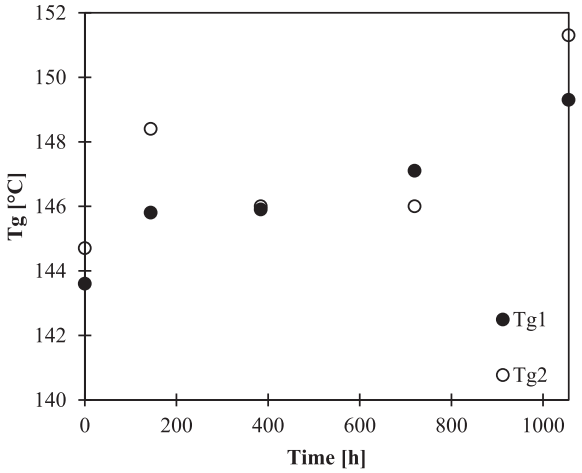

Fig. 9. Glass transition temperatures of UV irradiated PEEK fibres.

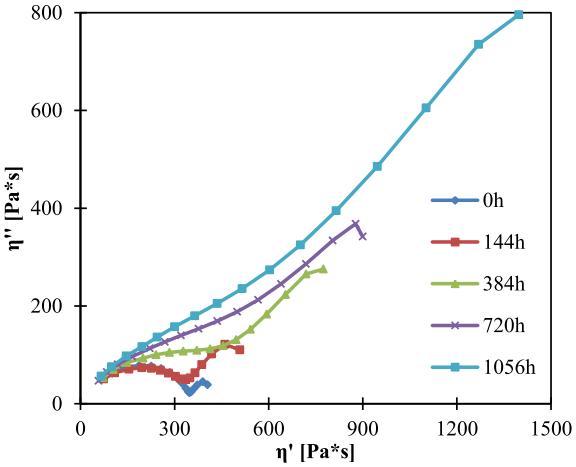

Fig. 11. Cole–Cole plot for UV irradiated PEEK fibres.

The zero shear viscosity of PEEK increases due to the crosslinking that was also evident in the tensile tests and in DSC scans. As previously mentioned, UV- or ion irradiation has been shown to increase the glass transition temperature because of crosslinking [36–38].

The Cole–Cole plot is an old but often used experimental rheological model that can be used to study the changes in polymer morphology [25,26,39].

$$\eta^*\left(\omega\right) = \frac{\eta_0}{1 + (i\omega\lambda_0)^{1-h}}$$

where η^* is the complex viscosity, ω angular frequency, η_0 zero shear viscosity, λ_0 average relaxation time and h parameter of the relaxation-time distribution. This model predicts that the η'' versus η' curve (where η'' is the imaginary component of the complex viscosity and η' the real component) is an arc of a circle in the complex plane and that the extrapolated crossing point of the arc and the real axis is the zero shear viscosity η_0. The zero shear viscosity η_0 and the molecular weight M_w have a well-known power law connection [40]

$$\eta_0 \propto M_w^a$$

which means that changes in the arc radius correspond to changes in the molecular weight. According to the Cole-Cole-plot of PEEK, shown in Fig. 11, the crosslinking behaviour is very dominant after 144 h of irradiation. The samples that have been irradiated for 0–384 h seem to have double distribution behaviour because a straight line follows the arc of circle. For 720 h and 1056 h irradiated samples the crosslinking rate is higher, with the curve being almost a straight line from the beginning. This is a typical sign of fully crosslinked material [25].

3.5. TGA

TGA tests were used to estimate the thermal resistance of the UV irradiated PEEK samples. The results measured in air (Fig. 12) and nitrogen (Fig. 13) show that even a rather short exposure to UV light weakens the thermal resistance significantly. The decrease in mass starts much earlier in aged samples than in pristine PEEK and depending on the definition of the starting point of the mass loss the difference can be up to 100 °C. The difference in the onset temperature is much smaller, only 10–20 °C as can be seen in Fig 14.

The differences between samples are larger when using synthetic air instead of nitrogen, since thermal degradation occurs faster in the presence of oxygen. Nitrogen purging inhibits the initiation of thermal degradation, even for photodegraded samples.

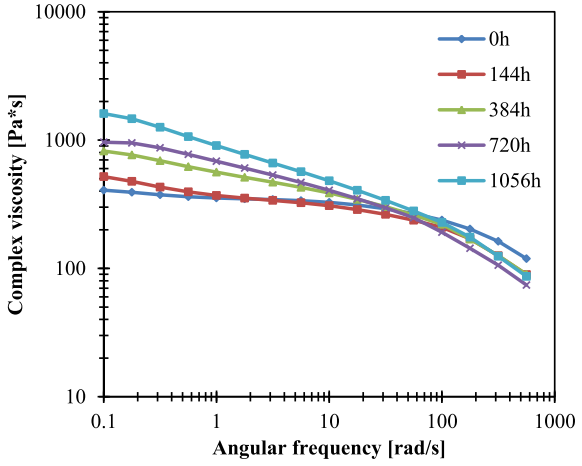

Fig. 10. Complex viscosity of UV irradiated PEEK fibres.

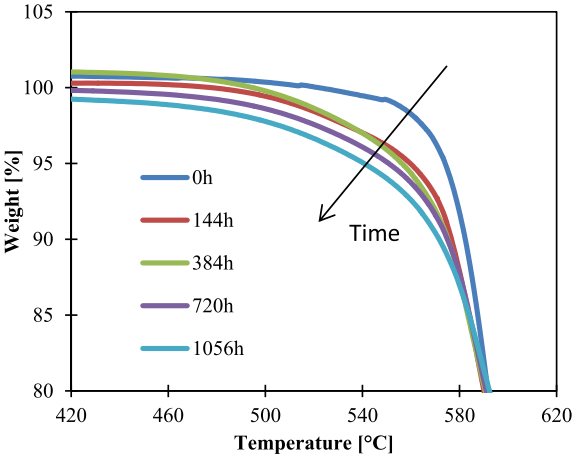

Fig. 12. TGA curve of UV irradiated PEEK fibres measured in air.

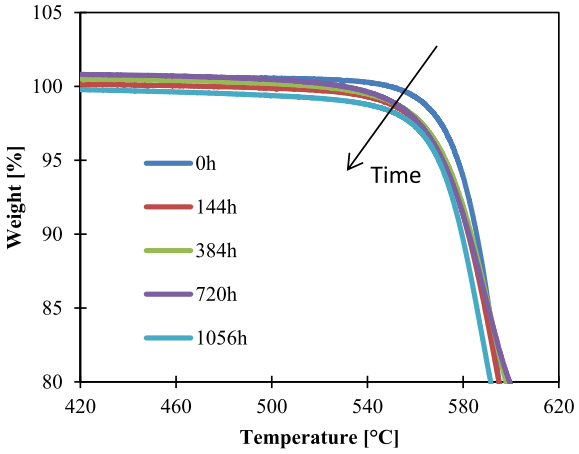

Fig. 13. TGA curve of UV irradiated PEEK fibres measured in nitrogen.

The thermal properties of PEEK fibres are weakened significantly, which indicates a lower energetic barrier for the initiation of thermal degradation. The by-products formed in the photo-degradation process are typically very labile radical and peroxide compounds, which significantly lowers the temperature barrier needed to start the thermal degradation process. One explanation of the weakened thermal properties is also found in the rheological tests that show significant changes in the molecular mass of the PEEK fibres.

3.6. SEM

In the longitudinal SEM photos there are no visible cracks even in the most irradiated 1056 h sample (Fig. 15A and B), although there is a clear reduction in the mechanical properties. There are some particles and roughness on the surface of the fibres, but these are most likely impurities or scratches not related to the UV irradiation. However, changes are clearly visible in the transverse SEM photo of the end face of the fibre that was cut by using liquid nitrogen (Fig. 15C and D). The cracks go to a depth of 20 μm which is a significant depth in the case of fibres. Surprisingly, the cracking is not visible in the longitudinal investigations.

Previous studies have shown that it is possible to estimate the polymer degradation level using an optical or scanning electron microscope in polypropylene (PP) [22,23,41]. Reconstruction of the

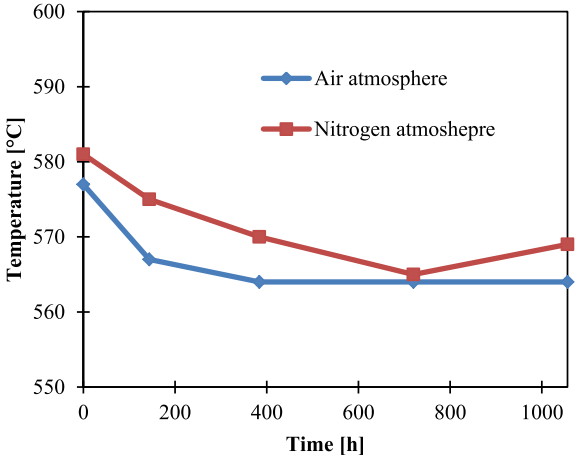

Fig. 14. Onset temperatures in TGA curves for UV irradiated PEEK fibres.

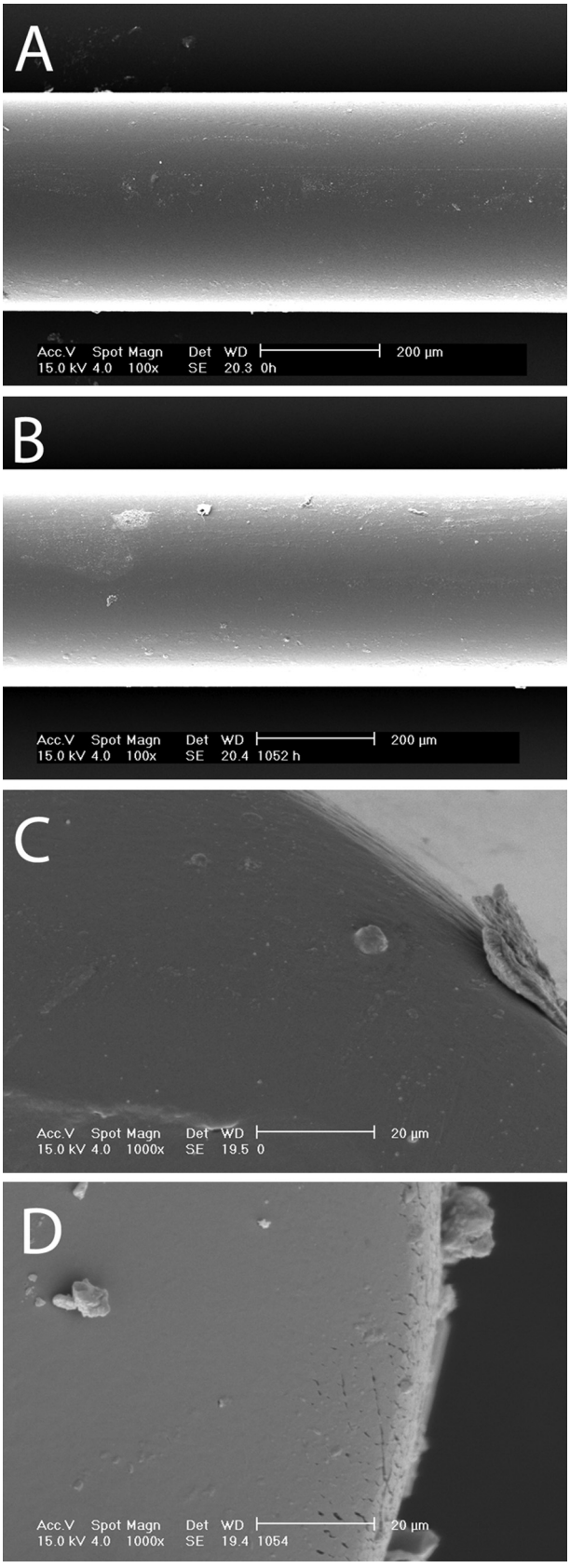

Fig. 15. Longitudinal SEM photo of pristine PEEK fibre (A), longitudinal SEM photo of 1056 h irradiated PEEK fibre (B), transverse SEM photo of pristine PEEK fibre (C) and transverse SEM photo of 1056 h irradiated PEEK fibre (D).

amorphous content in the surface and increased crystallization shrinks the outer layer of the sample which leads to cracking. The amount of cracking in PP is so significant that it is easily visible in the longitudinal investigations. The behaviour of the PEEK fibres is different because only transverse cracks were observed in the 1056 h irradiated sample. It is estimated that also these cracks are born randomly as a result of the shrinkage of the outer layer of the fibre. It is possible that longitudinal cracks would have emerged if the ageing would have been continued.

DSC tests indicate a stable crystallization degree of 36% in all the samples which is very close to the theoretical maximum of 40%. At least in the case of PP the high degree of crystallinity protects the fibres to some level from degradation and cracking [41]. PP studies have shown that changes in the mechanical properties can be observed before the changes in SEM photos because of micro cracks in the material [23]. Previous studies [7], DSC, and rheological tests have shown PEEK to harden by crosslinking, which can be confirmed from the transverse photos. Longitudinal investigations cannot be described as a very effective technique to estimate the degradation level of PEEK.

4. Conclusion

According to these tests PEEK fibres should not be stored in direct sunlight and limitations in outdoor use must be carefully considered to avoid safety problems. A few weeks in direct sunlight significantly increases the crosslinking rate and makes the fibres brittle. Changes in the material properties can be observed from the tensile tests, FTIR, TGA, SEM and rheological tests with some limitations. DSC cannot be considered a good technique to estimate the ageing of PEEK fibres. The carbonyl index measured by FTIR is a standard technique to show the first signs of photodegradation and is suitable for PEEK fibres as well. To observe changes in deeper portions of the fibres TGA, rheological or tensile tests can be used.

Acknowledgements

The authors would like to acknowledge the financial support received from the Academy of Finland (Grant no 253655) for the UVIADEM project. The authors also wish to thank MSc Anu Heikkilä from the UV chamber characterization and Sinikka Pohjonen from carrying the TGA, DSC and SEM tests.

References

[1] White J, Turnbull A. Weathering of polymers: mechanism of degradation and stabilization, testing strategies and modelling. J Mater Sci 1994;29:584–613.
[2] Bedia E, Paglicawan M, Bernas C, Bernando S, Tosaka M, Kohjiya S. Natural weathering of polypropylene in a tropical zone. J Appl Polym Sci 2003;87:931–8.
[3] Philippart J-L, Sinturel C, Arnaud R, Gardette J-L. Influence of the exposure parameters on the mechanism of photooxidation of polypropylene. Polym Degrad Stab 1999;64:213–25.
[4] Rajakumar K, Sarasvathy V, Thamarai Chelvan A, Chitra R, Vijayakumar C. Natural weathering studies of polypropylene. J Polym Environ 2009;17:191–202.
[5] Mailhot B, Jarroux N, Gardette J-L. Comparative analysis of the photo-oxidation of polystyrene and poly(a-methylstyrene). Polym Degrad Stab 2000;68:321–6.
[6] Dever J, Messer R, Powers C, Townsend J, Wooldridge E. Effects of vacuum ultraviolet radiation on thin polyimide films. High Perform Polym 2001;13:s391–9.
[7] Nakamura H, Nakamura T, Noguchi T, Imagawa K. Photodegradation of PEEK sheets under tensile stress. Polym Degrad Stab 2006;91:740–6.
[8] Giancaterina S, Rossi A, Rivaton A, Gardette J-L. Photochemical evolution of poly(ether ether ketone). Polym Degrad Stab 2000;68:133–44.
[9] Rivaton A, Gardette J-L. Photodegradation of polyethersulfone and polysulfone. Polym Degrad Stab 1999;66:385–403.
[10] Platt DK, editor. Engineering and high performance plastics market report. Shawbury: Smithers Rapra Technology; 2003.
[11] Sabu T, Visakh PM, editors. Handbook of engineering and speciality thermoplastics. Polyethers and polyesters, vol. 3. New York: Wiley; 2011. p. 55.
[12] Zyex Ltd. Manufacturer of PEEK fibers. Available from: http://www.zyex.com, [accessed 26.03.14].
[13] Patel P, Hull R, McCabe R, Flath D, Grasmeder J, Percy M. Mechanism of thermal decomposition of poly(ether ether ketone) (PEEK) from a review of decomposition studies. Polym Degrad Stab 2010;95:709–18.
[14] Nandan B, Kandpal L, Mathur G. Poly(ether ether ketone)/poly(aryl ether sulphone) blends: thermal degradation behaviour. Eur Polym J 2003;39:193–8.
[15] Day M, Suprunchuk T, Cooney J, Wiles M. Thermal degradation of poly(aryl-ether–ether-ketone) (PEEK): a differential scanning calorimetry study. J Appl Polym Sci 1988;36(5):1097–106.
[16] Xi DK, Tian JJ, Zhang DP, Yuan CS, Lu J, Sun HL, et al. High-pressure crystallized PEEK: degradation and stability. Appl Mech Mater 2011;71–78:698–701.
[17] Shard A, Badyal J. Surface oxidation of polyethylene, polystyrene, and PEEK: the synthon approach. Macromolecules 1992;25:2053–4.
[18] Munro HS, Clark DT, Recca A. Surface photo-oxidation of phenoxy resin and polyetheretherketone. Polym Degrad Stab 1987;19(4):353–63.
[19] Ferain E, Legras R. Modification of PEEK model compounds and PEEK film by energetic heavy ion and ultraviolet irradiations. Nucl Instrum Methods B 1993;83:163–6.
[20] Said M, Dingwall B, Gupta A, Seyam A, Mock G, Theyson T. Investigation of ultra violet (UV) resistance for high strength fibers. Adv Space Res 2006;37:2052–8.
[21] Lipp-Symonowicz B, Sztajnowski S, Kardas I. Influence of UV radiation on the mechanical properties of polyamide and polypropylene fibres in aspect of their restructuring. Autex Res J 2006;6(4):196–203.
[22] Schmidt H, Witkowska B, Kamińska I, Twarowska-Schmidt K, Wierus K, Puchowicz D. Comparison of the rates of polypropylene fibre degradation caused by artificial light and sunlight. Fibres Text East Eur 2011;19(4):53–8.
[23] Aslanzadeh S, Haghighat Kish M. Photo-oxidation of polypropylene fibers exposed to short wavelength UV radiations. Fibres Polym 2010;11(5):710–8.
[24] Massey L. The effect of UV light and weather on plastics and elastomers. 2nd ed. New York: William Andrew publishing; 2007.
[25] Commereuc S, Askanian H, Verney V, Celli A, Marchese P, Berti C. About the end life of novel aliphatic and aliphatic-aromatic (co)polyesters after UV-weathering: structure/degradability relationships. Polym Degrad Stab 2013;98:1321–8.
[26] Commereuc S, Askanian H, Verney V, Celli A, Marchese P. About durability of biodegradable polymers: structure/degradability relationships. Macromol Symp 2010;296:378–87.
[27] Verney V, Commereuc S. Molecular evolution of polymers through photo-ageing: a new UV in situ viscoelastic technique. Macromol Rapid Commun 2005;26:868–73.
[28] Q-lab technical bulletin LU-8160. A choice of lambs for the QUV accelerated weathering tester, accessed March 26 at http://www.q-lab.com/documents/public/d6f438b3-dd28-4126-b3fd-659958759358.pdf.
[29] Mylläri V, Syrjälä S, Skrifvars M, Järvelä P. The effect of melt spinning process parameters on the spinnability of polyetheretherketone. J Appl Polym Sci 2012;126:1564–71.
[30] Chalmers J, Gaskin W, Mackenzie M. Crystallinity in poly(aryl-ether-ketone) plaques studied by multiple internal reflection spectroscopy. Polym Bull 1984;11:433–5.
[31] Harris L. A study of the crystallisation kinetics in PEEK and PEEK composites. Master of research thesis. The University of Birmingham; 2011.
[32] Jonas A, Legras R, Issi J-P. Differential scanning calorimetry and infra-red crystallinity determinations of poly(aryl ether ether ketone). Polymer 1991;32(18):3364–70.
[33] ASTM international. Standard test method for measurement of percent crystallinity of polyetheretherketone (PEEK) polymers by means of specular reflectance Fourier transform infrared spectroscopy (R-FTIR). ASTM F2778–09; 2009.
[34] Jaekel DJ. Development and fabrication of silver composite PEEK to prevent microbial attachment and periprosthetic infection. Dissertation. Drexel University; 2012.
[35] Chalmers J, Everall N, Hewitson K, Chesters M, Pearson M, Grady A, et al. Fourier transform infrared microscopy: some advanced in techniques for characterization and structure-property elucidations of industrial material. Analyst 1998;123:579–86.
[36] Claudea B, Gonon L, Duchetb J, Verneya V, Gardette J. Surface cross-linking of polycarbonate under irradiation at long wavelengths. Polym Deg Stab 2004;83:237–40.
[37] Vaughan A, Stevens G. Irradiation and the glass transition in PEEK. Polym 2001;42:8891–5.
[38] Sasuga T, Kudoh H. Ion irradiation effects on thermal and mechanical properties of poly(ether–ether–ketone) (PEEK). Polymer 2000;41:185–94.
[39] Vega JF, Muñoz-Escalona A, Santamaria A, Muñoz ME, Lafuente P. Comparison of the rheological properties of metallocene-catalyzed and conventional high-density polyethylenes. Macromolecules 1996;29:960–5.
[40] Han CD, editor. Rheology and processing of polymeric materials. Polymer rheology, vol. 1. New York: Oxford University Press; 2007. p. 92.
[41] Rabello M, White J. The role of physical structure and morphology in the photodegradation behaviour of polypropylene. Polym Deg Stab 1997;56:55–73.

Polymer Degradation and Stability 120 (2015) 419–426

Contents lists available at ScienceDirect

Polymer Degradation and Stability

journal homepage: www.elsevier.com/locate/polydegstab

Characterization of thermally aged polyetheretherketone fibres – mechanical, thermal, rheological and chemical property changes

Ville Mylläri [a, *], Tero-Petri Ruoko [b], Jyrki Vuorinen [a], Helge Lemmetyinen [b]

[a] Department of Material Science, Tampere University of Technology, Tampere 33101, Finland
[b] Department of Chemistry and Bioengineering, Tampere University of Technology, Tampere 33101, Finland

ARTICLE INFO

Article history:
Received 18 June 2015
Received in revised form
3 August 2015
Accepted 4 August 2015
Available online 6 August 2015

Keywords:
PEEK
Fibre
Thermal degradation

ABSTRACT

This paper investigates the effects of thermal degradation on polyetheretherketone (PEEK) fibres. PEEK samples were aged at a constant temperature of 250 °C for 1–128 days and characterized with mechanical tests, FTIR (Fourier Transform Infrared Spectroscopy), DSC (Differential Scanning Calorimetry), rheology, TGA (Thermogravimetric Analysis), SEM (Scanning Electron Microscopy), and UV–Vis diffuse reflectance spectroscopy. The short-term thermal annealing had a positive effect on the mechanical properties, due to the formation and growth of secondary crystals. Crosslinking in the material was verified by rheological inspections. The crosslinking increased the mechanical strength and modulus but reduced the elongation at break of the fibres. FTIR tests showed that carbonyl and hydroxyl groups were slowly formed on the surface of the fibres while ring opening reactions took place. The thermal ageing reduced the thermal stability of PEEK. The decreased stability was observed in the decomposition onset temperature after 8 d and in the melting point and the glass transition temperature after 32 d. The first signs of degradation, crosslinking, embrittlement, and reduced thermal stability, were visible roughly after 8 d of ageing, whereas the deterioration in general usability occurred after 64 d.

1. Introduction

Polyetheretherketone (PEEK) is a linear, semicrystalline thermoplastic polymer and is probably best known for its outstanding thermal properties. A continued use temperature of 250–260 °C combined with excellent mechanical properties and chemical resistance make it an excellent candidate for replacing metals in demanding applications. A melt spinning of PEEK has been conducted from the 1980's, and the spinnability of the fibres is typically excellent [1]. The applications of the fibres are similar to those of bulk PEEK, extreme environmental conditions where conventional thermoplastic are inadequate. The PEEK fibres are currently used in process conveyor belts, filters, protective braids, reinforced rubber gaskets, industrial bristles, protective clothing, sports strings, music strings, and thermoplastic composites [2]. The chemical structure of PEEK is presented in Fig. 1, where a PEEK monomer is composed of three phenyl rings, linked to each other with either a carbonyl or ether group.

The high temperature behaviour of PEEK under both short- and long-term exposures, as well as the decomposition products formed have been well characterized with different approaches and methods, including FTIR (Fourier Transform Infrared Spectroscopy) [3,4], TGA (Thermogravimetric Analysis) [5–7], mass spectroscopy [8,9], UV–Vis [10], and NMR (Nuclear Magnetic Resonance) [10] spectroscopies, DSC (Differential Scanning Calorimetry) [11–13], WAXS (Wide Angle X-ray Scattering) [11], and mechanical tests [12–15]. However, most of the studies have concentrated only on one or two methods making the comparison between the results difficult. To the best of the authors' knowledge, any systematic studies regarding the thermal degradation of the PEEK fibres have not yet published. Fibres have typically high degree of orientation and crystallinity, and small diameter, which can cause differences in results compared to other sample forms.

Initially, the thermal ageing of PEEK has many advantages. Annealing PEEK between the glass transition (T_g) and melting temperature (T_m) for various time periods has been studied since the 1980's. According to the manufacturer recommendations, a typical annealing time is 40 h at 250 °C [13]. The annealing increases the crystallinity [13] and changes the crystal morphology [12,16,17]. According to the TEM (Transmission Electron Microscope) micrographs, PEEK has two populations of crystals [18]. The annealing grows these secondary crystals, which can be observed in the DSC scans as a minor secondary peak at a temperature a little

* Corresponding author.
E-mail address: ville.myllari@tut.fi (V. Mylläri).

http://dx.doi.org/10.1016/j.polymdegradstab.2015.08.003
0141-3910/

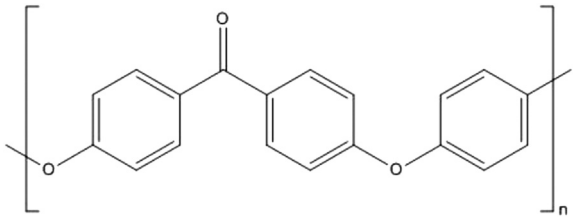

Fig. 1. The chemical structure of PEEK.

bit higher than the annealing temperature [12].

The goal of this article is to study the effects of the maximum use temperature (250 °C) on PEEK fibres using numerous complementary characterization methods. By using a long timescale, the onset of different phenomena, whether positive or negative or occurring on a microscopic or macroscopic scale, should be observed during the tests. In addition, the results are compared with our previous research on the photodegradation of PEEK fibres [19]. This research offers valuable information for the applications of PEEK fibres in different environments.

2. Experimental

2.1. Samples and ageing

Samples were made of Victrex (Lancashire, UK) PEEK grade 151G, a semicrystalline, easy flow grade PEEK with no inherent UV stabilizers. PEEK fibres were manufactured by a melt spinning process using a Göttfert Rheograph 6000. The processing temperature was 380 °C, capillary dimensions 30/1 mm and piston speed 0.5 mm/s. Fibres were drawn by gravity since the use of a spinning motor would have led to unnecessarily small fibre diameters. The draw ratio ($v_{capillary}/v_{final}$) of the fibres was 5.9, resulting in a very homogenous final diameter of 410 ± 10 μm.

2.2. Ageing

The samples were aged using a modified Ahma GO600 oven. The original temperature controller was replaced with an Omron E5CN control unit and a PT100 platinum resistance thermocouple. The annealing conditions were kept stable at a temperature of 250 ± 0.1 °C during the artificial ageing process. The samples were attached to a horizontal grill attached on the same level as the thermocouple. The aged fibres were cut from the grill so that the fibres in close contact with metal were discarded because the high thermal conductivity of the grill results in accelerated ageing.

2.3. Measurements

DSC thermograms were recorded with a Netzsch DSC 204 F1 heat-flux DSC. All measurements were performed under a nitrogen atmosphere. During the DSC tests, materials were heated from room temperature to 400 °C, cooled to room temperature, and heated once more. The heating rate was 20 °C/min. Two samples from each fibre were measured.

FTIR spectra of the fibres were measured with a Bruker optics tensor 27 using ATR (attenuated total reflectance) mode in the wavenumber range 400–4000 cm^{-1} with a resolution of 4 cm^{-1} and averaging 32 scans. Measurements were performed using three parallel fibres and results were an average of three measurements. A baseline correction was performed using the average absorbance between 3800 and 4000 cm^{-1} as a reference. The carbonyl index was calculated as the ratio of the aged and unaged peak intensities at 1740 cm^{-1}, corresponding to a carbonyl vibration in ester groups produced by the oxidation of carbonyl groups [3].

Oscillatory shear measurements within the linear viscoelastic range were carried out with an Anton Paar Physica MCR 301 rheometer. All experiments were performed with a 25 mm plate–plate geometry under a nitrogen atmosphere. The measuring points with decreasing frequency in the angular frequency range of 0.1–562 rad/s were recorded at 380 °C.

TGA thermograms were recorded with a PerkinElmer TGA 6. The samples were heated from room temperature to 995 °C in synthetic air (20% O_2/80% N_2) with a heating rate of 10 °C/min. The onset temperature was defined as the intersection point of the extrapolated baseline and the tangent of the inflection point.

The tensile properties of the fibres were tested with an Instron 5967 according to the ISO 5079:1995 standard. The initial length was 50 mm with a crosshead speed of 20 mm/min. Instead of the recommended 50 measurements, only 15 samples per annealing time were measured due to the long total duration of the mechanical tests. The modulus was calculated using linear regression techniques according to the EN10002 and ASTM E8 standards. A 2 kN force shell was used in the measurements.

The morphology of the PEEK fibres was investigated with a Philips XL30 scanning electron microscope (SEM). The fibres were broken in liquid nitrogen for transverse imaging.

UV–Vis diffuse reflectance spectra were measured with a Shimadzu UV-3600 UV–Vis–NIR spectrophotometer and ISR-3100 integrating sphere. All spectra were recorded in the wavelength range 350–750 nm.

3. Results and discussion

3.1. DCS tests

The annealing induces a secondary endotherm slightly above the maximum use temperature of PEEK, as observed also in previous studies [12,13,16]. After 1 d of ageing this peak is at 275 °C, shifting to higher temperature during the ageing so that it merges with the primary melting peak for the 128 d aged samples (Fig. 2). Melting of PEEK removes this secondary endotherm and it is not visible during the second DSC scan due to the thermal history of the sample being wiped in the first scan (Fig. 3). The disappearance of the secondary peak reduces the melting endotherm area of the 128 d aged sample to almost half compared to the first scan.

The melting point of PEEK remains at 345 °C for the first 32 d of ageing (Fig. 4). A sudden drop in T_m is noticeable with the additional ageing. By 128 d of ageing the T_m is 15 °C lower, a sign of significant degradation in the bulk of the fibres.

The glass transition temperature of the PEEK fibres increased with the ageing (Fig. 5). According to the previous literature, this change is caused by significant crosslinking induced decrease in the molecular mobility [20,21]. The latter study claims that if both the T_g and Young's modulus are increased simultaneously, this can only be justified by the material crosslinking. T_{g2} (glass transition during the second heating run) starts to increase after 16 d of ageing. Even 1 d of ageing increases T_{g1} (glass transition during the first heating run) from 148 °C to 164 °C presumably due to the formation of secondary crystals, leading to chemical and mechanical changes in the amorphous portions of the fibres and crosslinking induced tensions inside the fibres.

3.2. FTIR

The most common changes in the FTIR spectrum during the polymer degradation is the formation of an absorption band

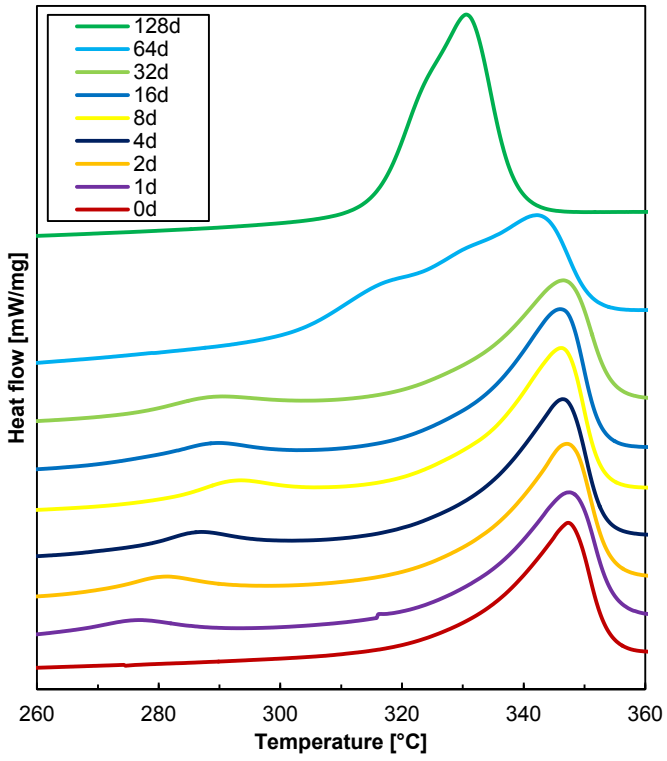

Fig. 2. DSC traces of thermally aged PEEK fibres, first heating.

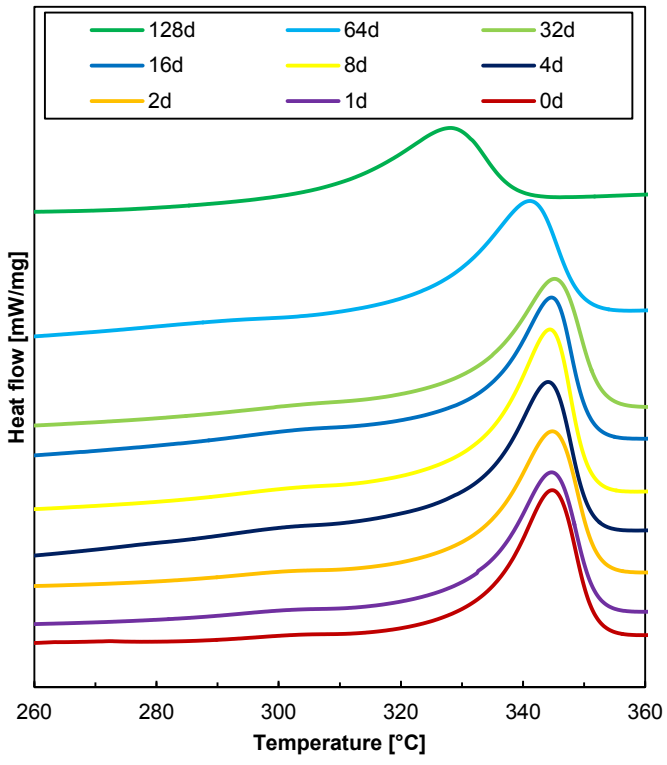

Fig. 3. DSC traces of thermally aged PEEK fibres, second heating.

specific to the carbonyl absorption. The carbonyl group (C=O) absorbs the IR radiation in the wavenumber region of 1540–1870 cm^{-1}, with the exact wavenumber depending on the

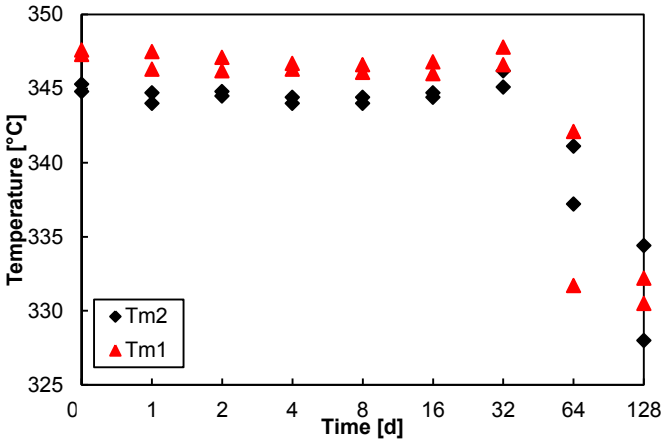

Fig. 4. Melting temperature of thermally aged PEEK fibres. T_{m1} during the first heating and T_{m2} during the second.

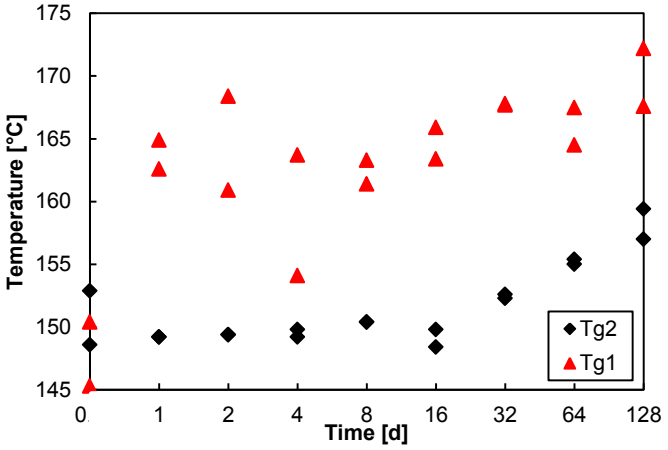

Fig. 5. Glass transition temperature of thermally aged PEEK fibres. T_{g1} during the first heating, T_{g2} during the second heating.

chemical structure of the polymer chain (Fig. 6). Another typical change during the ageing of PEEK is the formation of a broad hydroxyl group (–OH) absorption at 2800–3700 cm^{-1} with a maximum at ~3260 cm^{-1} (Fig. 7).

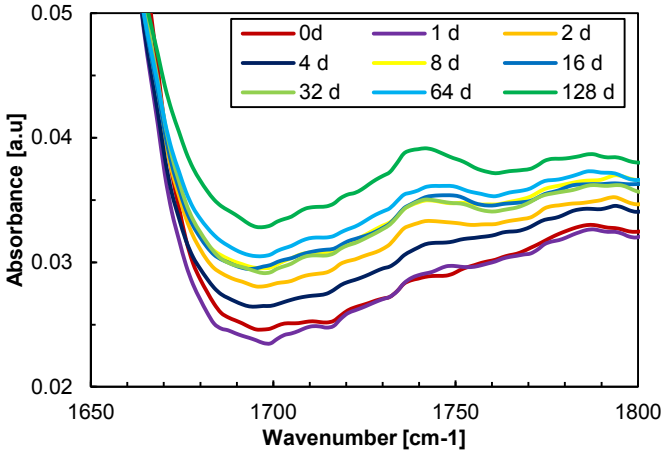

Fig. 6. FTIR spectra of thermally aged PEEK fibres in the carbonyl region.

The rise in the carbonyl index is steady, but moderate compared to the photodegradation (Fig. 8). The carbonyl peak intensity maximum is located at 1740 cm^{-1} which is different from the photodegradation study where the intensity maximum was at 1716 cm^{-1}. This is an interesting result because it indicates that the ageing goes through a different degradation route between the thermal- and photodegradation and illustrates the fact that the photodegradation of aromatic polymers rarely occurs by the well-known hydroperoxide mechanism that is typical for aliphatic polymers and general thermal degradation [22,23].

The good thermal stability of PEEK, and many other polymers, is connected to aromatic groups in the molecular structure. The repeating unit of PEEK includes three phenyl rings. According to the FTIR tests (Fig. 9), the relative number of the phenyl rings decreases and the number of aliphatic groups increases during ageing, which indicate that ring opening reactions occur during ageing. This is one probable reason for the decreased thermal stability at longer degradation times, which is observed as a reduction in the melting point with DSC.

3.3. Rheology

Rheology is not a commonly used tool for studying the ageing of polymer fibres. The challenge is obtaining a sufficient volume of fibres, up to several kilometres of length which are needed in the case of ultrafine fibres when using a typical rheometer. On the other hand, rheology is a powerful tool in estimating changes occurring in the whole fibre, not just at the surface. When studying materials degradation, rheology can be utilized to estimate which of the two competitive reactions is dominant, the chain scission or the crosslinking. Due to PEEK's aromatic structure, it has a tendency to crosslink when aged with the UV light [20], which can be observed as increased zero shear viscosity and shear thinning [19].

With regard to rheology, the thermal ageing (Fig. 10) causes somewhat similar effects as photodegradation [19]. The zero shear (or 0.1 1/s in this case) viscosity increases slowly in the early phases of ageing and very rapidly after 16 d. Even 1 d of the thermal ageing causes a significant reduction in the viscosity at the high angular frequencies. This behaviour is different from the photodegradation, where more changes occurred at low angular frequencies. The 32 d aged sample was the last that could be measured. The 64 and 128 d aged samples had very interesting properties, since they did not melt during the tests (Fig. 11). Evidently, at that point the material is highly crosslinked, behaving more like a thermoset than a thermoplastic.

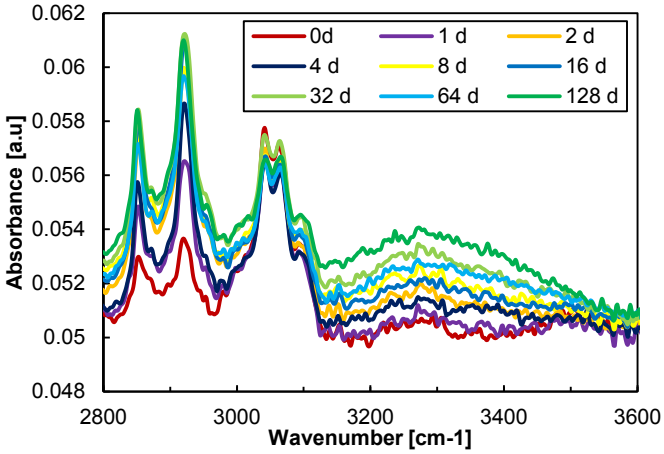

Fig. 7. FTIR spectra of thermally aged PEEK fibres in the hydroxyl region.

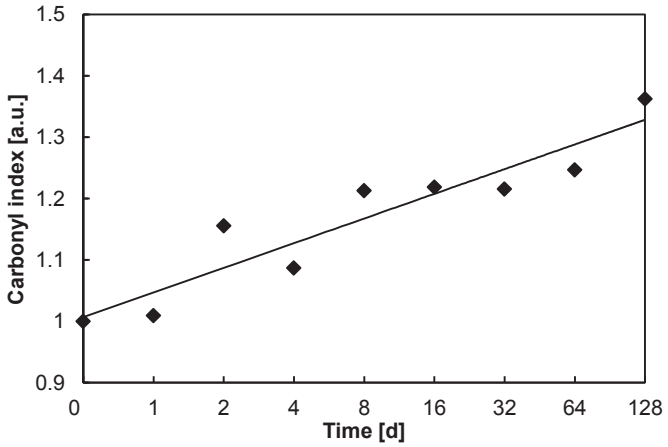

Fig. 8. Carbonyl index [1740 cm^{-1}/1740 cm^{-1} (t = 0)] of PEEK fibres aged at 250 °C.

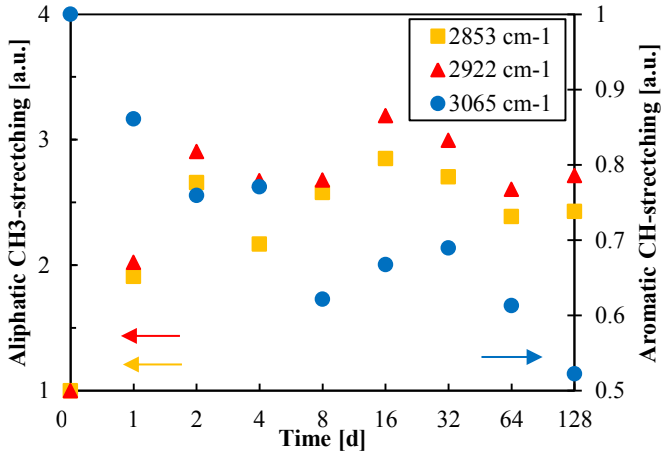

Fig. 9. Methylene CH_3- and aromatic CH-stretching vibrations of thermally aged PEEK fibres as a function of ageing time.

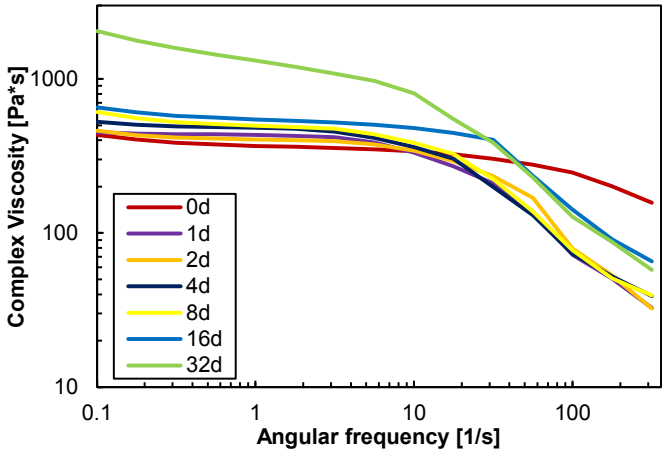

Fig. 10. Complex viscosity curves of PEEK fibres aged at 250 °C.

Relative molecular weights were estimated using the experimental Cole–Cole model [24,25]. In theory, the curves should form a circular arc where the x-axis crossing point is the zero shear viscosity. The curves were extrapolated using 2nd degree polynomial fitting, and the relative molecular weights were calculated

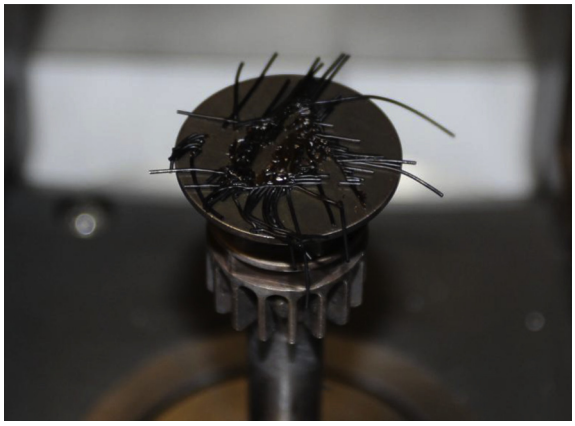

Fig. 11. 128 d aged PEEK fibres after rotational rheometer measurement. The fibres were heated 15 min at 450 °C using 50 N compression without changes in the fibre form. The photo was taken while heating was still on.

with Equation (1) [26].

$$\eta_0 \propto M_w^{3.4} \tag{1}$$

where η_0 is the zero shear viscosity and M_w the average molecular weight. The results shown in Fig. 12 indicate that a slow increase in M_w happens until 16 d, after which the crosslinking rate increases, thus significantly increasing the average molecular weight. T_m and T_{g2}, measured with DSC, start to change roughly at the same time (32 d) as the increased crosslinking is observed with the rheology. This is an expected correlation, since a high amount of crosslinking leads to changes in the relative amounts of crystalline and amorphous material, directly observed as changes in the melting point and the glass transition temperature with DSC.

3.4. TGA

TGA tests (Fig. 13) show that thermal ageing reduces the thermal stability of PEEK, a result observed in the DSC tests as well. The first significant changes are observed after 8 d of ageing. Even though the difference in degradation onset temperature (Fig. 14) is only 13 °C between the virgin sample and the 128 d aged sample, the curvatures of the mass loss curves are drastically different. With the increased ageing the mass loss begins at noticeably lower

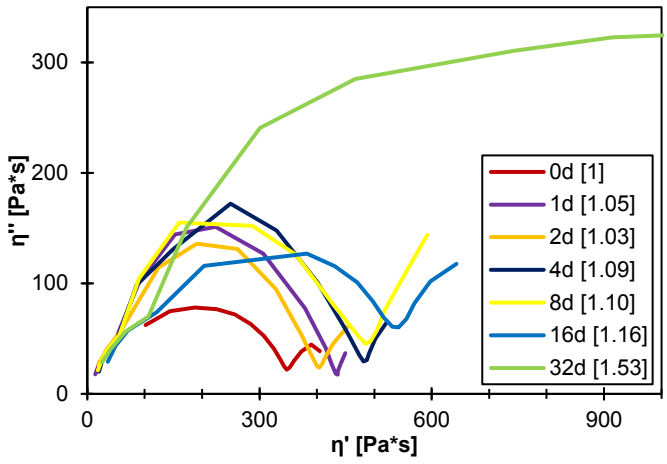

Fig. 12. Cole–Cole plot of PEEK fibres aged at 250 °C. Calculated relative molecular weights are within the brackets.

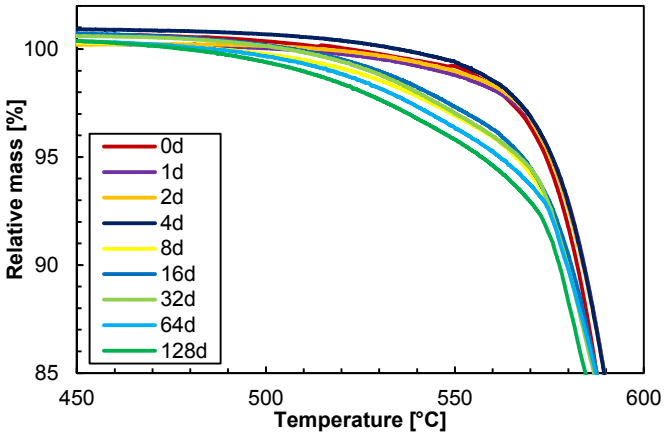

Fig. 13. TGA of PEEK fibres aged at 250 °C.

temperatures. Thermal degradation causes similar effects in TGA as photodegradation [19].

Even though the 64 d and 128 d aged samples did not melt during the rheological investigations, they have the worst thermal stability according to TGA. The confirmed crosslinking of the material during the ageing evidently reduces the gap between the material melting point and the decomposition temperature. In the case of virgin PEEK the gap is over 200 °C but it decreases to almost zero, like in the case of the thermosets. The loss of aromaticity that is observed with FTIR also supports this decrease in thermal stability, since phenyl rings are much more stable than aliphatic chains in the polymers. Both TGA and rheology give information on the whole samples volume, not only surface, and their ability to detect degradation in the bulk of the PEEK fibres is fairly similar. On the other hand, FTIR method is surface sensitive, thus observing the changes in aromaticity long before the lowered bulk thermal stability becomes visible.

3.5. Tensile properties

The tensile properties changed significantly during the first day of ageing; the tensile strength (Fig. 15) increased from 92 to 105 MPa and the modulus (Fig. 16) from 2.6 to 2.9 GPa. The properties were unchanged within standard errors until 64 d of ageing. The maximum values were reached after 128 d; a tensile strength of

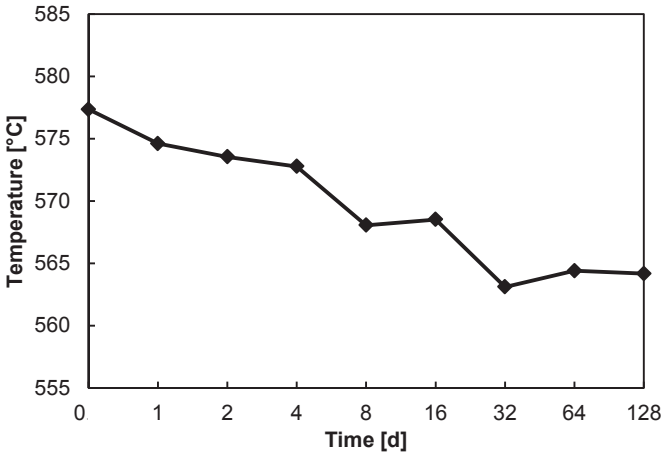

Fig. 14. Oxidation onset temperature of PEEK fibres measured in air.

123 MPa and a modulus of 3.0 GPa. PEEK typically turns brittle during the ageing. The elongation (Fig. 17) was reduced step by step from 315 % to 8 %. An untypical testing procedure, where the elongation was the maximum value of 15 measurements, was chosen because of equipment limitations. A stress concentration was generated near the jaws which often caused the fibre to break at the yield point. The modified method turned out to be suitable in this case. It provided a good way to estimate the elongation and reduced the amount of measurements needed compared to the conventional method. Typical tensile testing curves can be found in Fig. 18.

The effect of the annealing on the mechanical properties of PEEK has been intensively studied. According to literature, the annealing improves both short- and long-term mechanical properties of PEEK [12,15,18]. This was clearly visible in our short-term tensile tests as well. Crosslinking of the material, confirmed in Section 3.3, is another explanation for the improved mechanical properties and reduced elongation [14,20]. On the other hand, the crosslinking is not desirable in the case of fibres because they become very brittle, thus reducing usability.

3.6. SEM

There are no observable changes in the SEM micrographs during the ageing (Fig. 19). The photodegradation has been shown to cause solidification and shrinkage of the outer layer of the fibre causing observable cracking, but this was not evident with the thermal degradation. This is logical considering that the thermal degradation affects the whole sample, whereas the photodegradation mostly the sample surface.

3.7. UV–Vis

The originally yellowish PEEK fibres turned brownish red with the increased ageing. The diffuse reflectance spectra of the samples (Fig. 20) show how pristine PEEK fibres mainly absorb the UV radiation below 410 nm, which explains the yellow colour. With the increased ageing, the onset of the absorption gradually moves to higher wavelengths with an absorption band forming in the visible region between 400 and 750 nm. The 128 d aged fibres have an absorption onset of 550 nm, corresponding to a brownish red colour. The colour changes are presumably due to surface oxidation of the material, similar to what is observed during the burning of polymers.

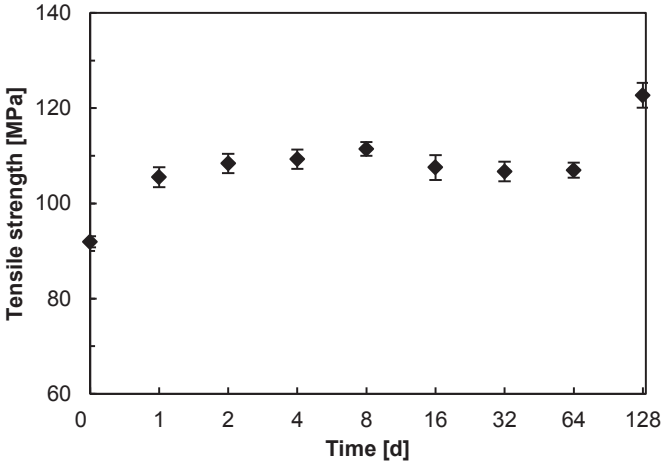

Fig. 15. Tensile strength of PEEK fibres aged at 250 °C.

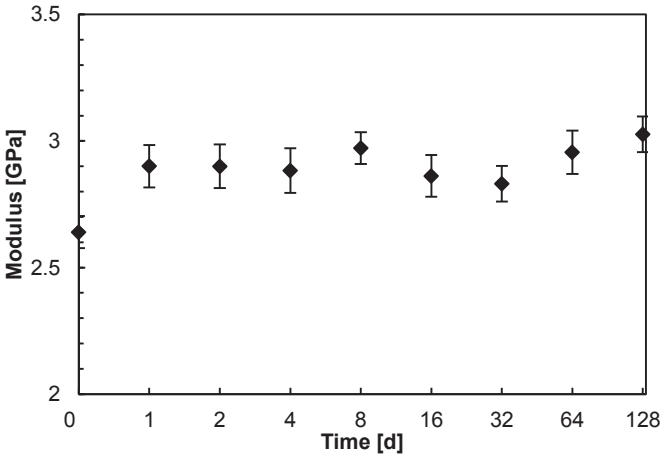

Fig. 16. Modulus of PEEK fibres aged at 250 °C.

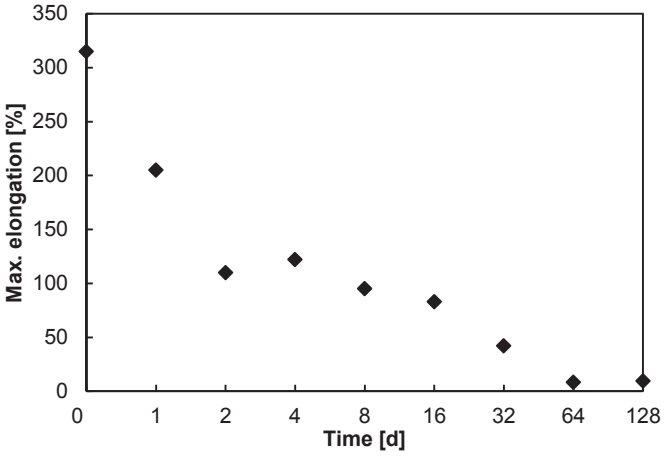

Fig. 17. Maximum elongation of PEEK fibres aged at 250 °C.

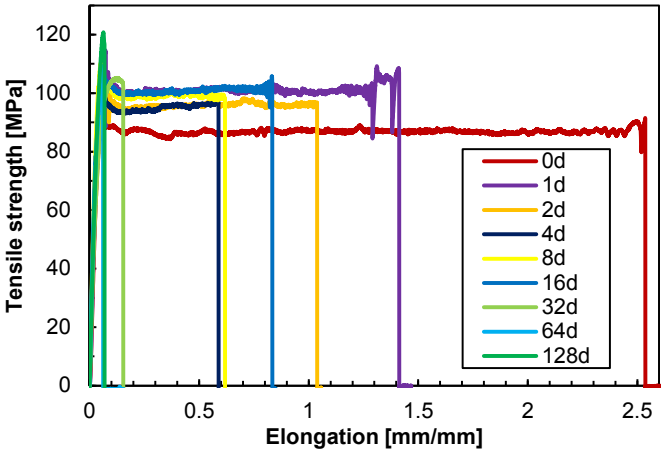

Fig. 18. Typical tensile testing curves.

Since the PEEK fibres are completely opaque, the absorption of the samples can be presented as $A = 1 - R$, where A is absorptance and R is reflectance. The relative changes in absorption at 500 nm (Fig. 21) show a clear logarithmic increase in the absorption of the PEEK fibres with increased annealing time, as illustrated by the

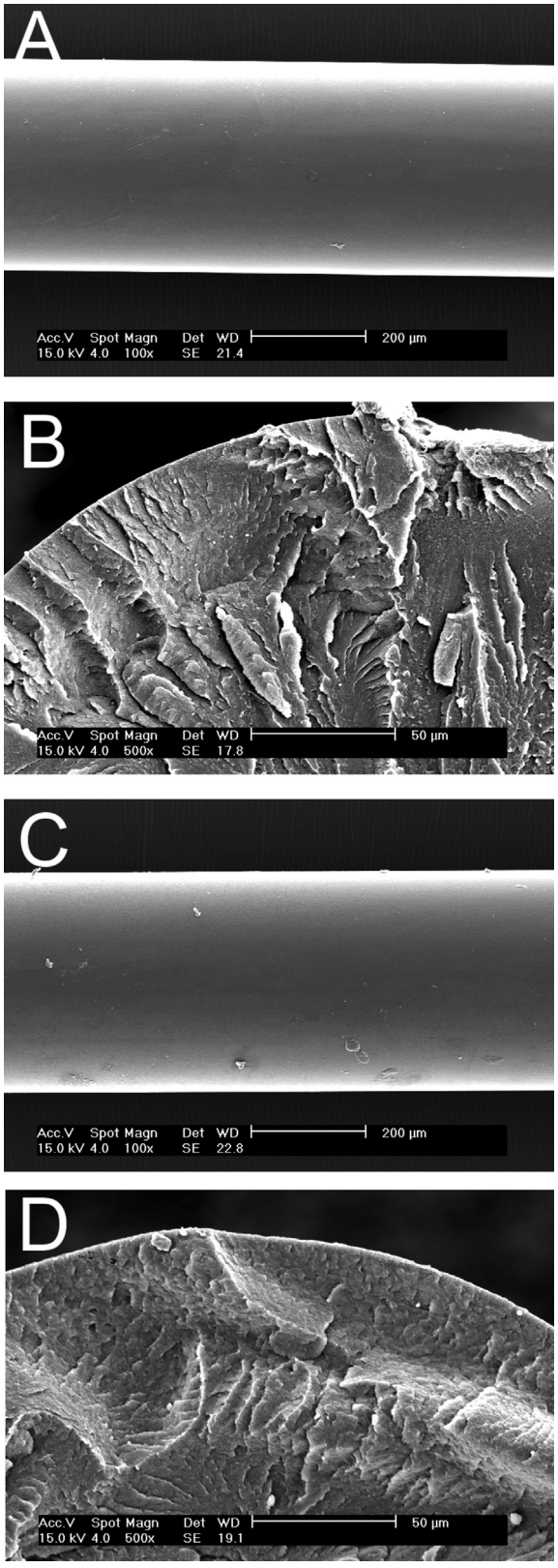

Fig. 19. Longitudinal SEM photo of pristine PEEK fibre (A), transverse SEM photo of pristine PEEK fibre (B), longitudinal SEM photo of 128 d aged PEEK fibre (C), and transverse SEM photo of 128 d aged PEEK fibre (D).

logarithmic trend line ($R^2 = 0.94$). The colour changes are mainly due to the formation of conjugation of the PEEK chains and the formation of small molecular degradation products.

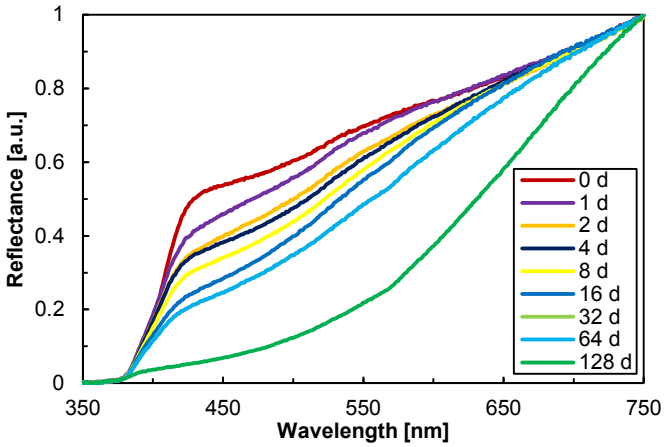

Fig. 20. UV–Vis diffuse reflectance spectra of PEEK fibres aged at 250 °C.

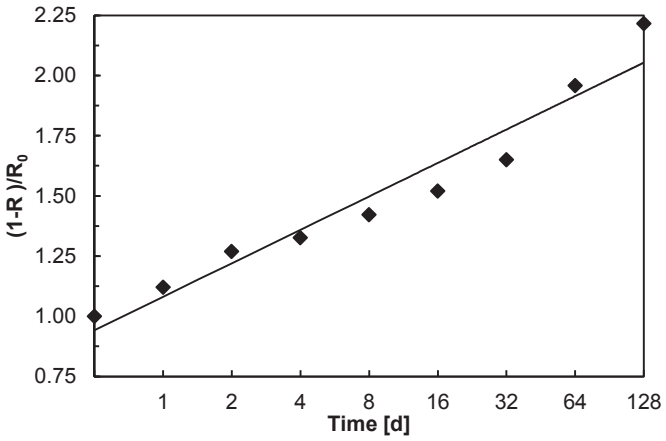

Fig. 21. Relative change in the absorbance of the PEEK fibres at 500 nm.

3.8. Comparison with photodegradation

The changes caused by thermal degradation were only partly similar to those caused by photodegradation [19]. Both ageing methods induced crosslinking in the material, increasing the zero-shear-viscosity and shear thinning, and making the most aged samples brittle. Both ageing methods also increased the mechanical strength, more so due to thermal degradation because of the positive effects of annealing the samples. The photodegradation increased both T_{g1} and T_{g2} but did not affect T_m. On the other hand, thermal ageing increased significantly T_{g1} due to the formation of secondary crystals, whereas there were no observable changes in T_{g2} and T_m before 32 d of the ageing. The carbonyl index rose more rapidly due to photodegradation compared to thermal ageing, and the main peak was located at a slightly different wavenumber, indicating that a different carbonyl group containing degradation product was dominant. According to the FTIR tests, both ageing types caused ring breaking reactions in the polymer chain. TGA revealed reduced thermal stability, however, it was inaccurate for quantitative analysis. SEM was not considered a good method for studying the degradation of PEEK fibres, since no changes were observable in the thermal degradation and only minor changes in the photodegradation. Combining both studies, the carbonyl index is the most accurate method to study the degree of degradation on the PEEK fibres. It can even separate the degradation source because the intensity maximum is located at a different

wavenumber in the thermal and photodegradation. If no equipment is available, colour changes or elongation at break can be used as easy alternatives.

4. Conclusion

The PEEK fibres were aged 1–128 d at 250 °C. The ageing process can be divided into four steps. The first step is the formation of secondary crystals in the first phases of ageing. The effects of the initial annealing are mostly positive: the mechanical strength and modulus increase without changes in the thermal properties or rheology. The second step occurs roughly between 8 and 16 d when the first signs of degradation become visible mainly with the surface sensitive methods, but the usability of the fibres remains good. The crosslinking is observed with the rheology, elongation of the material decreases, TGA demonstrates changes in the thermal decomposition behaviour, FTIR indicates the opening of phenyl rings, and the colour of the material is turning darker. The third step, the reduced usability, depends strongly on the intended application, but is located roughly between 32 and 64 d of the ageing. The material has become highly crosslinked and brittle. The decrease in the melting point can be measured with DSC and the colour of the fibres has turned brown. The fourth step would have been the degradation beyond the point of usability. However, this would have required a longer degradation time than 128 d.

Acknowledgements

The research was partly funded by the Academy of Finland UVIADEM project (Grant no 253655). The authors would like to thank Sinikka Pohjonen and Maija Järventausta for performing the TGA, DSC, and SEM measurements.

References

[1] M. Golzar, Melt Spinning of Fine PEEK Filaments (Dissertation), Technischen Universität Dresden, 2004.
[2] J. Hearle (Ed.), High Performance Fibres, Woodhead Publishing, Boca Raton, 2001, p. 344.
[3] K. Cole, I. Casella, Fourier transform infra-red spectroscopic study of thermal degradation in poly(ether ether ketone)-carbon composites, Polymer 34 (1993) 740–745.
[4] K.C. Cole, I.G. Casella, Fourier transform infrared spectroscopic study of thermal degradation in films of poly(ether ether ketone), Thermochim. Acta 211 (1992) 209–228.
[5] F. Yao, J. Zheng, M. Qi, W. Wang, Z. Qi, The thermal decomposition kinetics of poly(ether-ether-ketone) (PEEK) and its carbon fiber composite, Thermochim. Acta 183 (1991) 91–97.
[6] B. Nandan, L.D. Kandpal, G.N. Mathur, Poly(ether ether ketone)/poly(aryl ether sulphone) blends: thermal degradation behaviour, Eur. Polym. J. 39 (2003) 193–198.
[7] R.-Z. Huo, Y.-F. Luo, L.-K. Hang, X.-G. Jin, F.E. Karasz, Kinetic studies on thermal degradation of poly(aryl ether ether ketone) and sulphonated poly(aryl ether ether ketone) by thermogravimetry, J. Funct. Polym. 4 (1990) 426–433.
[8] L.H. Perng, C.J. Tsai, Y.C. Ling, Mechanism and kinetic modelling of PEEK pyrolysis by TG/MS, Polymer 49 (1999) 7321–7329.
[9] C.J. Tsai, L.H. Perng, Y.C. Ling, A study of thermal degradation of poly(aryl-ether-ether-ketone) using stepwise pyrolysis/gas chromatography/mass spectrometry, Rapid Commun. Mass Spectrom. 11 (1997) 1987–1995.
[10] M. Day, D. Sally, D.M. Wiles, Thermal degradation of poly(aryl-ether-ether-ketone): experimental evaluation of crosslinking reactions, J. Appl. Polym. Sci. 40 (1990) 1615–1620.
[11] M. Buggy, A. Carew, The effect of thermal ageing on carbon fibrereinforced polyetheretherketone (PEEK). Part II morphological changes, J. Mater. Sci. 29 (1994) 2255–2259.
[12] P.-Y. Jar, H.H. Kausch, W.J. Cantwell, P. Davies, H. Richard, The effect of annealing on the short and long term behavior of PEEK, Polym. Bull. 24 (1990) 657–664.
[13] M. Berer, Z. Major, G. Pinter, D.M. Constantinescu, L. Marsavina, Investigation of the dynamic mechanical behaviour of polyetheretherketone (PEEK) in the high stress tensile regime, Mech. Time Depend. Mater. 18 (2014) 663–684.
[14] M. Buggy, A. Carew, The effect of thermal ageing on carbon fibre reinforced polyetheretherketone (PEEK). Part I static and dynamic flexural properties, J. Mater. Sci. 29 (1994) 1925–1929.
[15] P.-Y. Jar, H.H. Kausch, Annealing effect on mechanical behavior of PEEK, J. Polym. Sci. B Polym. Phys. 30 (1992) 775–778.
[16] L.H. Lee, J.J. Vanselow, N.S. Schneider, Effects of mechanical drawing on the structure and properties of peek, Polym. Eng. Sci. 28 (1988) 181–187.
[17] G.M.K. Ostberg, J.C. Seferis, Annealing effects on the crystallinity of polyetheretherketone (PEEK) and its carbon fiber composite, J. Appl. Polym. Sci. 33 (1987) 29–39.
[18] M.P. Lattimer, J.K. Hobbs, M.J. Hill, P.J. Barham, On the origin of the multiple endotherms in PEEK, Polymer 33 (1992) 3971–3973.
[19] V. Mylläri, T.-P. Ruoko, P. Järvelä, The effects of UV irradiation to polyetheretherketone fibres – characterization by different techniques, Polym. Degrad. Stab. 109 (2014) 278–284.
[20] H. Nakamura, T. Nakamura, T. Noguchi, K. Imagawa, Photodegradation of PEEK sheets under tensile stress, Polym. Degrad. Stab. 91 (2006) 740–746.
[21] B. Claude, L. Gonon, J. Duchet, V. Verney, J.L. Gardette, Surface cross-linking of polycarbonate under irradiation at long wavelengths, Polym. Degrad. Stab. 83 (2004) 237–240.
[22] D. Carlsson, D. Wiles, The photodegradation of polypropylene films. II. Photolysis of ketonic oxidation products, Macromolecules 2 (1969) 587–597.
[23] D. Carlsson, D. Wiles, The photodegradation of polypropylene films. III. Photolysis of polypropylene hydroperoxides, Macromolecules 2 (1969) 597–606.
[24] J.M. Dealy, R.G. Larson (Eds.), Structure and Rheology of Molten Polymers, Hanser Publishers, Munich, 2006, p. 530.
[25] S. Commereuc, H. Askanian, V. Verney, A. Celli, P. Marchese, C. Berti, About the end life of novel aliphatic-aromatic (co)polyesters after UV-weathering: structure/degradability relationships, Polym. Degrad. Stab. 98 (2013) 1321–1328.
[26] C.D. Han, Rheology and Processing of Polymeric Materials: Volume 1: Polymer Rheology, Oxford University Press, New York, 2007, p. 736.

Journal of Applied Polymer Science

Sulfonated Polyetheretherketone/Polypropylene Polymer Blends for the Production of Photoactive Materials

Enrico Fatarella,[1] Ville Mylläri,[2] Marco Ruzzante,[1] Rebecca Pogni,[3] Maria Camilla Baratto,[3] Mikael Skrifvars,[4] Seppo Syrjälä,[2] Pentti Järvelä[2]

[1]Next Technology Tecnotessile Società Nazionale di Ricerca s.r.l. via del Gelso 13, 59100 Prato, Italy
[2]Department of Material Science, Tampere University of Technology, Korkeakoulunkatu 6, FI-33720 Tampere, Finland
[3]Department of Biotechnology, Chemistry and Pharmacy, University of Siena, Via A. Moro 2, 53100 Siena, Italy
[4]Swedish Centre for Resource Recovery, School of Engineering, University of Borås, S-501 90 Borås, Sweden
Correspondence to: E. Fatarella (E-mail: chemtech@tecnotex.it)

ABSTRACT: Sulfonated polyetheretherketone (SPEEK) was synthesized via a mono-substitution reaction of PEEK in concentrated sulphuric acid and was blended with polypropylene (PP) in 2–10%w/w concentration to be used for the production of photoactive thermoplastic products. SPEEK and SPEEK/PP blends were characterized using FTIR, DSC, TGA, NMR, rheology, SEM, and EPR. Under UV-Vis irradiation, stable benzophenone ketyl (BPK) radicals were generated by hydrogen extraction from PP. By increasing the amount of SPEEK in the polymer blend a linear increase in the BPK radicals was achieved according to the EPR data. DSC and TGA tests indicated weaknesses in the thermal stability of SPEEK but according to the rheological tests this should not have a major effect on processabililty. The optimal amount of SPEEK in the blend was obtained at 5%w/w. This concentration provided a good compromise between radical concentration, material processability, and cost. © 2014 Wiley Periodicals, Inc. J. Appl. Polym. Sci. **2015**, *132*, 41509.

KEYWORDS: blends; photochemistry; polyolefins

Received 4 June 2014; accepted 7 September 2014
DOI: 10.1002/app.41509

INTRODUCTION

Good indoor air quality is important for health, comfort and well-being. Despite the fact that a lot of efforts have been paid for the abatement of outdoor pollutants,[1–4] it has been stated that the levels of air pollution inside houses are often two to five times higher than outdoor levels.[5] Typical sources for indoor air pollution are cleaners, waxes, paints, pesticides, adhesives, cosmetic products, automotive products, and hobby supplies.[6] Conventional methods to remove the indoors decontaminants are often ineffective, chemically and energetically intensive and suitable only for large systems.[7] In addition, these intensive chemical treatments can even be the source of new contamination problems.

An effective alternative to conventional methods is represented by photocatalysis. Semiconductors such as TiO_2, ZnO, ZrO_2, CdS, MoS_2, Fe_2O_3, and WO_3 have been examined and used as photocatalyst.[7–11] Among these, titanium dioxide (TiO_2) has remained as the benchmark against which alternative photocatalysts are compared. TiO_2 is widely used because it is inexpensive, harmless, and its photostability is very high.[12–14] To enhance the redox potential of the valence-band holes and the conduction band electrons, particle size must be decreased. Furthermore, the highest surface area to volume ratio enhances their catalytic activity.[15]

However, TiO_2 nanoparticles have recently been classified by the International Agency for Research on Cancer (IARC) as an IARC Group 2B carcinogen "possibly carcinogenic to humans."[16] Therefore, the identification of polymeric photoactive compounds is recommended in order to reduce health concerns induced by nanoparticle handling. Within this study, SPEEK-based (sulfonated polyetheretherketone) polymeric photocatalytic blends have been studied, as an alternative enabling to realize micro- and nanosized materials, such as filaments, particles, and thin layers.

PEEK (polyetheretherketone or poly (oxy-1,4-phenyleneoxy-1,4-phenylenecarbonyl-1,4-phenylene)) is a linear semicrystalline thermoplastic with rather unique set of properties.[17] It has excellent mechanical and thermal properties and chemical resistance. Its water absorption is low, radiation resistance good and flammability low. Because of these properties PEEK is often used in high-tech applications and in extreme environments. The use of PEEK is mainly limited by its high price (100 €/kg).

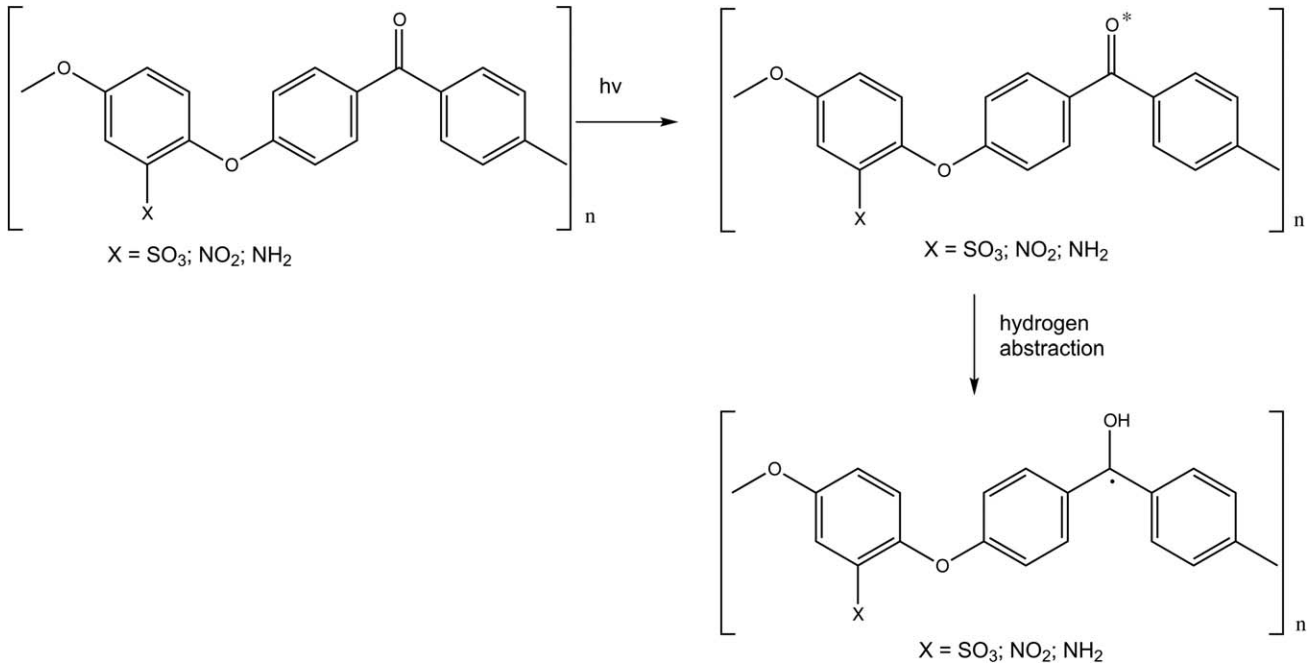

Figure 1. Excitation reaction and radical formation of modified PEEK. X can be SO_3, NH_2, or NO_2.

Sulfonation of PEEK has become a standard procedure and the effects of different parameters are well known.[18–20] The antimicrobial properties of benzophenone incorporated materials have been studied[21–23] but not in the case of SPEEK-based polymer blends. SPEEK has been, however, blended (in solution) with polymers such as polyvinyl alcohol (PVA) and polyvinyl butyral (PVB) to be used as a direct methanol fuel cell (DMFC),[24,25] metal reduction material[26,27] and for the production of functional thermoplastic materials such as advanced composites.[28] On the contrary, the idea to mechanically compound SPEEK with a polyolefin is rather new.

Chemical modifications of PEEK, such as sulfonation, enhance its solubility in organic solvents through electrophilic substitution reactions and promote the formation of benzophenone ketyl radicals (BPK) that could be effectively used to promote photocatalytic reactions. In fact, UV irradiation of a polar benzophenone induces an n to π^* transition (Figure 1) generating a triplet state that is highly reactive toward hydrogen atom abstraction by forming a stable radical.[29–31]

A hydrogen transfer reaction is involved in the initial production of the reactant radical and the generation of the final product. The selection of the appropriate hydrogen transfer agent depends on the kinetics of H-atom transfer agent and on the stabilisation of the radical induced by the chemical groups on the acceptor. Polyolefins possess a labile hydrogen atom and can therefore act as efficient chain transfer agents, whilst the sulfonated group stabilizes the radicals.

Within this study PP has been selected as the most promising partner in the photocatalytic activation because it is easy to process, largely available and very cheap polymer. The goal is to develop a new, safe, and affordable photocatalytic polymer blend that can be used in a wide range of applications (such as the production of filters for air purifier devices, filter masks, curtains, and carpet).

EXPERIMENTAL

Materials

Victrex (Lancashire, UK) PEEK grade 704 in powder form with an average molar mass of 4.5×10^4 g/mol is the primary source for the production of modified benzophenone compounds. In the sulfonation process Carlo Erba (Val de Reuil, France) 98% sulphuric acid (H_2SO_4) was used. The PP grade was Total Petrochemicals (Houston, USA) PPH 4050 homopolymer having a melt index of 3 (2.16 kg, 230°C, g/10').

Synthesis of SPEEK

The sulfonation of PEEK in powder form was carried out in a reactor in air atmosphere at a constant temperature of 45°C. 5%w/v of PEEK was added to a solution of concentrated sulphuric acid, and the solution was mechanically stirred for a period of 3 h. The obtained SPEEK was then precipitated by dropwise addition of the solution to 500 mL of ice cooled distilled water. The precipitate was washed till the excess acid was removed and then dried in an oven at 70°C for 12 h.

SPEEK/PP Compounding

The SPEEK/PP was compounded by using a DSM Xplore micro compounder. The equipment has two counter rotating screws and a maximum batch size of 5 mL. The materials were weighted, loaded into the compounder and mixed for 5 min at 200°C at a screw speed of 150 RPM.

FTIR

The chemical composition was characterized by ATR (attenuated total reflectance) FTIR spectroscopy. The equipment used was Perkin

Elmer Spectrum One spectrometer in HATR reflection mode. A zinc selenide crystal and a resolution of 4 cm^{-1} were used.

DSC

DSC tests were made with a Mettler Toledo 822 e. Samples were heated in nitrogen (flux 80 mL/min) at a heating rate of 10°C/min. They were heated only once due to the degradative behavior of SPEEK at higher temperatures.

TGA

TGA tests were made with a PerkinElmer TGA 6. Samples were heated from room temperature to 995°C in nitrogen atmosphere with a heating rate of 20°C/min.

NMR

The ^{1}H-NMR spectra were recorded using a Bruker 200 MHz spectrometer. The spectra were recorded at 60°C, without internal standard and using deuterated dimethyl sulfoxide (DMSO-d6) as a solvent, with a polymer concentration of about 30 mg mL^{-1}. Experimental data were elaborated with 1D Win-NMR software, applying the Lorentze Gauss enhance function and using appropriate Line broadening and Gaussian broadening parameters in order to improve the peaks resolution.

Rheological Measurements

Oscillatory shear measurements within the linear viscoelastic range (strain amplitude of 10%) were carried out for the samples using an Anton Paar Physica MCR 301 rheometer. All the experiments were performed under a nitrogen atmosphere using a 25-mm plate-plate geometry. The measuring points in the angular frequency range of 0.1–562 rad/s were recorded with decreasing frequency. Each sample was measured two times and the average of these measurements was used. The time-dependence of viscosity was tested using a constant angular frequency of 10 rad s^{-1}, strain amplitude of 10% and measuring time of 30 min.

Scanning Electron Microscopy

The morphology of PP, SPEEK, and SPEEK/PP blends were investigated by a Philips XL30 scanning electron microscope (SEM). The materials were cut with liquid nitrogen and mounted vertically under the SEM for the investigations. The materials were gold sputtered before investigations in order to increase their conductivity.

Electron Spin Resonance Measurements

Electron paramagnetic resonance (EPR) spectroscopy was used to confirm the free-radical characteristics of the photoactive species. Continuous wave (CW) X-band (9 GHz) EPR measurements were carried out at room temperature on a Bruker E500 ELEXSYS Series, using the Bruker ER 4122 SHQE cavity. The sample was placed into a 4.0 mm ID Suprasil tube, exposed to UV irradiation generated by a UV lamp (effective irradiative power 8 W/m^2 in the range 390−490 nm) at a distance of 11 cm for 15 min. Then the specimen was immediately measured by EPR spectroscopy. The relative radical amount was calculated from the EPR peak areas.

RESULTS AND DISCUSSION

SPEEK Sulfonation and SPEEK/PP Compounding

The processing parameters for PEEK sulfonation were chosen according to a previous study[18] in which a reaction temperature of 45°C, a reaction time of 3 h and PEEK concentration of 5%w/v provided the highest degree of sulfonation. Sulfonation is an electrophilic aromatic substitution reaction in which a hydrogen atom attached to the PEEK repeating unit is replaced by a sulfonic acid group via a monosubstitution reaction on the benzene ring connected with two ether linkages.[18]

SPEEK was compounded with a high viscosity (melt flow index of 3 g/10') PP grade. The selection of this grade was based on the assumption that compounding would decrease viscosity, which indeed was the case according to the rheological tests. Thermal characterization of SPEEK indicates poor thermal stability that had to be taken into consideration during the material compounding: the compounding time and temperature had to be a compromise between proper mixing and as low material degradation as possible. The obtained SPEEK/PP blend had a homogenous character and was brown in colour. An increase of the processing time lead to a darker color, which is a typical sign of thermal degradation.

FTIR

The results of the FTIR analysis correspond with the results from previous studies, where PEEK[32,33] and SPEEK[18] were characterized. Typical absorption bands of PEEK are 1653, 1648, and 1252 cm^{-1} associated with carbonyl stretching frequency, 1490 cm^{-1} characteristic of ring absorption, 1227 cm^{-1} associated with carbon-oxygen-carbon stretching vibration, 863, 841, and 700 cm^{-1} associated with ring deformation modes, and 1305, 1280, 965, and 952 cm^{-1} that are related to PEEK crystallinity.

In SPEEK, typical absorption bands associated with sulphuric acid groups are 3440, 1252, 1080, 1024, and 709 cm^{-1}.[18] The broad band at 3440 cm^{-1} is related to the —OH vibrations of —SO_3H and to the absorbed moisture, 1252 cm^{-1} to asymmetric stretching of O═S═O, 1080 cm^{-1} to symmetric stretching of O═S═O, 1024 cm^{-1} to stretching of S═O and 709 cm^{-1} to stretching of S—O.

Literature data[18] suggests that the intensity of aromatic C—C absorption band at 1492 cm^{-1} should decrease and the intensity of the 1472 cm^{-1} band (associated with the aromatic absorption of a substituted ring) increase as the sulfonation degree increases. The FTIR analysis confirms that the intensity of the 1492 cm^{-1} band decreases significantly during the sulfonation. An absorption peak at 869 cm^{-1}, associated with out-of-plane C—H bending of isolated hydrogen in a tri-substituted phenyl ring, appears during the sulfonation.

DSC

Significant changes in the thermal behaviour of the SPEEK polymer in comparison with PEEK were observed in the DSC tests. In PEEK, an endothermic transition peak at 346°C is recorded. In SPEEK, no crystallization peak is observed, which indicates that after the sulfonation reaction a complete amorphous polymer is produced. The T_g (glass transition temperature) midpoint temperature is higher in SPEEK than in PEEK, 225°C and 159°C, respectively (Table I).

In SPEEK/PP blends a single melting temperature (T_m) around 168°C and two different T_g's around 3°C and 223°C were

Table I. Thermal Properties of PP, PEEK, SPEEK, and SPEEK/PP 2 : 98, 5 : 95, and 10 : 90 Blends Measured by DSC (10°C/min, N_2)

Sample	T_{g1}	T_{g2}	T_m
PEEK	159.4°C	–	346.6°C
SPEEK	–	225.2°C	–
PP	2.3°C	–	168.2°C
SPEEK/PP 2 : 98	3.1°C	221.9°C	169.4°C
SPEEK/PP 5 : 95	2.0°C	225.8°C	167.5°C
SPEEK/PP 10 : 90	2.8°C	219.7°C	168.6°C

observed. The differences between different blend compositions are rather small. T_m corresponds to the melting temperature of PP whilst it is well known[34] that T_g for a homogeneous mixture of bicomponent blends can be considered the weighted mean of the T_g of the single components according to the eq. (1):

$$T_{gmix} = T_{g1} w_1 + T_{g2} w_2 \quad (1)$$

where T_{g1} and T_{g2} are the glass transition temperatures and w_1 and w_2 the weight portions of the components 1 and 2, respectively. Because the thermal profile shows two different T_gs (Figure 2), this means that an immiscible (heterogeneous) polymer blend is obtained. This result was confirmed by the SEM analysis.

TGA

The TGA analysis in Figure 3 shows that the mass of PEEK remains constant until the decomposition temperature of 580°C, which is rather unique for a thermoplastic polymer. PEEK sulfonation changes the thermal properties of the material totally, lowering the decomposition temperature of SPEEK below 250°C. The mass loss from 50 to 250°C is shown to happen due to chemically and physically bound water, the mass loss from 250 to 450°C is due to the decomposition of acid group which induces the elimination of SO_3 and the decomposition of the $–SO_3H$ group. The mass loss above 450°C is due to the breakdown of the polymer backbone.[18] If the SPEEK is dried 30 min at 200°C, the curve stays at a significantly higher level as a result of the removed water. It is also possible that the drying evaporates some of the most unstable components which change the decomposition behaviour compared with undried SPEEK/PP.

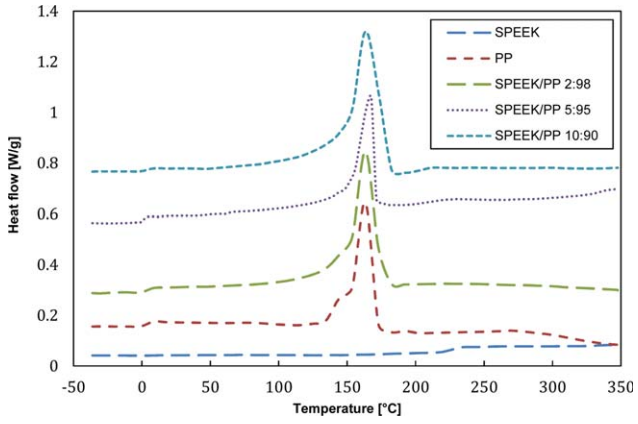

Figure 2. DSC curve of SPEEK, PP, SPEEK/PP 2 : 98, 5 : 95, and 10 : 90 (10°C/min, N_2 80 mL/min). [Color figure can be viewed in the online issue, which is available at wileyonlinelibrary.com.]

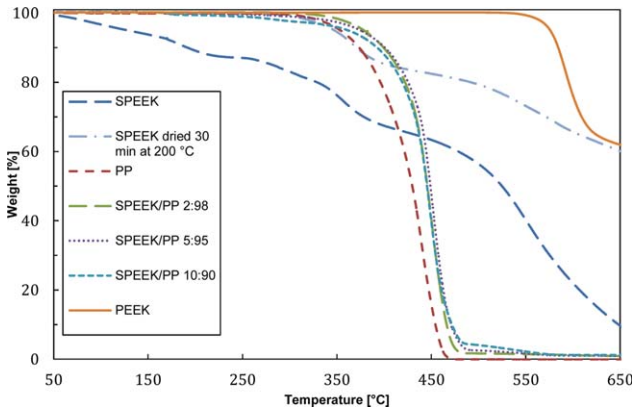

Figure 3. TGA curve of PEEK, SPEEK dried, SPEEK, SPEEK/PP 2 : 98, 5 : 95, 10 : 90, and PP (20°C/min, N_2). [Color figure can be viewed in the online issue, which is available at wileyonlinelibrary.com.]

In the SPEEK/PP blend, the mass loss starts earlier with increased SPEEK concentrations. Surprisingly SPEEK/PP seems to have an improved thermal stability compared with neat PP, at least at low SPEEK concentrations. This could be related to the degradation of the SPEEK that promotes clustering of the sulfonated groups, enabling to thermally stabilize the polymer.

The degree of sulfonation (DS) for SPEEK can be evaluated from the weight losses (WL) according to the eq. (2):

$$DS = \frac{WL_m}{WL_t} \times 100\ \% \quad (2)$$

where WL_m is the measured weight loss between 250 and 450°C and WL_t the theoretical maximum of the weight loss; the mass of the SO_3 group from the whole unit according to the eq. (3):

$$WL_t = \frac{[SO_3]}{[C_{19}H_{12}O_6S]} \times 100\ \% \quad (3)$$

WL_t is thus 21.7% for completely sulfonated samples (exactly one sulfonic acid group per repeating unit is present, Figure 4).

The WL_m measured is 23.7% (Table II), giving a theoretical DS of 109%. The explanation why this value is over 100% is that the acid groups may cause random chain scission reactions, which lead to a loss of phenol groups as well.[35] In addition, the limits for SO_3 volatilization can be considered somewhat

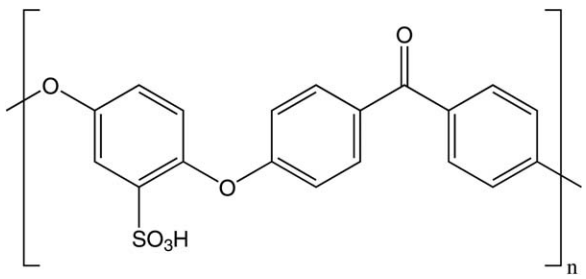

Figure 4. The chemical structure of synthesized SPEEK. NMR and TGA studies are confirming that a monosubstituted SPEEK is produced.

Table II. Results of the TGA Analysis for PEEK and SPEEK (20°C/min, N_2)

	Mass loss (%)			
Sample	50–250°C	250–450°C	450–650°C	Char residue
PEEK	0.1	0.0	38.3	61.6
SPEEK	12.4	23.7	53.6	9.6

inaccurate. According to the previous study,[18] the DS (measured by elemental analysis and ^{1}H-NMR) is around 70–80% with the same processing parameters.

NMR

To confirm that a monosubstitution has arisen, DS has been assessed by ^{1}H-NMR measurement. In fact, PEEK sulfonation generates a single signal for H proton in ortho position to SO_3H and its intensity is equivalent to the SO_3H group content.[36] The ratio between the area of this proton peak (centered at 7.5 ppm) and the area of the other protons corresponds to a degree of sulfonation that equals of 93%. It confirms the achievement of a higher reaction yield compared to previous study[18] and the contribution of acid group random chain scission during thermal degradation.

Rheological Characterization

It is important to know the rheological properties of the SPEEK/PP blend when the material is further processed into an actual product. The results of the rheological tests in Figure 5 show that compounding decreases the complex viscosity. Compounded PP has ~10% lower viscosity compared with neat PP. This is in line with previous studies[37] where several extrusion cycles have shown to cause a rapid increase in chain scission reactions and thus a decrease in molecular weight and complex viscosity. SPEEK/PP 2 : 98 has similar viscosity as compounded 100% PP but at a 5 : 95 concentration the viscosity is significantly lower. The drop in viscosity from a concentration of 5 : 95 to 10 : 90 is relatively small. The decrease in viscosity could be explained by the degradation behavior of SPEEK at elevated temperatures and the following chain scission reactions in the material caused by the decomposition products of SPEEK, such as the acid groups mentioned in the TGA paragraph. A similar degradation has been seen when adding compatibilizating maleic anhydride to PP[38] and peroxides[39] or nitroxyl radical generators[40] to PP for rheology control.

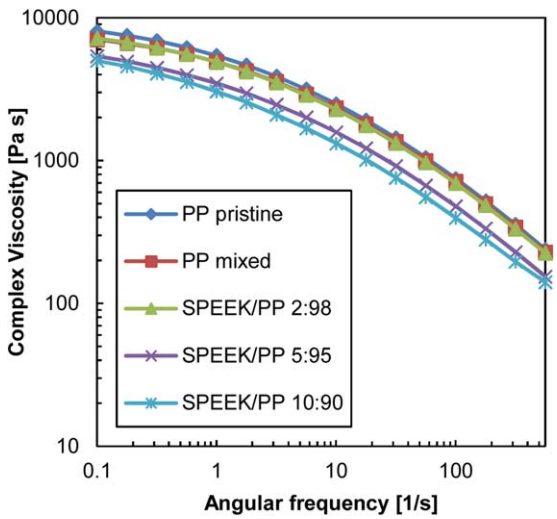

Figure 5. Complex viscosity of PP, PP mixed, and SPEEK/PP 2 : 98; 5 : 95; 10 : 90 (200°C, N_2). [Color figure can be viewed in the online issue, which is available at wileyonlinelibrary.com.]

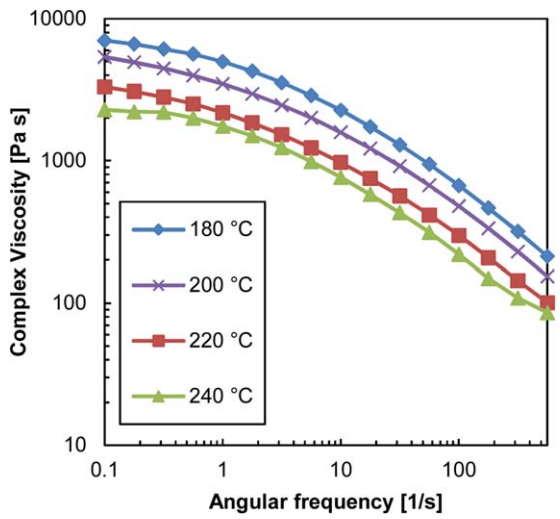

Figure 6. Complex viscosity of SPEEK/PP 5 : 95 (180, 200, 220, and 240°C, N_2). [Color figure can be viewed in the online issue, which is available at wileyonlinelibrary.com.]

There are no significant differences in the shear thinning behavior of SPEEK/PP 5 : 95 blend up to temperature of 220°C (Figure 6). At 240°C the shape of the curve is different from the other curves, indicating that thermal degradation occurs at the end of the measurement. The total measuring time is ~10 min, and the three last points (lowest angular frequencies) take most of this time.

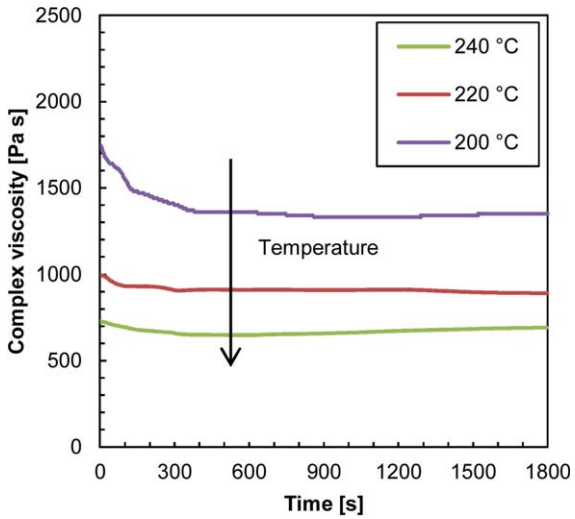

Figure 7. Complex viscosity of SPEEK/PP 5 : 95 as a function of time (200, 220, and 240°C, N_2). [Color figure can be viewed in the online issue, which is available at wileyonlinelibrary.com.]

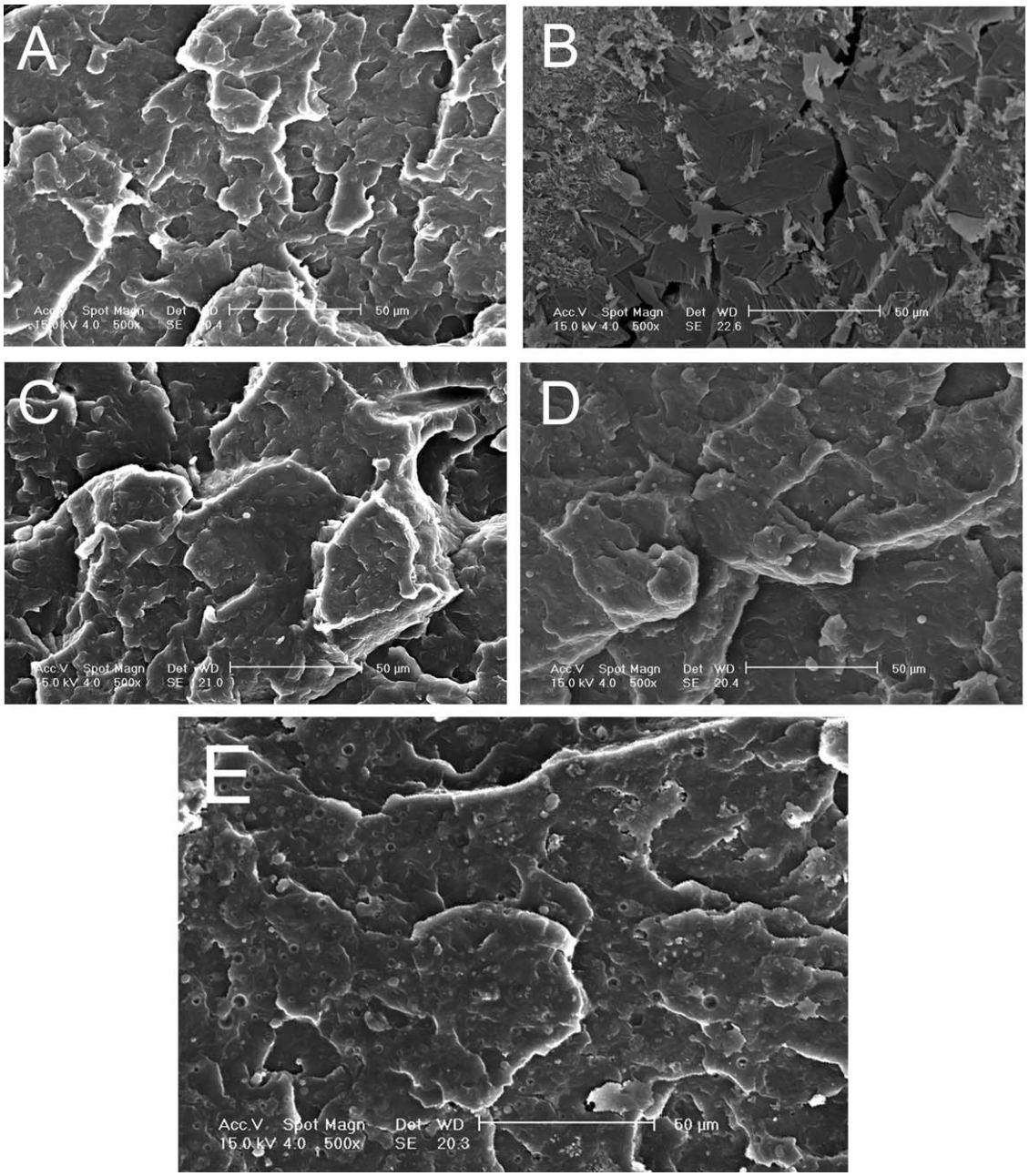

Figure 8. SEM micrograph of PP (A), SPEEK (B), SPEEK/PP 2 : 98 (C), SPEEK/PP 5 : 95 (D), and SPEEK/PP 10 : 90 (E).

Figure 7 shows that viscosity decreases as a function of time, which confirms that thermal degradation occurs. At 200°C the drop is the largest, ~20% during the first 5 min. As a comparison, the drop at 220°C and 240°C is 8–9%. The explanation for this behavior can be found from the measuring setup. It takes a few minutes to melt the material, trim it and then start the measurement. Evidently most of the chemical reactions occur during this time if the temperature exceeds 200°C. This also explains the observed variations in the results with 5 : 95 and 10 : 90 concentrations at 200°C.

The high viscosity PP grade was originally selected to compensate the decrease in viscosity during the compounding and according to these tests the rheological properties of 0–10%w/w compounds should be sufficient for further processing. Processing times and temperatures are recommended to be minimized in order to avoid thermal degradation of the material.

SEM Analysis

SEM analysis has been carried out for PP [Figure 8(A)], SPEEK [Figure 8(B)] SPEEK/PP 2 : 98 [Figure 8(C)], SPEEK/PP 5 : 95 [Figure 8(D)], and SPEEK/PP 10 : 90 [Figure 8(E)]. There are two different domains in the SPEEK/PP blends which mean that the two polymers are not miscible, even if the shear forces in the compounder seem to be able to homogenously disperse the photoactive SPEEK polymer into the polypropylene. This result was confirmed by the DSC tests where two separate T_g's were observed in SPEEK/PP. A typical size of the SPEEK

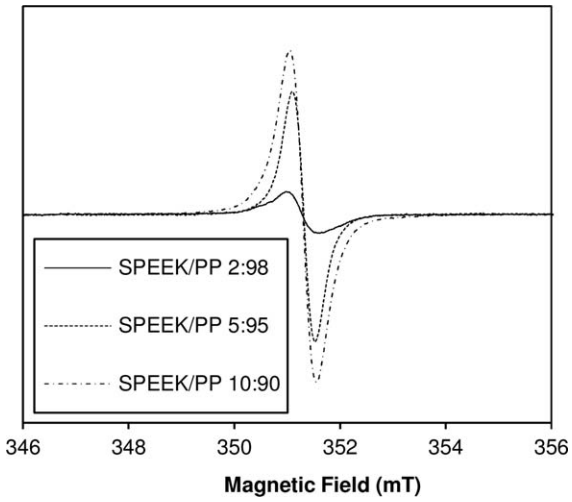

Figure 9. RT X-band EPR spectra of the SPEEK/PP blends (2 : 98; 5 : 95; 10 : 90) recorded after 15 min of irradiation ($\nu = 9.86$ GHz, 0.63 mW power, 0.2 mT modulation amplitude).

particles in the blend seems to be a few micrometers which should not be a problem during the further processing of the material. Even melt spinning of the blend should be possible.

Photochemical Properties

In order to evaluate the photocatalytic effectiveness of the made polymer blends, EPR spectroscopy was performed. Room temperature EPR analysis performed on a transparent casted film made from 100% SPEEK showed that after exposure to UV irradiation for 15 min free radicals are generated. The presence of PP in the SPEEK sample with increasing molar ratio significantly improves the radical formation efficiency. In Figure 9, the room temperature X-band EPR spectra of the SPEEK/PP blends are reported.

X-band EPR spectrum of 100% SPEEK exhibits a single line with a g value of 2.0035 ($\pm$0.0003). The g value obtained for the investigated sample is in agreement with the value reported in the literature for a phenyl ketyl radical of benzophenone.[41] In the EPR spectrums reported for SPEEK/PP 2 : 98, 5 : 95, and 10 : 90, where the donor is polyolefins, the radical signal may derive from the coexistence of both BPK radical and diphenylhydroxy methyl radical. However, the very slight difference in the g values for both specimens does not allow discriminating the single contributions, and the simultaneous presence of the radicals cannot be excluded.

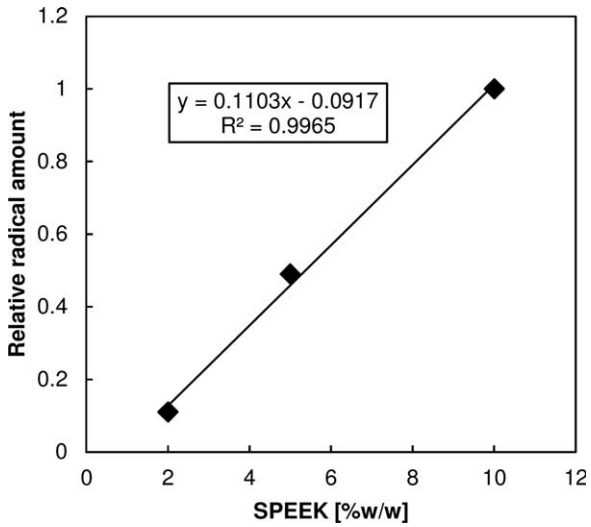

Figure 10. Relative radical concentration as a function of the polymer blend composition.

The analysis of the spectral area showed that by increasing the polyolefin content in the range 2–10% a linear increase in the production of the radical is achieved (Figure 10). Higher SPEEK concentrations in the SPEEK/PP blend have not been investigated due to the higher costs of the SPEEK polymer and the high efficiency of the system at low SPEEK content. The relative radical amount of 100% SPEEK was 1/20 of that of SPEEK/PP 10 : 90.

CONCLUSIONS

The combination of SPEEK and PP generates a stable BPK radical formation, enabling to promote the degradation of chemicals. The increase in the radical concentration is almost linear as a function of SPEEK concentration. An optimal amount of modified PEEK in the polymer blend is seen at 5%w/w. This concentration was observed to provide good photochemical properties at a competitive price. The synthesis of SPEEK as well as SPEEK/PP compounding were relatively problem-free and, according to the SEM analysis, SPEEK particles are homogenously dispersed into the PP matrix. Inferior thermal properties of SPEEK compared with PEEK were evident in the thermal tests, and also the rheological tests showed signs of material degradation as a result of chain scission reactions. Further processing of the material into commercial products should be possible when the optimal processing parameters have been determined.

ACKNOWLEDGMENTS

The authors thank the European Commission for funding this study within the FP7 "SAFEPROTEX" (FP7-NMP-2008-SME-2 contract number 228439), the Federation of Finnish Textile and Clothing Industry (Finatex) and Finnish Foundation for Technology Promotion (TES).

REFERENCES

1. Shen, S.; Burton, M.; Jobson, B.; Haselbach, L. *Constr. Build. Mater.* **2012**, *35*, 874.
2. Justin, M.; Langridge, R.; Gustafsson, J.; Griffiths, P. T.; Cox, R. A.; Lambert, R. M.; Jones, R. L. *Atmos. Environ.* **2009**, *43*, 5128.
3. Ângelo, J.; Andrade, L.; Madeira, L. M.; Mendes, A. *J. Environ. Manag.* **2013**, *129*, 522.
4. Paz, Y. *Appl. Catal. B: Environ.* **2010**, *99*, 448.
5. US Department of Health and Human Services Center for Environmental Health. Healthy Housing Reference Manual, Atlanta, **2006**.

6. Maroni, M.; Seifert, B.; Lindvall, T. Air quality monograps Vol. 3. Indoor air quality; Elsevier: Amsterdam, **1995**.
7. Rajesh, K. M. Studies on photocatalysis by nano titania modified with non-metals. Doctoral thesis. Cochin University of Science and Technology; India, **2011**.
8. Quanjun, X.; Jiaguo, Y.; Po, K. W. *J. Colloid. Interface Sci.* **2011**, *357*, 163.
9. Kitano, M.; Matsuoka, M.; Ueshima, M.; Anpo, M. *Appl. Catalysis A: Gen.* **2007**, *325*, 1.
10. Lin, C.-C.; Chiang, Y.-J. *Chem. Eng. J.* **2012**, *181*, 196.
11. Siriwong, C.; Wetchakun, N.; Inceesungvorn, B.; Channei, D.; Samerjai, T.; Phanichphant, S. *Prog. Cryst. Growth Charact. Mater.* **2012**, *58*, 145.
12. Sato, K.; Hirakawa, T.; Komano, A.; Kishi, A.; Nishimoto, C. K.; Mera, N.; Kugishima, M.; Sano, T.; Ichinose, H.; Negishi, N.; Seto, Y.; Takeuchi, K. *Appl. Catalysis B: Environ.* **2011**, *106*, 316.
13. deRichter, R.; Caillol, S. *J. Photochem. Photobiol. C: Photochem. Rev.* **2011**, *12*, 1.
14. Ramirez, A. M.; Demeestere, K.; Belie, N. D.; Mäntylä, T.; Levänen, E. *Build. Environ.* **2010**, *45*, 832.
15. Beydoun, D.; Amal, R.; Low, G.; Mc Evony, S. *J. Nanopart. Res.* **1999**, *1*, 439.
16. World health organization International Agency for Research on Cancer. IARC monograps on the evaluation of carcinogenic risks to humans. Vol. 93 carbon black, titanium dioxide and talc. Lyon, **2010**.
17. Sabu, T.; Visakh, P. M., Eds. Handbook of Engineering and Speciality Thermoplastics: Polyethers and Polyesters, Vol. 3; Wiley: New York, **2011**.
18. Muthu Lakshmi, R. T. S.; Choudhary, V.; Varma, I. K. *J. Mater. Sci.* **2005**, *40*, 629.
19. Jin, X.; Bishop, M. T.; Ellis, T. S.; Karasz, F. E. *Br. Polym. J.* **1985**, *17*, 4.
20. Shibuya, N.; Porter, R. S. *Macromolecules* **1992**, *25*, 6495.
21. Hong, K. H.; Sun, G. *J. Appl. Polym. Sci.* **2009**, *112*, 2019.
22. Hong, K. H.; Sun, G. *J. Appl. Polym. Sci.* **2008**, *109*, 3173.
23. Hong, K. H.; Sun, G. *J. Carbohydr. Polym.* **2008**, *71*, 598.
24. Yang, T. *Int. J. Hydrog. Energy* **2008**, *33*, 6772.
25. Molla, S.; Compan, V. *Int. J. Hydrog. Energy* **2014**, *39*, 5121.
26. Korchev, A. S.; Konolova, T.; Cammarata, V.; Kispert, L.; Slaten, L.; Mills, G. *Langmuir* **2006**, *22*, 375.
27. Korchev, A. S.; Bozack, M. J.; Slaten, B. L.; Mills, G. *J. Am. Chem. Soc.* **2004**, *126*, 10.
28. Conceição, T. F.; Bertolino, J. R.; Barra, G. M. O.; Pires, A. T. N. *Mater. Sci. Eng. C* **2009**, *29*, 575.
29. Korchev, A. S.; Shulyak, T. S.; Slaten, B. L.; Gale, W. F.; Mills, G. J. *Phys. Chem. B* **2005**, *109*, 7733.
30. Gilbert, A.; Baggott, J. Essentials of Molecular Photochemistry; CRC Press: Boca Raton, **1991**.
31. Rånby, B.; Rabek, J. F. ESR Spectroscopy in Polymer Research; Springer: Berlin, **1977**.
32. Harris, L. A study of the crystallisation kinetics in PEEK and PEEK composites. Master of research thesis; The University of Birmingham, **2011**.
33. Chalmers, J.; Gaskin, W.; Mackenzie, M. *Polym. Bull.* **1984**, *11*, 433.
34. Guaita, M.; Ciardelli, F.; La Mantia, F.; Pedemonte, E. Fondamenti di Scienza dei Polimeri, Pacini Ed. Nuova; Cultura, **1998**.
35. Luo, Y.; Huo, R.; Jin, X.; Karasz, F. J. *Anal. Appl. Pyrolysis* **1995**, *34*, 229.
36. Zaidi, S. M. J.; Mikhailenkoa, S. D.; Robertson, G. P.; Guiver, M. D.; Kaliaguine, S. *J. Membr. Sci.* **2000**, *173*, 17.
37. da Costa, H. M.; Ramos, V. D.; Rocha, M. C. G. *Polym. Test.* **2005**, *24*, 86.
38. Machado, A. V.; Covas, J. A.; Van Duin, M. *Adv. Polym. Technol.* **2004**, *23*, 196.
39. Azizi, H.; Ghasemi, I.; Karrabi, M. *Polym. Test.* **2008**, *27*, 548.
40. Psarreas, A.; Tzoganakis, C.; McManus, N.; Penlidis, A. *Polym. Eng. Sci.* **2007**, *47*, 2118.
41. Yoshida, H.; Warashida, T. *Bull. Chem. Soc. Jpn.* **1971**, *44*, 2950.

Journal of Applied Polymer Science

Production of sulfonated polyetheretherketone/polypropylene fibers for photoactive textiles

Ville Mylläri,[1] Enrico Fatarella,[2] Marco Ruzzante,[2] Rebecca Pogni,[3] Maria Camilla Baratto,[3] Mikael Skrifvars,[4] Seppo Syrjälä,[5] Pentti Järvelä[1]

[1]Tampere University of Technology, Department of Material Science, Korkeakoulunkatu 6, 33720 Tampere, Finland
[2]Next Technology Tecnotessile Società Nazionale di Ricerca s.r.l., via del Gelso 13, 59100 Prato, Italy
[3]Department of Biotechnology, Chemistry and Pharmacy, University of Siena, Via A. Moro 2, 53100 Siena, Italy
[4]Swedish Centre for Resource Recovery, University of Borås, S-501 90 Borås, Sweden
[5]Tampere University of Technology, Department of Mechanical Engineering and Industrial Systems, Korkeakoulunkatu 6, 33720 Tampere, Finland
Correspondence to: V. Mylläri (E-mail: ville.myllari@tut.fi)

ABSTRACT: New photocatalytic fibers made of sulfonated polyetheretherketone (SPEEK)/polypropylene (PP) are melt compounded and melt spun, first on laboratory scale and then on a semi-industrial scale. Fiber spinnability is optimized and the fibers are characterized using mechanical testing, electron paramagnetic resonance (EPR) spectroscopy, and scanning electron microscopy (SEM). According to the results, the fiber spinnability remains at a good level up to 10 wt % SPEEK concentration. Optimal processing temperature is 200°C due to the thermal degradation at higher temperatures. EPR measurements show good and long-lasting photoactivity after the initial irradiation but also decay in the radical intensity during several irradiation cycles. Mechanical tenacity of the SPEEK/PP 5 : 95 fiber is approximately 20% lower than for otherwise similar PP fiber. The fiber is a potential alternative to compete against TiO2-based products but more research needs to be done to verify the real-life performance. © 2015 Wiley Periodicals, Inc. J. Appl. Polym. Sci. **2015**, *132*, 42595.

KEYWORDS: blends; fibers; functionalization of polymers; photochemistry; textiles

Received 26 February 2015; accepted 3 June 2015
DOI: 10.1002/app.42595

INTRODUCTION

The use of photocatalytic textiles in antimicrobial, self-cleaning, and anti-pollution products has increased during the last few decades. These functionalities are based on the highly reactive radicals and oxidants that are generated under band-gap light irradiation. Photocatalysts can be used as an alternative to conventional biocides to prevent the deterioration of textiles caused by insects, fungi, algae, and microorganisms.[1] The self-cleaning property of a photoactive textile is based on the discoloration of organic stains by reactive radicals.[2] Photocatalytic oxidation (PCO) is an emerging technology in air purification, and is also based on the decomposition of harmful substances.[3]

Although several semiconductors have been used as photocatalysts,[4] titanium dioxide (TiO_2) has dominated the research because of its low price, high photostability, and safety.[5] In this study, a photoactive polymer fiber made of sulfonated polyetheretherketone (SPEEK)/polypropylene (PP) blend is manufactured as an alternative to TiO_2-based fibers. According to the previous characterization of the SPEEK/PP blend,[6] the material provides good photochemical properties but has problems in thermal stability. The main competitive advantage of SPEEK/PP is the safety of the material because it does not contain nanoparticles and it has been demonstrated to be biocompatible with minor effect on cytotoxicity induced by residual content of sulphuric acid used in the synthesis.[7] By contrast, the particle size of TiO_2 is reduced to nanoscale to increase the total surface area per volume ratio and thus efficiency. The increased use of nanoparticles in many applications has raised questions about their safety, and recent research suggests that TiO_2 nanoparticles are possibly carcinogenic to humans.[8]

Sulfonated polyetheretherketone (SPEEK) is manufactured through a sulfonation process of polyetheretherketone (PEEK), which is a linear semicrystalline thermoplastic polymer with excellent mechanical and thermal properties and chemical

Additional Supporting Information may be found in the online version of this article.

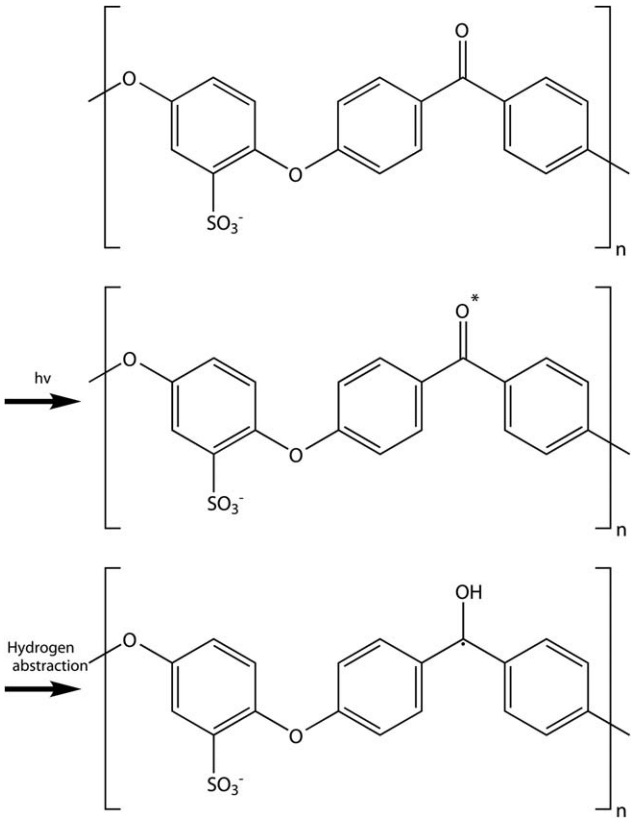

Figure 1. Excitation reaction and radical formation of SPEEK.

resistance.[9] Compared to PEEK, SPEEK alone has poor thermal properties and processability[6] and has to be blended with other polymers.[10–12] The photoactivity of SPEEK is based on the formation of benzophenone ketyl radicals (BPK) in the polymer chain. When polar benzophenone of SPEEK is exposed to UV irradiation, the n-to-π^* transition induces a generation of a triplet state.[11] This triplet state is highly reactive to form a stable BPK radical by abstracting a hydrogen atom (Figure 1). The antimicrobial effectiveness of benzophenone has been previously confirmed with different polymers.[13] PP is an excellent candidate to assist SPEEK in the hydrogen abstraction since it possesses a labile hydrogen atom. Furthermore, PP is an inexpensive commodity plastic widely used in fibers.

The SPEEK/PP fibers are made by first compounding the materials in a melt mixing process, and then melt spinning the compound. During the melt mixing, it is important that the SPEEK particles are homogenously dispersed into the PP matrix and that there remain no large particles or particle agglomerates which could lead to a spinline failure in the melt spinning. It has been observed that when the particle size approaches close to the fiber diameter, the spinning stability is reduced drastically.[14] According to the performed characterization of previously made SPEEK/PP blends, the blend is homogenous with a SPEEK particle size of a few micrometers,[6] which should be small enough for the fiber spinning.

Textile fabrics made of SPEEK/PP filament yarn would have potential for use in photocatalytic textiles. The closest competitor, a PP/TiO_2 nanocomposite fiber, has been evaluated[15] and, according to antimicrobial testing, this blend should have antimicrobial properties in proper compositions.[16] Antimicrobial textiles are currently used in products such as tents, tarpaulins, awnings, blinds, parasols, sails, waterproof clothing, in some consumer textiles, and medical settings.[17] Conventional antimicrobial textiles are based on biocides like silver,[18,19] quaternary ammonium salts,[20] halamine structures,[21,22] triclosan, or zinc pyrithione.[17] These biocides have been criticized due to their limited efficiency, high costs, toxicity, and environmental concerns.[16] A self-cleaning property is desirable especially in the clothing industry and, therefore, the research has focused on that sector.[2,23,24] However, these products are not largely available yet and they raise health concerns due to the nanoparticles they contain. There are many commercial air purifiers on the market that use photocatalytic oxidation to turn harmful substances, including volatile organic compounds (VOCs), into less harmful compounds such as CO_2 and H_2O.[3,25]

In this study, SPEEK/PP-based photoactive fibers are manufactured as an alternative to TiO_2 and conventional methods to provide antimicrobial, self-cleaning, and anti-pollution properties. The fibers are manufactured in a melt spinning process, first on laboratory scale and then on a semi-industrial scale. The fibers are characterized regarding their mechanical properties, photochemical effectiveness, and morphology. Based on the obtained results, their suitability in commercial textile applications is estimated. In addition to the new polymer-based textile material, the novelty of this study is the melt spinning of an unconventional polymer blend containing two totally different components and time-dependent processability.

EXPERIMENTAL

Materials

Victrex (Lancashire, UK) PEEK grade 704 in powder form with an average molar mass of 4.5×10^4 g/mol is the primary source for the synthesis of modified benzophenone compounds. In the sulfonation process, 98% sulphuric acid (H_2SO_4) (Carlo Erba, Val de Reuil, France) was used. The PP grade was PPH 4050 homopolymer (Total Petrochemicals, Houston, USA) having a melt index of 3 g/10 min (2.16 kg, 230°C) according to the supplier's information.

Synthesis of SPEEK

The sulfonation of PEEK in powder form was carried out in a 250 mL reactor in air atmosphere at a constant temperature of 45°C. 5% w/v of PEEK was added to a solution of concentrated sulphuric acid (98%), and the solution was mechanically stirred for a period of 3 h. The obtained SPEEK was then precipitated by dropwise addition of the solution to 500 mL of ice-cooled distilled water. The precipitate was washed till the excess acid was removed and then dried in an oven at 70°C for 12 h.

SPEEK/PP Compounding

The SPEEK/PP blend was batchwise compounded by using a DSM Xplore micro compounder. The equipment has two counter rotating screws and a maximum batch size of 5 mL. The materials were weighed, loaded into the compounder, and mixed for 5 min at 200°C at a screw speed of 150 RPM.

Table I. Processing Parameters for the Laboratory Scale Melt Spinning Process

Number of filaments	1
Die length (mm)	30
Die diameter (mm)	1
Drawing speed (m/min)	100
Spinning path length (m)	0.05
Tex number (g/km)	2–4

The required material amounts are larger in a semi-industrial fiber spinning process, and therefore, the compounding was performed in a Brabender W50 single-screw extruder. The processing temperature was 200°C and the extruder screw speed was 30 RPM. The material was repeatedly processed four times to provide a homogenous compounding quality.

SPEEK/PP Melt Spinning

The laboratory scale melt spinning system was based on a modified Göttfert Rheograph 6000 capillary rheometer.[26] It is a piston-based system for monofilaments with a volume of 26 cm^3 and a maximum processing temperature of 400°C. The most important processing parameters used can be found in Table I.

The semi-industrial multifilament melt spinning of SPEEK/PP 5 : 95 was performed in a Fourne melt spinning system comprised of a single-screw extruder system with a filament count of 1–100. The equipment has the possibility to use heatable godets with different speed settings but these were not used due to the lack of material. The most important processing parameters for this system can be found in Table II.

Electron Paramagnetic Resonance Measurements

Electron paramagnetic resonance (EPR) spectroscopy was used to study the free-radical formation and life time of the photoactive species. Continuous wave (CW) X-band (9 GHz) EPR measurements were carried out at room temperature on a Bruker E500 ELEXSYS Series, using the Bruker ER 4122 SHQE cavity. The sample was placed into a 4.0 mm ID Suprasil tube, exposed to UV irradiation generated by an UV lamp (effective irradiative power 8 W/m^2 in the range of 390–490 nm) at a distance of 11 cm for 15 min. Then the specimen was immediately measured by EPR spectroscopy and the radical was monitored until 16 h. Then, it was irradiated again for 15 min and the radical signal was followed for other 24 h. This was repeated for a total of 10 times. The relative radical amount was calculated from the EPR peak areas by a double integration of the signal, centered at $g = 2.0035 \pm 0.0003$ with a narrow scan of 50 G avoiding Mn(II) contribution.[6]

Table II. Processing Parameters for the Semi-Industrial Melt Spinning Process

Number of filaments	10
Die length (mm)	8
Die diameter (mm)	0.5
Tex number (g/km)	23
Screw speed (RPM)	57
Drawing speed (m/min)	250
Winder traverse (1/min)	198
Spinning path length (m)	4.8

Table III. Spinning Quality Table

Quality	Description
Excellent	No problems in fiber quality or spinning stability.
Good	Fiber spinning was possible but there were problems in the spinning stability or fiber quality and spinning of very thin fibers was not possible.
Not spinnable	Fiber spinning was not possible or the process was stable for a few seconds at best.

Tensile Testing

Tensile tests were performed according to the ISO 2062 standard using ADF brustio Tessile tensile testing machine. A 200 mm clamping length and 1800 mm/min drawing speed were used. A total of 10 measurements per sample were made. Young's modulus was calculated in 0–10% strain. Prior to the mechanical analyses, the samples were conditioned at 20°C and a humidity of 65% for 24 h.

Scanning Electron Microscopy

The morphology of the SPEEK/PP 5 : 95 fibers was investigated by a Philips XL30 scanning electron microscope (SEM). The materials were gold sputtered before investigations in order to increase their conductivity.

Table IV. The Results of the Melt Spinning Tests

Test number	Processing temperature (°C)	SPEEK concentration (%)	Quality
1	180	0	Good
2	200	0	Excellent
3	220	0	Excellent
4	180	5	Good
5	200	5	Excellent
6	220	5	Excellent → good → not spinnable (depending on the residence time)
7	180	10	Good
8	200	10	Excellent
9	220	10	Excellent → good → not spinnable (depending on the residence time)

Figure 2. Melt spun SPEEK/PP 5 : 95 filaments. [Color figure can be viewed in the online issue, which is available at wileyonlinelibrary.com.]

RESULTS AND DISCUSSION

SPEEK Sulfonation and SPEEK/PP Compounding

The SPEEK/PP material has been previously characterized at different blend ratios.[6] According to these tests, the compounding should provide a homogenous blend. The biggest challenge was found in the thermal properties of the blend, and therefore, the blend spinnability was evaluated at different processing temperatures.

SPEEK/PP Fiber Spinning on a Laboratory Scale

The same Göttfert capillary rheometer-based fiber spinning system has been used in previous PEEK melt spinning experiments and the process parameters were thoroughly characterized for PEEK.[26] Although the processing temperatures are very different for the SPEEK/PP blend compared to neat PEEK, the previously found optimal spinning path length (5 cm), capillary dimensions (30/1 mm), and motor speed (100 m/min) for this equipment were used for the SPEEK/PP blend. The goal of these current laboratory scale tests was not to optimize the process as far as possible; instead the aim was to get a good overview of the spinnability at different SPEEK concentrations and temperatures.

For evaluation of the fiber spinning properties, a very simple three-step grading scale was created. The descriptions for different spinning qualities can be found in Table III.

Fiber spinning of the SPEEK/PP blend was easy at best and the fiber quality turned out to be excellent despite the fact that the system has no filters to remove impurities or unmelted particles. Generally an increase in the processing temperature improves spinnability[26–28] and this was evident with the SPEEK/PP blend as well. At 180°C, the spinnability was the worst regardless of the SPEEK concentration. This is not surprising considering how close this temperature is to the melting point of PP. However the processing temperature cannot be increased endlessly because the thermal properties of SPEEK are poor.[6] This was evident at 220°C where spinnability worsened drastically as the residence time increased. At first, the spinnability was excellent but after about 5 min, it had reduced to good and after 10–15 min, it was impossible to keep the

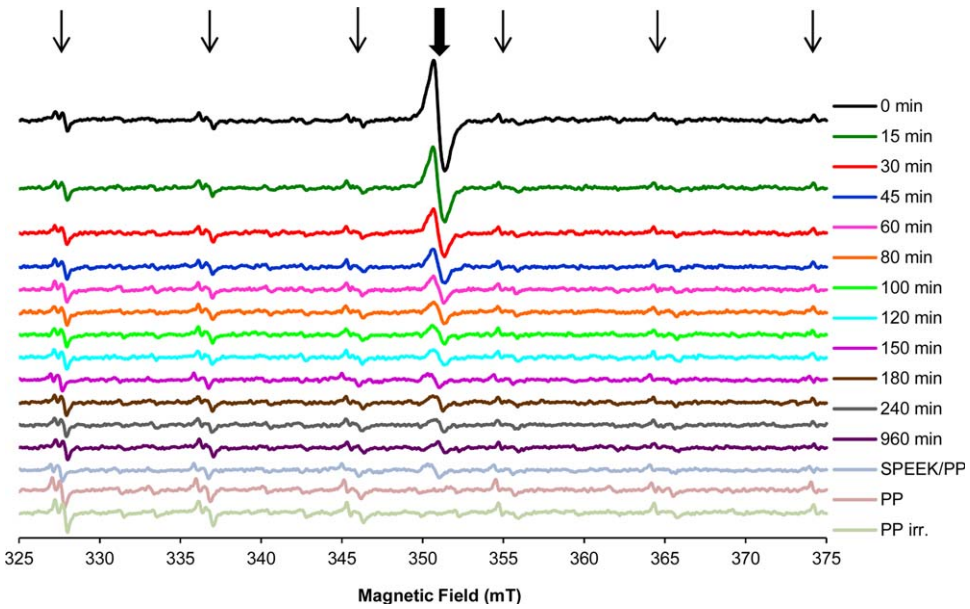

Figure 3. X-band EPR spectra of the sample recorded at different times after the irradiation. $\nu = 9.84$ GHz, 0.1 mT modulation amplitude, 2 mW power, 298 K. [Color figure can be viewed in the online issue, which is available at wileyonlinelibrary.com.]

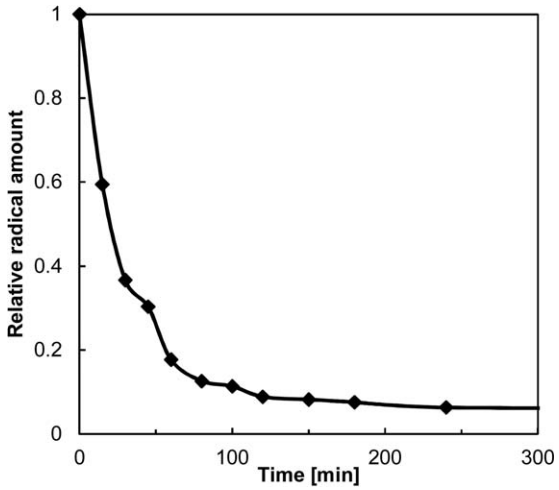

Figure 4. Relative radical amount after the first irradiation compared to I_{max} as a function of time.

process stable at all. The spinnability of PP remained excellent at 220°C so this problem is due to the thermal properties of SPEEK.

The differences in spinnability between different concentrations are small. PP and SPEEK/PP 10 : 90 blend have almost similar spinnability at the same processing temperature (with a short residence time). This is in line with the rheological characterization, where the concentration had only a small effect on viscosity.[6] Although the limits of spinnability were not tested, the best spun SPEEK/PP 5 : 95 blend fibers (at 200°C) were approximately 45 μm in average diameter. This should be easy to improve even further by optimizing the process and the PP grade. The results of the spinning tests can be seen in Table IV.

Semi-Industrial Fiber Spinning of the SPEEK/PP

The goal of the semi-industrial melt spinning was primarily to test the spinnability of the SPEEK/PP 5 : 95 blend under conditions that are closer to the industrial scale, and second, to manufacture a sufficient amount of multifilament yarns for characterization. The fiber properties are more stable in the semi-industrial process as a result of a more stable material flow, a 50 μm filter used to remove impurities, and a more accurate drawing system. The results from the laboratory scale spinning tests were used as a base for the upscaling and therefore a processing temperature of 200°C was used.

The spinnability was excellent from the beginning and no fine tuning was needed for the process to be stable. No broken filament was observed during the spinning of 4 bobbins. According to the SEM micrographs of the previously tested SPEEK/PP bulk blend,[6] the material did not contain any particles larger than a few micrometers, and this was also confirmed by the good spinnability. Figure 2 shows a picture of the bobbins obtained. The photocatalytic filaments have a brown color compared to light-colored PP ones.

Radical Formation

Figure 3 reports the X-band (9 GHz) EPR spectra of the samples recorded at different times after the irradiation. The BPK radical signal, marked as a thick arrow, is detected. The EPR signals, marked as a thin arrow, are the six lines due to Mn(II) impurities. The BPK signal reaches the maximum (I_{max}) immediately after the irradiation, then starts to decay reducing its intensity, and reaches its minimum in 150 min. The radical signal decay has been monitored for 16 h without any further changes in the intensity. A small intensity BPK peak is observed also in non-irradiated SPEEK/PP samples because the photocatalytic reaction is promoted by light sources during material

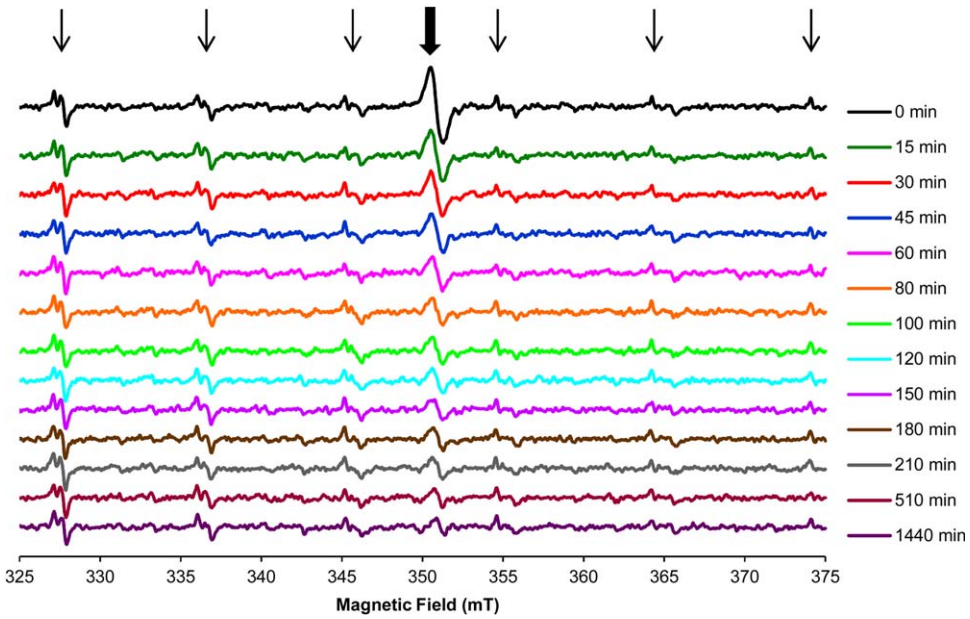

Figure 5. X-band EPR spectra of the sample recorded at different times after the second 15 min irradiation. $v = 9.84$ GHz, 0.1 mT modulation amplitude, 2 mW power, 298 K. [Color figure can be viewed in the online issue, which is available at wileyonlinelibrary.com.]

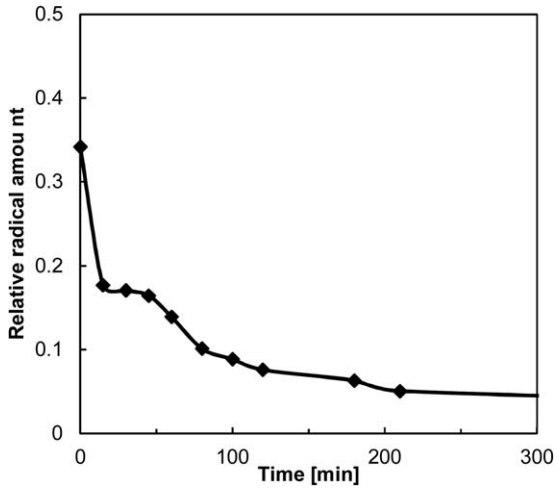

Figure 6. Relative radical amount after the second irradiation compared to I_{max} as a function of time.

handling (cutting of the fibers and displacement in the EPR capillary), demonstrating that material photocatalytic activity is very high. In PP samples, with or without irradiation, this peak was not visible. The reason for the long lifetime of the BPK radicals is their slow dimerization/disproportionation coupling reaction.[29] In the solid state, the mobility of the radicals is slow increasing the life-time.

Figure 4 presents the EPR signal area, obtained by double integration of the experimental spectra, as a function of time. The lifetime of the radical is rather long. After 15 min, the radical intensity is reduced to 59% and after 60 min to 18% of the I_{max}. The residual radical intensity is approximately 5% of the I_{max}.

The same sample was irradiated a second time for 15 min in order to see if the radical was reformed, and its decay was followed. As shown in Figures 5 and 6, the radical is visible again, however, at a lower intensity (approximately one-third of the I_{max}). Based on the previous studies, this result is expected.[29] The radical intensity drops rapidly during the first 15 min. The evolution of the signal was followed for 24 h even though the minimum signal intensity was reached in 3 h.

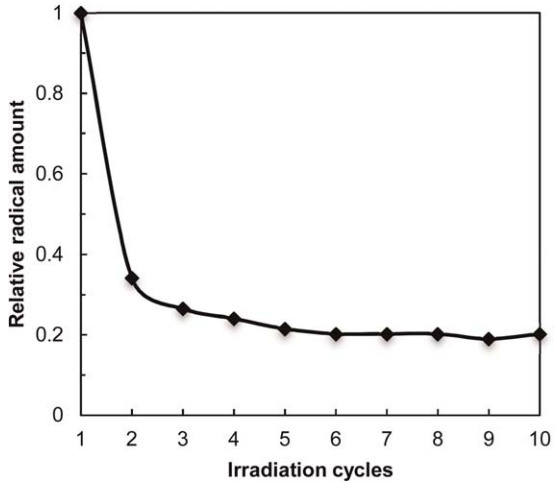

Figure 7. Relative radical amount after irradiation compared to I_{max} as a function of irradiation cycles.

Table V. Mechanical Properties for SPEEK/PP 5 : 95 and PP Filaments

Sample	Tex (g/km)	Tenacity at break (cN/tex)	Strain at break (%)	Young's modulus (cN/tex)
SPEEK/PP 5 : 95	23	9.1 ± 1.2	267 ± 59	19.5 ± 2.9
PP	23	11.6 ± 1.8	268 ± 47	24.7 ± 2.2

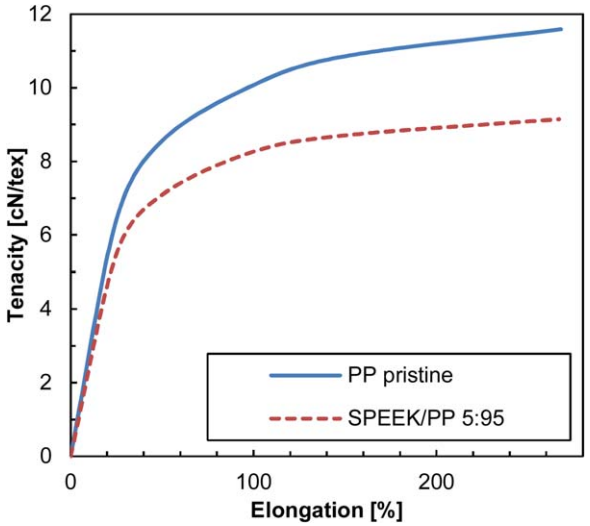

Figure 8. Typical tensile testing curves for PP and SPEEK/PP 5:95. [Color figure can be viewed in the online issue, which is available at wileyonlinelibrary.com.]

Relative radical amount was monitored up to 10 continuous irradiation cycles to simulate the fiber effectiveness in use. According to these results (Figure 7), the effectiveness immediately after the irradiation drops significantly during the first few irradiation cycles, and then quickly reaches the residual radical intensity of approximately 15% of the I_{max}. Evidently, the radical formation ability reduces in use and the actual usability has to be verified with, e.g., antimicrobial tests.

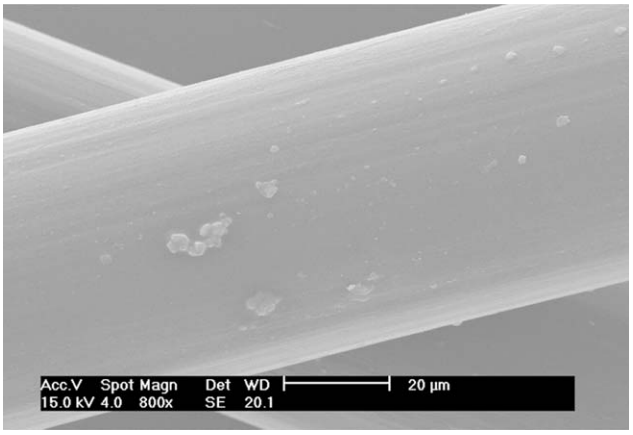

Figure 9. SEM micrograph of the PP fiber.

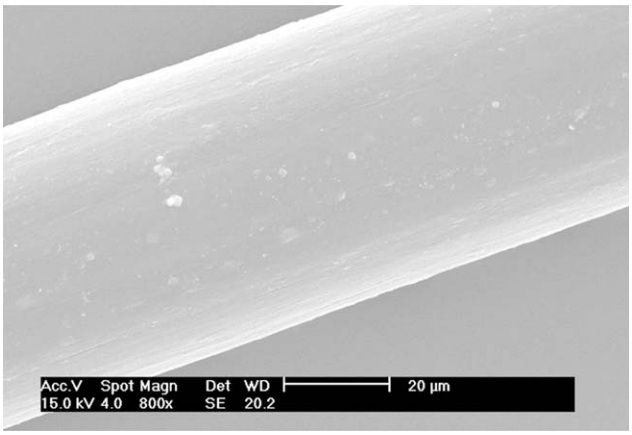

Figure 10. SEM micrograph of the SPEEK/PP 5 : 95 fiber.

Mechanical Properties

The mechanical properties of the yarns are listed in Table V. The mechanical tenacity of the 5 : 95 SPEEK/PP yarn is 20% lower than that of otherwise similar PP yarn. Tenacity values are a little low compared to commercial PP yarns, even with similar linear density.[30] Cold drawing using heatable godets and incrementally increased drawing speed would have improved the orientation of the polymer chains and thus increased the mechanical strength. Unfortunately, the lack of material limited the testing, and only the simplest option, drawing the yarns directly into the bobbin, was performed. Another reason for the low mechanical properties may have been the low melt index of the PP grade used. Even though its use was justified to improve the compounding quality, higher melt index grades are typically preferable in melt spinning. In contrast to the low mechanical strength, the polymer yarns are highly elastic with over 250% strain at break. Typical tensile testing curves for PP and SPEEK/PP 5 : 95 can be found in Figure 8 and the raw data of the measurements in Supporting Information, in Table S1.

SEM Analysis

The analysis of the SPEEK/PP 5 : 95 fibers reveals no problems in the fiber quality. There are only small differences between the surfaces of the PP (Figure 9) and the SPEEK/PP 5 : 95 (Figure 10) fibers according to the SEM micrographs. The surface of the SPEEK/PP 5 : 95 fiber is slightly rougher due to the SPEEK particles. The results are consistent with the previously performed characterization of the blend where SPEEK particles, a few micrometers in size, were found to be homogenously dispersed in the PP matrix. Unfortunately cross-sectional SEM micrographs could not be obtained due to sample manufacturing problems: very thin filaments were too difficult to break using liquid nitrogen.

CONCLUSIONS

The goal of this study was to provide a fiber with sufficient and long-lasting photoactivity and mechanical properties. There were many challenging aspects such as the new polymer blend, thermal degradation of the blend, and small SPEEK particles in the blend that could interfere with the fiber spinning. The overall performance of the fibers is good. Fiber spinnability is good when using optimal processing parameters, most importantly a proper processing temperature of approximately 200°C has to be used. Mechanical properties are only a little affected by the addition of SPEEK and they are sufficient for technical applications. The SPEEK/PP fiber is highly elastic, so the mechanical properties can be further improved by increasing the drawing speed and draw ratio.

UV-induced radicals on the fiber surface were characterized by the EPR technique: stable BPK radical was detected and the characterization of the stability of the radical over several irradiation cycles showed that decay during the first few cycles occurs. This cannot be directly related with the photocatalytic efficiency; however, a reduction on the effectiveness over time is expected as per conventional photoactive materials. The next goal is therefore to estimate the antimicrobial, antipollution, and self-cleaning performance of the final fabrics in order to fully characterize the efficiency of the new fibers.

ACKNOWLEDGMENTS

The authors would like to thanks the European Commission for funding this study within the FP7 "SAFEPROTEX" (FP7-NMP-2008-SME-2 contract number 228439), the Federation of Finnish Textile and Clothing Industry (Finatex), and the Finnish Foundation for Technology Promotion (TES).

REFERENCES

1. Lacasse, K.; Baumann, W. Textile Chemicals: Environmental Data and Facts; Springer: Berlin, **2004**.
2. Meilert, K. T.; Laub, D.; Kiwi, J. *J. Mol. Catal. A* **2005**, *237*, 101.
3. Zhong, L.; Lee, C.-S.; Haghighat, F. *J. Hazard. Mater.* **2012**, *243*, 340.
4. Quanjun, X.; Jiaguo, Y.; Po, K. W. *J. Colloid Interface Sci.* **2011**, *357*, 163.
5. deRichter, R.; Caillol, S. *J. Photochem. Photobiol. C: Photochem. Rev.* **2011**, *12*, 1.
6. Fatarella, E.; Mylläri, V.; Ruzzante, M.; Pogni, R.; Baratto, M. C.; Skrifvars, M.; Syrjälä, S.; Järvelä, P. *J. Appl. Polym. Sci.* **2015**, *132*, 41509.
7. Ma, R.; Tang, T. *Int. J. Mol. Sci.* **2014**, *15*, 5426.
8. World health organization International Agency for Research on Cancer. IARC monograps on the evaluation of carcinogenic risks to humans. Vol. 93 carbon black, titanium dioxide and talc. Lyon, **2010**.
9. Sabu, T.; Visakh, P. M. eds.; Handbook of Engineering and Speciality Thermoplastics: Vol. 3: Polyethers and Polyesters; Wiley: New York, **2011**.
10. Yang, T. *Int. J. Hydrogen Energy* **2008**, *33*, 6772.
11. Korchev, A. S.; Bozack, M. J.; Slaten, B. L.; Mills, G. *J. Am. Chem. Soc.* **2004**, *126*, 10.
12. Conceição, T. F.; Bertolino, J. R.; Barra, G. M. O.; Pires, A. T. N. *Mater. Sci. Eng. C* **2009**, *29*, 575.
13. Hong, K. H.; Sun, G. *J. Appl. Polym. Sci.* **2009**, *112*, 2019.
14. Lee, S. H.; Youn, J. R. *J. Appl. Polym. Sci.* **2008**, *109*, 1221.

15. Esthappan, S. K.; Kuttappan, S. K.; Joseph, R. *Mater. Des.* **2012**, *37*, 537.
16. Altan, M.; Yildirim, H. *J. Mater. Sci. Technol.* **2012**, *28*, 686.
17. Windler, L.; Height, M.; Nowach, B. *Environ. Int.* **2013**, *53*, 62.
18. Abdelgawad, A. M.; Hudson, S. M.; Rojas, O. J. *Carbohyd. Polym.* **2014**, *100*, 166.
19. Dubas, S. T.; Kumlangdudsana, P.; Potiyaraj, P. *Colloid Surf. A* **2006**, *289*, 105.
20. Liu, Y.; Liu, Y.; Ren, X.; Huang, T. S. *Appl. Surf. Sci.* **2014**, *296*, 231.
21. Tan, K.; Obendorf, S. K. *J. Membr. Sci.* **2007**, *305*, 287.
22. Sun, Y.; Sun, G. *Ind. Eng. Chem. Res.* **2004**, *43*, 5015.
23. Uddin, M. J.; Cesano, F.; Scarano, D.; Bonino, F.; Agostino, G.; Spoto, G.; Bordiga, S.; Zecchina, A. *J. Photochem. Photobiol. A* **2008**, *199*, 64.
24. Yuranova, T.; Mosteo, R.; Bandara, J.; Laub, D.; Kiwi, J. *J. Mol. Catal. A-Chem.* **2006**, *244*, 160.
25. Yang, L.; Cai, A.; Luo, C.; Liu, Z.; Shangguan, W.; Xi, T. *Sep. Purif. Tehnol.* **2009**, *68*, 232.
26. Mylläri, V.; Skrifvars, M.; Syrjälä, S.; Järvelä, P. *J. Appl. Polym. Sci.* **2012**, *126*, 1564.
27. Golzar, M. Melt spinning of the fine PEEK filaments. Dissertation, Technische Universität Dresden: Dresden, **2004**.
28. Fourné, F. Synthetic Fibers: Machines and Equipment, Manufacture, Properties: Handbook; Hanser Gardner publications: Munich, **1999**.
29. Korchev, A. S.; Konovalova, T.; Cammarata, V.; Kispert, L.; Slaten, L.; Mills, G. *Langmuir* **2006**, *22*, 375.
30. Vitkauskas, A.; Miglinaite, R.; Vesa, P.; Puolakka, A. *Mater. Sci.-Medžiagotyra* **2005**, *11*, 407.

Tampereen teknillinen yliopisto
PL 527
33101 Tampere

Tampere University of Technology
P.O.B. 527
FI-33101 Tampere, Finland

ISBN 978-952-15-3926-8
ISSN 1459-2045